INTRINSIC HOST AND EXTRINSIC ENVIRONMENTAL DRIVERS OF CORAL HEALTH AND DISEASE

A Dissertation

Presented to the Faculty of the Graduate School

of Cornell University

In Partial Fulfillment of the Requirements for the Degree of

Doctor of Philosophy

by

Courtney Saltonstall Couch

January 2014

INTRINSIC HOST AND EXTRINSIC ENVIRONMENTAL FACTORS OF CORAL HEALTH AND DISEASE

Courtney Saltonstall Couch, Ph. D.

Cornell University 2014

Disease is an ecological process that regulates hosts, but does not affect all host populations and communities uniformly. The extent to which populations and communities are affected by disease is determined by a suite of intrinsic factors such as host demography, susceptibility, and immunocompetence, as well as environmental extrinsic factors, which can alter host-pathogen interactions.

Coral disease is a leading contributor to global coral reef decline, highlighting the importance of testing the role of intrinsic and extrinsic factors in disease affecting natural systems. Further, the ability of corals to respond to disease is influenced by the dynamics of innate immunity. The broad goals of this dissertation are to (1) address the patterns and processes of coral health and disease along the west coast of the Island of Hawai‘i (WHI), which has some of the highest disease levels in the Pacific; and (2) investigate the temporal dynamics of the cellular immune response, using a Caribbean sea fan as a model system.

Ecological processes including disease, competition for space, and predation strongly influence the health of coral communities. In **Chapter 1,** I characterize the spatial and temporal patterns in coral disease and other biological interactions, describes long-term changes in coral cover, and identifies sites of concern for

management action along WHI.

The spatial extent of disease in communities is determined by an integrated series of host population- and community-level processes. In **Chapter 2**, I test the effects of host demographics, coral species richness, predation and disease co-occurrence on the risk of three most common diseases affecting the scleractinian coral *Porites*.

In addition to host ecology, disease is often influenced by environmental stress. In **Chapter 3**, I identify the risk factors contributing to dynamics of *Porites* growth anomalies by testing the correlation between prevalence, severity and linear extension, and ecological and environmental parameters across gradients of terrestrial input.

Immune responses often determine an organism's success in pathogen and stress response. In **Chapter 4**, I use *G. ventalina* to characterize the temporal dynamics of cellular responses (granular amoebocyte aggregation and prophenoloxidase activation) to allogenic grafts in a series of laboratory and field experiments.

BIOGRAPHICAL SKETCH

Inspired by summers of searching for critters in the intertidal zones surrounding Vinalhaven, Maine, Courtney professed to her parents at the age of 10 that she was going to become a marine biologist. As a native to Ithaca, New York, Courtney takes great pride in the fact that, twenty years later, not only did she become a marine biologist, but she spends her days working on some of the world's most specular coral reef ecosystems.

With strong support from her parents, Courtney formally entered the world of marine science as a high school student at Sea Education Association in Woods Hole, Massachusetts, learning about oceanography and nautical science aboard the tall ship the SSV Westward. Fully committed to pursuing this career path, but longing for warmer climates, Courtney and her father became certified SCUBA divers in 2000. Her father often jokes that it became clear early on that Courtney was destined to study marine invertebrates rather than dolphins and sharks since she spent more time upside down looking under crevices than paying attention to the sharks swimming by.

During her four years at St. Lawrence University where she received her Bachelors of Science in Biology, her interest in marine science and coral reef ecology was further piqued by the diverse research opportunities in Prof. Brad Baldwin's lab. Under Prof. Baldwin's invaluable mentorship, Courtney conducted an independent research project on the feeding preferences of the sea urchin *Lytechinus variegatus* and was introduced to scientific diving in San Salvador, Bahamas where Prof. Baldwin's team investigated the impact of herbivory on coral communities and reef biodiversity.

Following her work in Prof. Baldwin's lab, Courtney worked as a marine science educator at Seacamp on Big Pine Key, Fl and an environmental consultant at PBS&J in Miami, Fl before returning to Ithaca. Courtney was introduced to the fields of coral disease ecology and coral immunology as a lab technician in Prof. Drew Harvell's lab at Cornell University. Under the mentorship of Prof. Harvell and her postdoctoral researcher Dr. Laura Mydlarz, Courtney conducted field and laboratory experiments to assess coral's immunological response to pathogens and environmental stress, focusing on the sea fan coral, *Gorgonia ventalina - Aspergillus sydowii* pathosystem. This research resulted in three peer-reviewed publications. In addition to her research, Courtney was the coordinator for the Coral Disease Working Group, which was one of six international working groups within the "Coral Reef Target Research and Capacity Building for Management" funded by the Global Environmental Facility and the World Bank. As the working group coordinator, Courtney conducted interdisciplinary research with the world's leading coral biologists and microbiologists, as well as co-edited a coral disease handbook for marine resource managers.

Inspired by the Coral Disease Working Group and the Harvell Lab's research on coral disease ecology and evolution of coral resistance, Courtney chose to pursue her doctorate with Prof. Harvell. Courtney applied her extensive background as a field ecologist to develop a new research project on the leeward coast of the Island of Hawai‘i aimed at identifying disease hot spots and understanding the role of ecological processes and environmental factors in mediating these patterns.

In addition to her doctoral research, Courtney is passionate about marine

conservation and has consistently strived to use her data and expertise to inform marine resource management. In collaboration with NOAA and Hawai‘i’s Division of Aquatic Resources, Courtney has not only improved managers’ capacity to respond to disease outbreaks in Hawai‘i, but has also helped target sites and disease risk factors necessary for corrective action. Courtney also sought to promote environmental stewardship through frequent outreach with community members and school groups.

Courtney is starting her ‘dream job’ as a postdoctoral researcher at the Hawai‘i Institute of Marine Biology in Kaneohe, HI on a project to promote Indo-Pacific coral health through the newly formed “Action Network for Coral Health and Resilience.” Courtney is honored to work with Dr. Randall Kosaki (NOAA), Dr. Eric Conklin (The Nature Conservancy) and Dr. Megan Donahue (HIMB) to standardize coral disease data across the world’s largest tropical marine protected areas, address local environmental drivers of coral disease through targeted research in the Main Hawaiian Islands, and build capacity and facilitate communication between marine resource managers and scientists to improve reef resilience planning.

This work is dedicated to my husband, Chris, who has taught me the meaning of balance, persistence and happiness.

To Peter and Tacie Saltonstall who are inspiration and love personified.

To Hattie and Lev Saltonstall for keeping me laughing.

To Jean and Fargo Balliett who always reminded me to "never turn down a new adventure."

To Alice Saltonstall for the many impromptu dinners and Dr. Megan Shull for the many inspirational talks.

To the Couch Clan for their unwavering moral support, patience during my many months away from home and love.

ACKNOWLEDGMENTS

It is with profound gratitude that I acknowledge all of the people that have helped make my dissertation possible, especially my academic mentors. First, I would like to thank my major advisor Prof. Drew Harvell who provided tremendous support from day 1, gave me intellectual freedom to explore my research interests and provided me with countless opportunities to study around the world and build an invaluable network of colleagues. I would also like to thank my supportive committee members Dr. Esther Peters, Dr. Ian Hewson and Prof. Jennifer Thaler, who provided invaluable feedback from start to finish. My entry into coral disease ecology is also largely thanks to the incredible team of PIs and graduate students involved in the Coral Reef Targeted Research & Capacity Building for Management (CRTR)'s Coral Disease Working Group. I would also like to thank Prof. Laura Mydlarz for her tremendous mentorship and providing research opportunities during my early days in the Harvell lab. Chapter 4 would not have been possible without mentorship, logistical support and enthusiasm from Prof. Ernesto Weil. I am grateful to Dr. Rebecca Vega Thurber for enfolding me into her lab, providing tremendous molecular support and advice on graduate school and beyond.

My research was generously funded by The Kohala Center, the National Science Foundation Graduate Research Fellowship Program, the NOAA Coral Reef Conservation Grant Program, National Geographic, GEF-World Bank CRTR program, and Cornell University. I am grateful to Bill Thornton and the Cornell AAUS dive program for helping me navigate difficult dive logistics. I am forever grateful to all of the members of the Harvell lab who profoundly shaped me

intellectually, read countless manuscripts, provided endless laboratory support, and who were always there for moral support. I am also grateful to the incredible team of undergraduate students, especially Reyn Yoshioka, Jillian Lyles and Catherine Kim who spent countless hours processing samples and analyzing data. I owe profound thanks to Dr. Joe Simonis, Dr. Brooks Miner, Dr. Diego Ruiz-Moreno, Ian Brosnan and Ben Dalziel who provided unbelievable statistical support. I thank my fellow disease ecologists especially, Katie Marchetto, Gui Becker, Ana Longo, Ben Dalziel for their inspiring intellectual curiosity and constant feedback. To all my Cornell friends, Dr. Morgan Mouchka, Ian Brosnan, Colleen Burge, Alison Tracy, Yula Kapetakanos, Ana Forsman, Dr. Cayelan Carey, and Angela Early, thank you for your years of moral support!

Mahalo nui loa to my Hawai‘i ‘ohana. There aren’t enough words to express how grateful I am to all of people on Hawai‘i Island who welcomed me with open arms and without whom my research wouldn’t have been possible. Mahalo to Dr. Bill Walsh and everyone at Hawai‘i Division of Aquatic Resources for providing invaluable logistical support, knowledge of Hawai‘i and so many wonderful memories on the water. I am forever indebted to Rich Lazear, Nora Judd, Camille Barnett and Shane Ramsey for giving me a place to call home when funding ran thin. I’m grateful to my dear friends at Kona Diving company who helped me with all my dive gear needs, great conversations and field support. I thank Keith Olson, Eric Grossman and Lisa Marrack for providing tremendous help with water quality assessments and a wealth of knowledge about Hawai‘i’s hydrology and biogeochemistry. Mahalo to Matt Hamabata, Cindi Punihaole, Caroline Carl and Sam Birch for enfolding me into The

Kohala Center Family and providing logistical and financial support.

Finally, I owe huge thanks to all of my incredible field assistants and friends who never complained about the ½ mile surface swims, spent over 1000 hours underwater with me, and kept me laughing even the worst conditions. Joao Garriques, Camille Barnett, Lindsey Kramer, Jonatha Giddens, Rebecca Most, Katie Gaab, Gavin Key, Petch Manopawitr, and Nigel Rozet-you are my heroes!

TABLE OF CONTENTS

LIST OF FIGURES

CHAPTER 4

APPENDIX I

APPENDIX II

LIST OF TABLES

CHAPTER 1

SPATIAL AND TEMPORAL PATTERNS OF CORAL HEALTH AND DISEASE ALONG LEEWARD HAWAI'I ISLAND

In Review as Couch, C. S., J. Garriques, C. Barnett, L. Preskitt, S. Cotton, J. Giddens, W. Walsh (in review). Spatial and Temporal Patterns of Coral Health and Disease along Leeward Hawai`i Island. Coral Reefs.

ABSTRACT

Ecological processes including disease, competition for space, and predation strongly influence coral reef health from the colony to reef level. The leeward/west coast of the island of Hawai‘i (WHI), consists of the largest expanse of intact reefs in the Main Hawaiian Islands, yet little is known about the health of its coral communities. We measured prevalence of coral diseases and non-disease conditions (biological interactions) at nine regions across two depths in the summer and winter months between 2010 and 2011. Mean disease prevalence 5 to 25 times greater than previously reported for the Main Hawaiian Islands (MHI). Prevalence of the three most common diseases, *Porites* growth anomalies (PorGA: 14.60 ± 0.85%), *Porites* trematodiasis (PorTRM: 9.92 ± 0.88%), and *Porites* tissue loss syndrome (PorTLS: 0.70 ± 0.07%) varied more across site and depth than survey month. Overall, spatial variation in disease prevalence was dependent on disease type and site, but was not uniform as a function of depth. Other biological interactions such as algal overgrowth (ALOG) and predation contributed to colony mortality and varied between sites. At the coast-wide level, percent coral cover did not change significantly between 2003 and 2011, but did increase significantly at Ho‘okena and declined significantly at Mauna Lani and Ka‘ūpūlehu. Puakō, Mauna Lani, Ka‘ūpūlehu and Hōnaunau were also of concern due to their high levels of PorGA, PorTLS, predation and ALOG. The high spatial variation in coral health not only advances our understanding of coral disease ecology, but also supports reef resilience planning by identifying vulnerable areas that would benefit most from targeted conservation and management efforts.

INTRODUCTION

Ecological processes including disease, competition for space, and predation play important roles in regulating healthy coral populations (reviewed by Birkeland 1997; Harvell et al. 2007). Although coral disease is a natural component of healthy ecosystems, it can have detrimental effects on ecosystem structure and function during outbreaks (Aronson and Precht 2001; Kim and Harvell 2004). Disease has become a major contributor to global coral mortality since the 1980s, especially in the Caribbean where disease, together with other local stressors has lead to widespread phase shifts to communities dominated by other coral genera or macroalgae (Aronson and Precht 2001). Although the effects of coral disease have been most pronounced throughout the Caribbean (Ruiz-Moreno et al. 2012) with 80% mortality of *Acropora* following disease outbreaks (Aronson and Precht 2001; Patterson et al. 2002), impacts to Pacific reefs remained largely undetected until the early 2000s (Willis et al. 2004).

While the causative agents of most coral diseases remain unknown, an estimated 25 diseases/syndromes affect Pacific corals ranging from chronic diseases such as growth anomalies to acute highly infectious diseases such as white syndrome and black-band disease (Vargas-Angel 2009). Preliminary evidence suggests that Pacific coral diseases are increasing both temporally (Willis et al. 2004; Ruiz-Moreno et al. 2012) and spatially, now reaching even remote reefs such as the Pacific Remote Island Areas (Vargas-Angel 2009), Palmyra Atoll (Williams et al. 2010b) and the Northwestern Hawaiian Islands (Aeby et al. 2011b). While the causes of this increase are not well understood, coral disease patterns have been linked to a combination of global and local factors. Tissue loss diseases often vary seasonally and have been

linked with seasonal increases in sea surface temperature and light (Boyett et al. 2007; Sato et al. 2009). On the local scale, disease is also affected by local environmental disturbances (e.g. Kaczmarsky and Richardson 2010; Haapkylä et al. 2011) as well as coral abundance (Bruno et al. 2007). Only through repeated coral health assessments at the same sites over time can we understand the broader role of disease and biological interactions in reef health, as well as the underlying mechanisms driving these patterns.

In addition to disease, other non-disease conditions (henceforth referred to as "biological interactions") such as competition and predation provide strongly influence reef ecosystems both directly and indirectly. Coral-macroalgal competition is a well-known contributor to colony and reef-level mortality. Under eutrophic conditions, accelerated algal growth can overgrow and kill coral tissue, inhibit coral recruitment, enhance microbial activity, or result in ecosystem phase shifts (Done 1992; Hughes 1994; Smith et al. 2006). Another important contributor to coral mortality and reef health is corallivore predation. Invertebrate corallivores such as the gastropod *Drupella* spp. and the crown-of-thorns-starfish (COTS) *Ancanthaster plancii* have become a major cause of coral cover decline (e.g. Turner 1994; De'ath et al. 2012) and facilitate disease by spreading pathogenic microorganisms and wounding tissue (Nugues and Bak 2009; Nicolet et al. 2013). To date, very few coral health monitoring programs have quantitatively assessed the role of these other ecological processes.

In Hawai'i, algal blooms, coral disease epizootics, and a variety of natural and anthropogenic disturbances have dramatically shaped coral health and reef resilience.

Human population growth and a burgeoning tourism industry in Hawai‘i have resulted in considerable land use change, mass sedimentation events, and eutrophication (Jokiel et al. 2004; Kittinger et al. 2011). These changes have been pronounced in regions such as Kāne‘ohe Bay, O‘ahu, where a combination of natural and anthropogenic disturbances have resulted in precipitous coral cover decline and widespread algal blooms (reviewed by Hunter and Evans 1995). Of the 12 diseases affecting Hawaiian corals (Aeby et al. 2011b), outbreaks of *Montipora* white syndrome in Kāne‘ohe Bay (Aeby et al. 2010), and the recent *Montipora* disease outbreak in Hanalei, Kaua‘i (Aeby and Work, pers. comm.) and anomalously high *Montipora* growth anomaly levels in southeastern Hawai‘i Island (Burns et al. 2011) have dramatically affected one of the region's dominant reef-building genera. To date, coral disease research has been focused on impacted reefs with ongoing disease outbreaks, with relatively less effort in describing disease dynamics of the most intact reefs such as those surrounding the Island of Hawai‘i (but see Takabayashi et al. 2008; Burns et al. 2011).

As the largest and youngest of the Hawaiian Islands, the Island of Hawai‘i has the highest coral coverage in the state (Battista et al. 2007; Franklin et al. 2013), and is also of particular concern due to its rapid human population growth rate (US Census Bureau 2007) and highly porous basaltic rock, which renders coastal ecosystems susceptible to coastal pollution (Street et al. 2008). The leeward/west coast (WHI) has the largest expanse of intact reef in Hawai‘i, and has not experienced the widespread coral cover loss observed on other islands, but is demonstrating localized reef decline (Walsh et al. 2013). Coral disease assessments have been conducted along WHI as

part of archipelago-wide studies (Vargas-Ángel and Wheeler 2009; Aeby et al. 2011b), but less is known about the spatiotemporal dynamics of WHI coral health and disease (but see, Walsh et al. 2013). To characterize coral health, determine whether coral cover is changing over time, and identify sites of specific concern for management action along WHI, we tested the following hypotheses: 1. Coral disease prevalence varies temporally and is correlated with temperature. 2. Coral disease and biological interactions vary as a function of depth and site. 3. Percent coral cover varies temporally during the last eight years.

METHODS

Study Sites

Surveys were conducted at nine locations along West Hawai‘i, chosen based on proximity to West Hawai‘i Aquarium Project (WHAP) long-term monitoring sites (Tissot et al. 2004), shoreline access, and expressed interest from Hawai‘i Division of Aquatic Resources (Fig. 1.1). See Table S1 for a list of acronyms. At each location, a shallow site was established by haphazardly choosing four coordinates within a 5,000 m^2 area (3 - 6m depth). At each coordinate, a 10-m transect was extended at a haphazard bearing parallel to shore and marked with GPS coordinates to relocate in future seasons. A deep site was also monitored at each region by surveying the first 10 m of the four established WHAP permanent transects (10–15m depth).

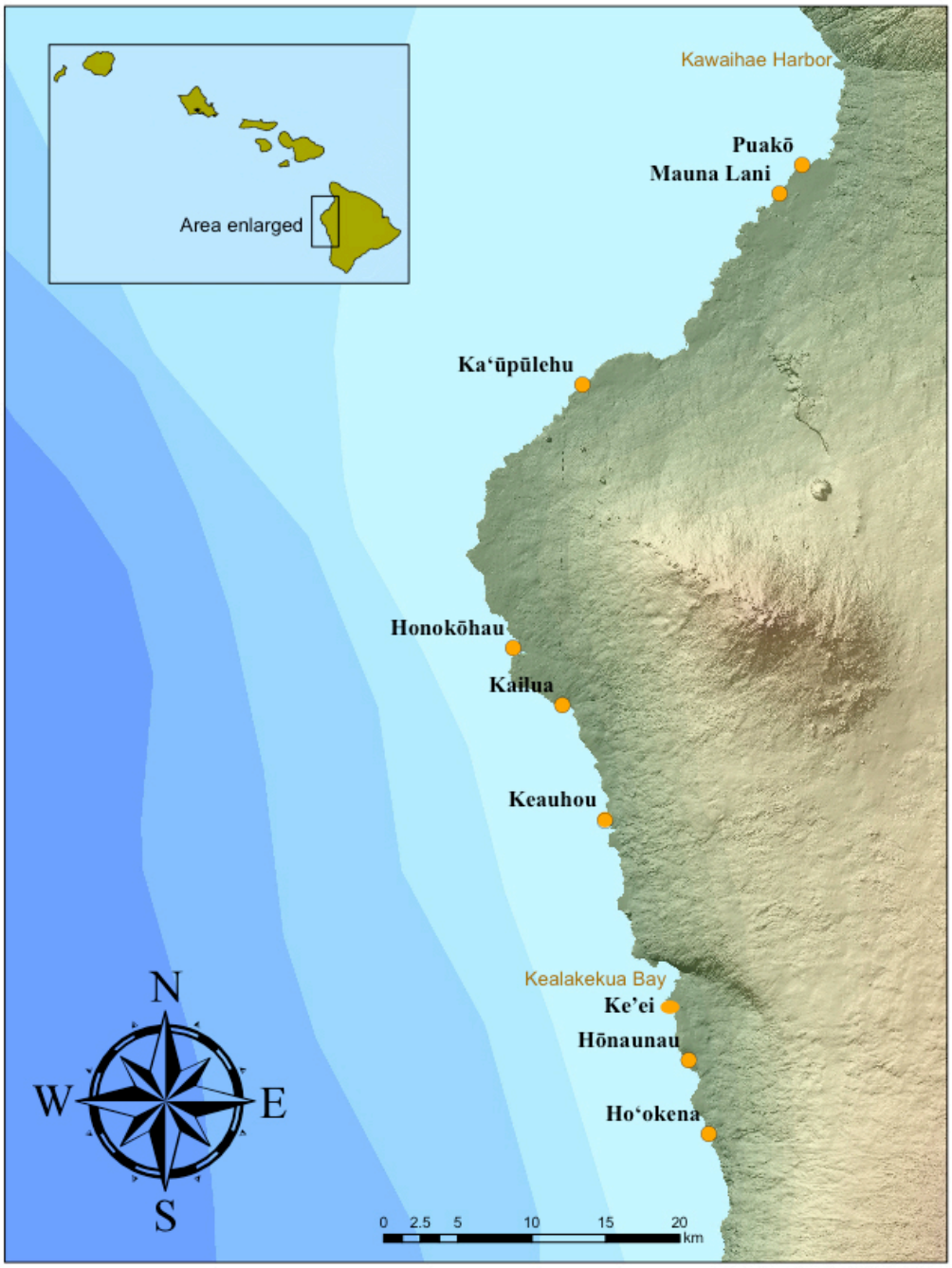

Figure 1.1 West Hawai'i study site locations, Main Hawaiian Islands, USA.

Coral Health Assessments

Coral health surveys were conducted on each of four 10 x 2 m belt transects (80 m^2) on which all colonies were counted and identified to species. Each colony was also inspected for disease (using categories described by Work et al. 2008a; Aeby et al. 2011b) and other biological interactions/sources of mortality (Fig. S1.1, Table S1.2). Shallow and deep sites were surveyed between January and March 2011 to determine the spatial (site and depth) variation in prevalence of each condition. Shallow sites were surveyed between January and March 2010, July to August 2010, January to March 2011, and July to August 2011 to assess seasonal fluctuations in coral health. The number of disease lesions on each colony was recorded at all shallow sites as a metric of severity during July through August 2011. HOBO Water Temperature Pro version 2 data loggers (HoboTemp; Onset Co., Pocasett, MA) were launched at 1-hour intervals and deployed at all shallow sites to monitor temperature continuously between July 2010 and August 2011.

Coral Cover Assessments

Long-term trends in benthic community structure at the deep WHAP sites (Fig. 1.1) were estimated in photoquadrats using the following digital cameras: Olympus 5060 in November and December 2003, Olympus 7070 in April 2007 and an Olympus E-PL1 camera (12.3 megapixels in an Olympus PT-EPO1 housing) in February through April 2011. The underwater housing was attached to a clear Plexiglas® spacer rod and used to take images at a fixed height (0.75 m) above the benthos with manual white balance. Images were taken at 1-m intervals along each of the four 25 m

transects, producing 26 images per transect and analyzed using the Coral Point Count with Excel extensions software program (CPCe, Kohler and Gill 2006). Data were pooled by transect using 30 randomly generated points per frame. The proportion of each benthic category was determined for each image and percent cover was calculated for each transect, total percent cover was obtained by calculating the mean percent cover of the four transects.

Statistical Analyses

Due to logistical constraints preventing the comparison of depth across multiple seasons, the depth and seasonal prevalence data were analyzed using separate generalized linear models (GLM) in R version 2.13.2. As a result of the high genus-specific disease patterns and to enable comparison with previous studies in HI (Williams et al. 2010a; Aeby et al. 2011b), prevalence of each disease was calculated for the primary reef-building genera. For example, PorGA prevalence = (number of *Porites* colonies with GAs/total number of *Porites* colonies surveyed) * 100. CIL prevalence was calculated for *Montipora* and *Pocillopora* only. The prevalence of colonies with other biological interactions was calculated for all colonies, except *Porites* PR. To estimate the spatial extent/commonality of each disease and biological interaction, we calculated the frequency of occurrence as the percent of transects surveyed having at least one colony with a particular condition.

To assess whether disease and biological interaction prevalence varied seasonally, we used separate binomial generalized linear mixed-effects models (GLMMs) for PorGA, PorTRM, PorTLS, ALOG, GastPRD and BLE. We treated

transect nested within site (shallow only) as a random effect and survey month/year (e.g. July/August 2010) as a fixed effect. We compared each fixed-effect model to the null model using Likelihood ratio tests (LRT) with chi-square test statistics (Burnham and Anderson 2002). Generalized linear hypothesis tests (glht function in the multcomp package) were used to identify significant differences between survey months. To determine whether seasonal variation in disease was attributed to thermal fluctuation, disease prevalence was regressed against average bimonthly mean and maximum daily temperature using GLMs (quasibinomial distribution; parameter estimates in logit form).

To determine whether disease and biological interaction prevalence varied spatially, we used separate quasibinomial GLMs for PorGA, PorTRM, PorTLS, ALOG, and GastPRD prevalence with site and depth as fixed effects during winter 2011. We compared quasi-corrected Akaike's information criterion to determine which fixed effects or interaction models best fit the data (Burnham and Anderson 2002). The best-fit models were selected when ΔqAICc <10 (Bolker et al. 2009). The goodness of fit for each model was also determined by calculating the % deviance ((Null deviance-residual deviance)/null deviance *100). To determine whether prevalence varies by depth at each site, we ran individual paired t-tests with Bonferroni corrections for multiple comparisons. GLMs (poisson distribution and log link) with LRTs were used to determine whether disease severity (number of lesions per colony) varied as a function of site during summer 2011 for PorGA, PorTRM, and PorTLS.

To determine whether percent coral cover changed between 2003 and 2011 at WHAP sites, mean percent coral cover was analyzed for the entire coast and then separately by site using linear mixed-effect models (LMEM). For each site LMEM, transect nested within site was treated as a random effect and year as a fixed effect. We used the Markov chain Monte Carlo (MCMC) simulation to detect differences between years (see Baayen et al. 2008). MCMC generates random samples from a posterior distribution of parameter values for fixed and random effects (Bolker et al. 2009). We conducted 50,000 iterations to estimate the highest posterior density (HPD) interval for each parameter, using 95% of the probability distribution (credible intervals). HPD intervals that did not overlap zero indicated conservative significant effects of the specified parameters $\alpha = 0.05$ (Pinheiro and Bates 2000).

RESULTS

WHI corals were affected by eight coral diseases that varied in their prevalence and frequency of occurrence (Table S1.2, Fig. S1.1). PorGA, PorTRM, and PorTLS were the most widespread diseases found at 100, 98, and 56% of all transects, respectively, followed by PorMFTL, PavHYP, CIL, MonGA, and PocTLS (Table S1.2). PorGA, PorTRM were the most prevalent diseases (Table S1.2). PavHYP was the third most prevalent disease, but was only found on 10% of the transects. No cases of MWS were observed during the course of this study. The three most widespread and prevalent types of biological interactions affecting WHI corals were ALOG, PR, and GastPRD, with very low COTSPRD (Table S1.2). ALOG and

GastPRD were the primary contributors to coral tissue mortality of all diseases and biological interactions (Couch pers. obs.).

Seasonal Patterns in Coral Health and Temperature

To determine whether the most common conditions vary seasonally along WHI, we analyzed each condition separately and found that PorTLS prevalence varied significantly between months when compared to the null model (LRT: χ^2=40.6, df= 3, p=0.039). There was an indication of PorTLS seasonality with elevated prevalence in the summer compared to winter months, but only significantly higher in summer 2010 compared to winter 2011 (Fig. 1.2A). ALOG prevalence was significantly elevated in summer months compared to winter months (Fig. 2B, GLM post hoc test p<0.05). BLE prevalence varied temporally (LRT: χ^2=763.9, df= 3, p<0.0001) and was significantly elevated in summer 2010 compared to other months (data not shown), but average prevalence remained <1 % (Table S1.2) with no strong seasonal patterns. PorGA, PorTRM, and GastPRD did not vary significantly over time when compared to the null model (LRT: PorGA χ^2=91.5, df= 3, p=0.542, PorTRM χ^2=226.7, df= 3, p=0.222, GastPRD χ^2=16.2, df= 3, p=0.544).

Overall, we found only minimal seasonal fluctuation in average mean daily (24.59°C to 26.40°C) and maximum daily (25.00°C to 26.76°C) temperature (Fig. 1.2), and no correlation between PorTLS prevalence and temperature and (GLM: mean daily temperature $\beta \pm$ s.e. 0.77 ± 0.55, z_{13}=1.4, p=0.1619; maximum daily temperature $\beta \pm$ s.e. 0.22 ± 0.30, z_{13}=0.72, p=0.472).

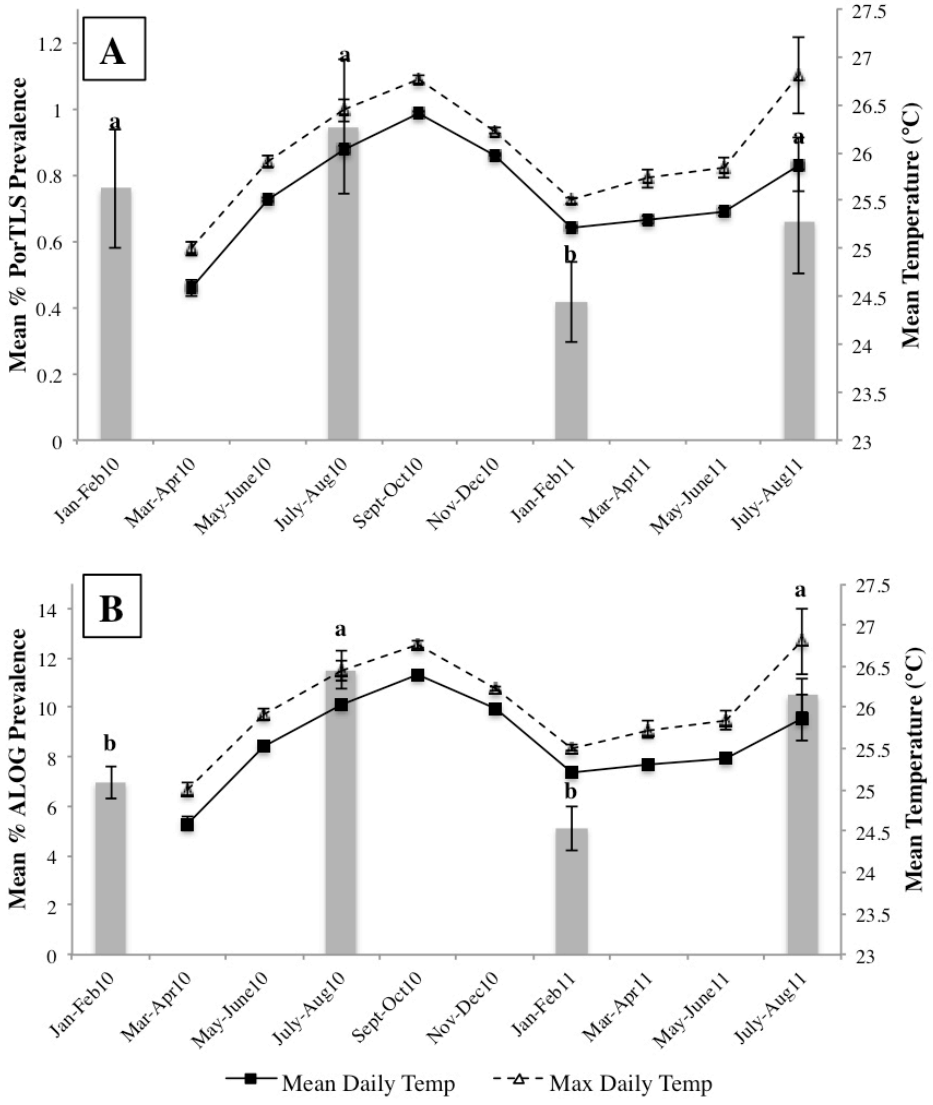

Figure 1.2. (A) *Porites* tissue loss syndrome (PorTLS) prevalence (gray bars) (mean ± SE, n= 9 sites/survey month), bi-monthly mean ± SE daily temperature (solid line) and mean ± SE maximum daily temperature (dashed line) across all shallow sites. (B) Algal Overgrowth (ALOG) (gray bars), bi-monthly mean ± SE daily temperature (solid line) and mean ± SE maximum daily temperature (dashed line) across all shallow sites. Letters indicate significant differences between survey months for each condition (post hoc HSD tests $p<0.5$).

Spatial Patterns in Coral Disease and Biological Interactions

We observed considerable spatial variation in the most common conditions. PorGA, PorTRM, and PorTLS prevalence was best predicted by the interaction of site and depth, which explained 58.2 to 91.9% of the variance in prevalence (Table 1.1). At the site level (Fig. 1.3A), PorGA prevalence was higher in the shallow zones at Mauna Lani and Ka‘ūpūlehu, but higher in the deep zones at Kaloko-Honōkohau and Ho‘okena. PorTRM prevalence was elevated in shallow zones at Mauna Lani, Kaloko-Honōkohau and Kailua (Fig. 1.3B), but higher in the deep zone at Ho’okena. PorTLS prevalence, was highest prevalence at Puakō, Keauhou and Hōnaunau deep zones and Ka‘ūpūlehu shallow zone (Fig. 1.3C). Overall, prevalence of the three most common diseases was highly spatially variable and dependent on disease type and unique site by depth interactions.

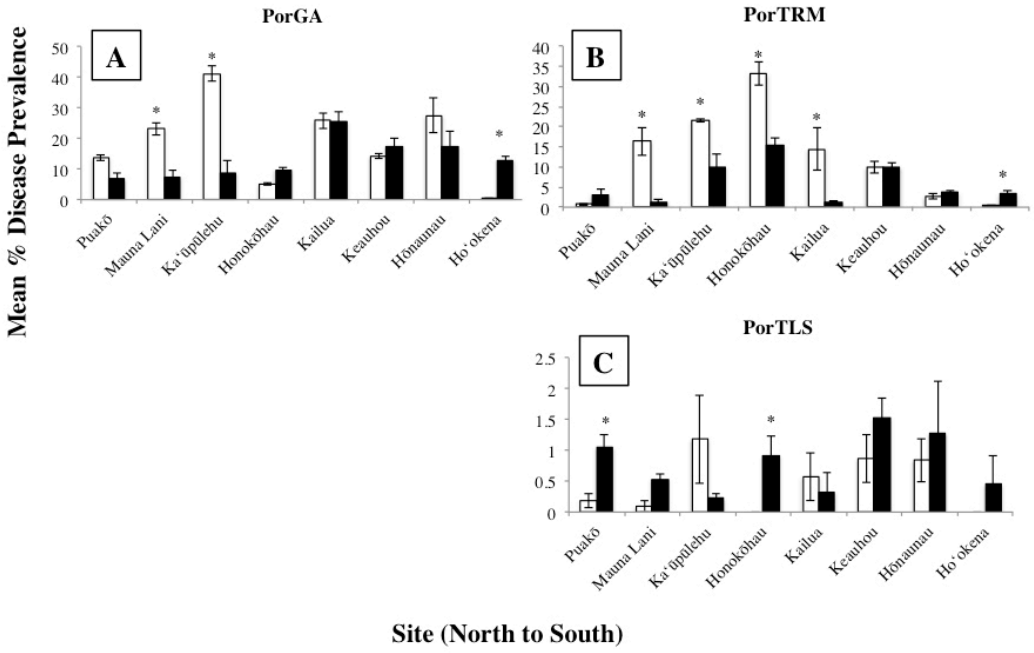

Figure 1.3. Percent disease prevalence during Winter 2011 (mean ± SE, n= 4 transects/site x 8 sites/depth): (A) *Porites* growth anomalies (PorGA) across shallow and deep sites; (B) *Porites* trematodiasis (PorTRM) across shallow and deep sites; (C) *Porites* tissue loss syndrome (PorTLS) across shallow and deep sites. Results do not include Ke`ei. Asterisks indicate significant difference between shallow and deep habitats after Bonferoni corrections ($\alpha = 0.006$).

The primary contributor to ALOG and coral tissue mortality was red filamentous turf algae (Fig. S1.1J). There were no cases of invasive algae observed during this study. The primary gastropod corallivores were *Drupella cornus* (Fig. S1.1K) and *Coralliophila violacea*. The interaction of site and depth best explained the unique spatial patterns in ALOG and GastPRD prevalence (Table 1.1). ALOG was especially high at Hōnaunau (19.02 ± 2.53%) and Puakō (15.2 ± 0.72%) (Fig. 1.4A). GastPRD prevalence was low at most sites (0.45 to 3.89%), but was as high as 8.30% in the deep zone at Hōnaunau (Fig. 1.4B).

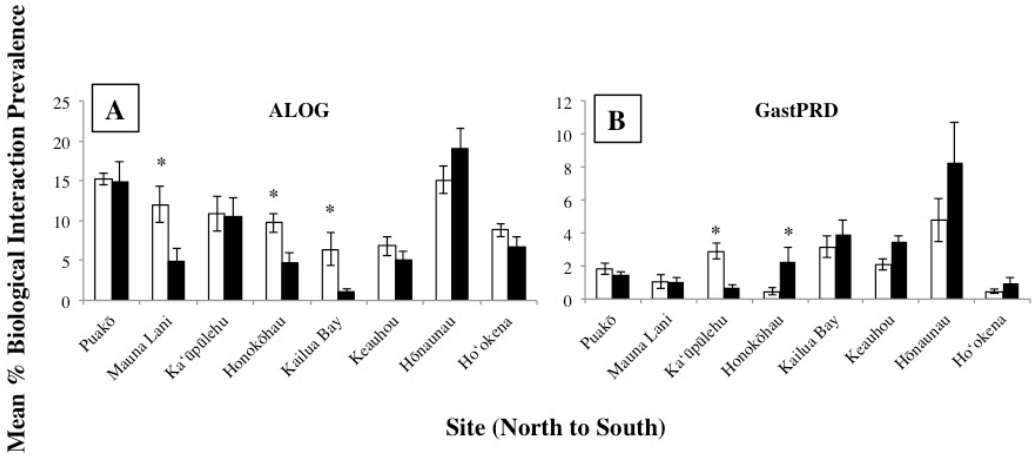

Figure 1.4. Percent biological interaction prevalence during Winter 2011 (mean ± SE, n= 4 transects/site x 8 sites/depth): (A) Prevalence of all colonies with algal overgrowth across shallow and deep sites; (B) Prevalence of all colonies with signs of gastropod predation across shallow and deep sites; n= 4 transects/site x 8 sites/depth (excluding Ke`ei). Asterisks indicate significant difference between shallow and deep habitats after Bonferoni corrections ($\alpha = 0.006$).

Table 1.1. Results of model selection for predicting spatial patterns in PorGA, PorTRM, PorTLS, ALOG and GastPRD prevalence (binomial GLMs). Fixed effects = site and depth. Includes the K, log likelihood (LL), % of deviance explained by the fitted model compared to the null model, corrected Akaike's Information Criteria (AICc), and corrected delta AIC (ΔAIC). Best fit models (<10 ΔAIC) are indicated in bold.

Model	% Deviance	df	qAICc	ΔqAICc
PorGA				
Site x Depth	**88.87**	**16**	**155.99**	**0.00**
Site + Depth	57.47	9	275.53	110.40
Site	50.92	8	301.36	135.40
Depth	0.66	2	503.05	334.20
PorTRM				
Site x Depth	**91.96**	**16**	**148.99**	**0.00**
Site + Depth	81.83	9	192.33	34.20
Site	70.85	8	252.45	93.50
Depth	2.85	2	625.31	463.40
PorTLS				
Site x Depth	**58.22**	**16**	**167.88**	**0.00**
Site + Depth	30.18	9	190.30	13.30
Site	23.49	2	196.98	18.70
Depth	12.34	8	199.46	19.10
ALOG				
Site + Depth	**53.39**	**9**	**167.3**	**0.00**
Site x Depth	**67.75**	**16**	**159.18**	**1.00**
Site	**47.55**	**8**	**174.29**	**6.20**
Depth	5.33	2	222.32	56.30
GastPRD				
Site x Depth	**75.01**	**16**	**209.62**	**0.00**
Site + Depth	**59.59**	**9**	**226.77**	**8.00**
Site	**58.13**	**2**	**227.71**	**8.10**
Depth	4.48	8	324.05	101.50

Overall, severity of the most common diseases mirror the spatial (site) patterns observed in prevalence. Severity of PorGA (range = 1–160 lesions/colony) and PorTRM (range = 1–50 lesions/colony) varied significantly between sites in shallow zones (LRT: PorGA χ^2 = 1139.8, df=8, p<0.0001; PorTRM: χ^2 = 1125.4, df=8, p<0.0001). Similar to prevalence, PorGA severity was highest at Ka'ūpūlehu, Kailua Bay, and Hōnaunau Bay (Fig. S1.2A), but was highest at sites near Kailua-Kona and decreasing north and south for PorTRM (Fig. S1.2B). PorTLS severity (range = 1-5 lesions/colony) did not vary significantly among sites (LRT: PorTLS: χ^2 = 8.30, df=8, p=0.1405).

Long-term Trends in Coral Cover

Overall, percent coral cover along the coast did not change significantly between 2003 and 2011 (Table 1.2, HPD interval: -1.30, 3.42). However, six of the eight deep sites declined by 2.19% to 12.01%, with significant coral decline at Mauna Lani and Ka'ūpūlehu between 2003 and 2011 (Table 1.2). Two sites increased in % coral cover between these years, from 4.06% to 4.92% with significant increases at Ho'okena (Table 2, HPD interval: -6.79, -0.28).

Table 1.2. Long-term % coral cover and change in coral cover between 2003 and 2011 in deep habitats (WHAP sites) by site and overall. HPD intervals that do not overlap 0 indicate significant changes in coral cover. Note Hōnaunau is not included due to insufficient within site replication.

Site	2003	2007	2011	2011-2003 % Cover	HPD intervals
Puakō	46.22	47.83	34.21	-12.01	-0.899, 7.940
Mauna Lani	38.12	31.21	28.43	**-9.69 ***	**2.728, 8.296**
Ka‘ūpūlehu	38.29	31.15	27.05	**-11.24 ***	**0.138, 11.749**
Honokōhau	44.26	48.55	48.32	4.06	-7.974, 2.444
Kailua	52.28	61.86	46.55	-5.73	-5.546, 3.037
Keauhou	30.19	31.1	28	-2.19	-6.608, 7.670
Ke‘ei	28.94	28.67	26.7	-2.24	-5.687, 7.539
Ho‘okena	34.02	39.62	38.94	**4.92 ***	**-6.791, -0.276**
Overall	39.04	40.00	34.78	-4.26	-1.30, 3.42

DISCUSSION

Comparison of WHI to MHI Patterns in Disease Prevalence

A striking result of this study is that disease prevalence is considerably higher along the *Porites*-dominated reefs of WHI than previously reported for the MHI and other Pacific regions. Unlike the Great Barrier Reef (Willis et al. 2004; Sato et al. 2009; Haapkyla et al. 2010), Indonesia (Haapkyla et al. 2009) and other Central Pacific regions (Work and Aeby 2011) experiencing outbreaks of acute coral tissue loss diseases (e.g., black-band disease and white syndrome), WHI corals are primarily affected by chronic and sub-acute diseases. PorGA and PorTRM were the most widespread/common and prevalent diseases, while PorTLS had low prevalence, but was widespread across 56% of all transects, which is similar to other regions of the MHI (Williams et al. 2010a; Aeby et al. 2011b). PorGA prevalence along WHI was 25 times greater than average PorGA prevalence across the MHI (Table 1.3, Aeby et al. 2011b). PorTRM was also highly variable and eight times greater than the average levels for the MHI, but was one-fold lower than the Northwestern Hawaiian Islands (Aeby et al. 2011b). PorTLS prevalence along WHI was very low, but still six times greater than average PorTLS prevalence across the MHI and 1.2 times lower than the Northwestern Hawaiian Islands (Table S1.3). These pronounced regional differences are also consistent with other Archipelago-wide assessments when prevalence of each disease is calculated for all colonies rather than by genus (Vargas-Ángel and Wheeler 2009).

While WHI's anomalously high disease prevalence is likely driven by a

combination of ecological and environmental factors unique to each disease's etiology, regional differences in host demographics may provide one explanation for these patterns. Coral abundance, specifically % coral cover, has been positively correlated with disease in Hawai'i (Williams et al. 2010a; Aeby et al. 2011b) and other Indo-Pacific reefs (Bruno et al. 2007; Myers and Raymundo 2009; Aeby et al. 2011a), and was on average 2.98 to 140.33 times higher in WHI than % *Porites* cover previously reported for the MHI, including Hawai'i Island (Aeby et al. 2011b). Colony size is also strongly positively correlated with PorGA and PorTLS prevalence (Chapter 2) and 2.13 to 5.0 times higher along WHI than previously reported for the MHI (Vargas-Angel unpub. data). Coral demography may also partially explain the absence of *Montipora* white syndrome in this study. On O'ahu, *Montipora* white syndrome is highest above 10% coral cover (Aeby et al. 2010), but *Montipora* % cover did not exceed 5.63% along WHI (Couch unpub. data), suggesting that coral abundance is not conducive for disease manifestation.

Seasonal Patterns in Coral Health and Temperature

On many Indo-Pacific reefs, thermal stress promotes disease outbreaks of acute tissue loss diseases (Boyett et al. 2007; Bruno et al. 2007; Sato et al. 2009). While these diseases are predicted to be especially sensitive to thermal stress due to elevated pathogen virulence and/or compromised immune function of the host (Harvell et al. 2007), PorTLS prevalence was only marginally elevated in summer months. Moreover, PorTLS temporal dynamics were not correlated with seasonal fluctuations in mean or maximum daily temperature. The highly patchy nature of PorTLS and

insufficient temporal replication makes it difficult to draw a conclusive link between PorTLS and seasonal fluctuation in WHI. The lack of strong seasonal effects are, however, consistent with patterns within the Hawaiian Archipelago (Aeby et al. 2011b) and may be due to Hawai‘i’s unique geography (Aeby et al. 2011b). Due to its higher latitude, exposure to deep oceanic waters and regular flushing from high wave energy, the MHI have been protected from severe thermal stress observed in regions such as the GBR (summer high = 32°C) (Sato et al. 2009). Additionally, WHI’s nearshore coastal water temperatures are influenced by submarine groundwater discharge, which bathes WHI reefs with cooler brackish water (Street et al. 2008). In Kāne‘ohe Bay, O‘ahu, PorTLS and *Montipora* white syndrome prevalence peaked when temperature exceeded 27°C (Williams et al. 2010a), suggesting that thermal stress in our study (daily max = 27°C) was not high enough to enhance disease establishment. The MHI have also historically escaped most of the major global bleaching events (Burke et al. 2011), including the severe 2010 event that resulted in severe bleaching. However, bleaching prevalence along WHI remained very low (0.55 ± 0.12%) throughout this study. While disease and bleaching did not vary much seasonally, ALOG increased from 1.7 to 2-fold from winter to summer months. Summer macroalgal blooms have also been observed on other reefs of the MHI and are hypothesized to be the result of increased water temperatures, nutrients, and UV irradiation during summer months (Smith et al. 2005). While Hawai‘i has been somewhat protected from extreme thermal stress associated with climate change, Hawaiian corals have a lower temperature threshold than corals at lower latitudes (Jokiel and Coles 1990). With global temperatures predicted to exceed the bleaching

threshold of 1°C summer maxima by 2100 (Hoegh-Guldberg 1999; IPCC 2007), it is increasingly important to monitor coral disease on subtropical reefs.

Spatial Patterns in Disease and Biological Interactions

We observed high spatial heterogeneity in coral health along WHI. The disease severity also varied significantly between sites and generally mirrored the site x depth patterns in prevalence. These unique spatial patterns are likely the result of each disease's etiology, as well as several environmental and ecological factors.

While PorGA prevalence in the MHI is generally higher in shallow zones (Domart-Coulon et al. 2006; Stimson 2010; Williams et al. 2010a; Aeby et al. 2011b), prevalence along WHI was only elevated in the shallows relative to deep in 3 of the 8 regions, suggesting that specific site-level factors are driving prevalence. Despite several decades of research, the etiology and transmissibility of GAs are still unclear (Peters et al. 1986; Gateno et al. 2003; Kaczmarsky and Richardson 2007). Elevated GA prevalence has been hypothesized to be linked to damage to UV-absorbing compounds (Coles and Seapy 1998). Although PorGA prevalence has been positively correlated with frequency of UV radiation anomalies (Aeby et al. 2011b), experimental UV irradiation did not result in increased rates of GA formation (Stimson 2010) and does not explain the variable depth-effects along WHI. PorGA prevalence has also been linked with local stressors, and was positively correlated with human population density (Aeby et al. 2011a), nutrient and chlorophyll *a* concentration (Kaczmarsky and Richardson 2010; Guilherme Becker et al. 2013), proximity to submarine groundwater plumes and boat ramps (Walsh et al. 2013).

These environmental factors, together with the role of host abundance likely explain why the relationship between PorGA and depth is not consistent.

PorTRM along WHI was elevated in shallow zones in 4 of the 8 regions. PorTRM is caused by the digenetic trematode, *Podocotyloides stenometra* (Aeby 1998) and disease prevalence is generally determined by the distribution of the parasite and hosts. The *P. stenometra* life cycle consists of a first intermediate molluscan host yet to be identified, *Porites* as a second intermediate host, and corallivorous butterflyfishes (Chaetodontidae) as the final host that transmits the parasite by feeding on infected polyps (Aeby 1998). While depth may not be a strong predictor of PorTRM, research along WHI and O'ahu suggests that PorTRM prevalence is highest at intermediate coral abundance (Aeby 2007; Williams et al. 2010a) and positively related to butterflyfish density (Williams et al. 2010a), suggesting that density-dependent transmission of the trematode *P. stenometra* is necessary for persistence of this disease. Butterflyfish density in deep zones was also 0-2.77 times higher than other MHI (Walsh unpub. data, Williams et al. 2010), possibly partially accounting for the interisland variation in PorTRM.

PorTLS was generally elevated in deep zones, but still highly variable spatially. PorTLS etiology is largely unknown and unlike white syndrome, which has been associated with helminthes, ciliates (Work et al. 2012), and bacterial agents (Sussman et al. 2008; Ushijima et al. 2012), no visible microorganisms have been identified within PorTLS lesions (Work unpub. data, Sudek et al. 2012). Given PorTLS's low prevalence, it is difficult to identify meaningful predictors of prevalence patterns. However, prevalence is weakly and positively correlated with % coral cover

(Aeby et al. 2011b) and colony size (Chapter 2). PorTLS prevalence has been positively correlated with gastropod and COTS predation (Chapter 2), indicating that predation may indirectly affect coral health by providing open wounds for pathogenic microorganisms to infect colonies, spreading causative agents, or causing physiological stress thus exacerbating disease prevalence.

In addition to disease, WHI corals were highly affected by other biological interactions. ALOG and GastPRD were the primary contributors to coral mortality (Couch pers. obs.), with low COTS predation (0.14 ± 0.03%). The MHI have experienced widespread coral cover loss following blooms of both native and invasive algal species since the 1950s (Martinez et al. 2012). However, in this study the primary contributors to coral mortality were native red turf algae, morphologically similar to *Corallophila huysmansii* and *Anotrichium tenue* (Fig. 1.2J). These Pan-Pacific algae are commonly associated with tissue mortality (Jompa and McCook 2003; Willis et al. 2004; Myers and Raymundo 2009) and are hypothesized to excrete allelotoxic compounds used to overgrow coral tissue (Jompa and McCook 2003). Our results highlight that while invasive algal blooms typically the most concerning in Hawai‘i due the speed and scale at which they alter communities, the role of native algal species in coral health should not be underestimated.

Our study is the first to highlight spatial variation of gastropod predation in Hawai‘i. There are no reported cases of *Drupella* outbreaks in Hawai‘i, but this corallivore is found throughout the Hawaiian Archipelago (Aeby and Vargas-Ángel pers. comm.) and is the most common gastropod corallivore throughout the Indo-

Pacific (Turner 1994). Along WHI, *Drupella* primarily consumed *Porites, Pocillopora*, and *Montipora*. While we did not measure gastropod density during this study, drupellids typically prefer the highly complex zones found in branching corals, which offer more shelter from predation and waves (Schoepf et al. 2010; Al-Horani et al. 2011), thus potentially explaining higher prevalence in *P. compressa*–rich habitat in deep reefs. Another hypothesis is that drupellids preferentially feed on *P. compressa*. Given *Drupella*'s broad geographic range and their potential to cause significant coral mortality, future studies should investigate *Drupella* demographics and their roles in Hawaiian reef ecosystems.

Long-term Trends in Coral Cover

On a coast-wide scale, mean percent coral cover did not change significantly between 2003 and 2011, but did decline significantly at several sites. These spatial patterns are consistent with coral community dynamics across the state, with significant changes in coral cover at the site and island level during the last 14 years (K. Rodgers pers. comm). At the site level, we detected a decline in percent coral cover at 6 of the 8 WHAP sites, which was most pronounced on reefs north of Kaloko-Honōkohau. Coral communities are, however, exposed to a variety of natural disturbances, which renders them naturally dynamic systems affecting community structure (Brown 1997; Connell 1997; Nystrom et al. 2000). Despite these natural fluctuations, three WHI sites (Puakō, Mauna Lani and Ka‘ūpūlehu) experienced coral cover loss close to or above the proposed 10% threshold that can be attributed to natural cycles (Jokiel et al. 2004), suggesting that other disturbances are affecting

long-term reef health. While significant coral cover decline has occurred in the Kohala District as a result of sedimentation (Walsh et al. 2013), coral cover loss does not appear to be restricted to sediment-impacted areas and may be linked to a number of local stressors discussed below. Despite these decreases in coral cover, Hawai‘i Island still has the highest number of sites with increasing coral cover in the state (K. Rodgers, pers. comm.), especially in the younger reefs of south Kona (this study, Walsh et al. 2013)

Regions of Concern for Coral Reef Management

Despite WHI's reputation as one of the most intact sections of reef in the Hawaiian Archipelago, our study highlights common patterns of impaired coral health and coral decline at several regions. Puakō and Mauna Lani, connected by the same reef system, have experienced 12.01% and 9.69% coral cover loss, respectively (Table 1.2). In a metanalysis of 40 years of biological and human use data in Puakō, Minton et al. (2012) also documented a 48% decline in coral cover and substantial declines in fish biomass, abundance, and diversity. During the last 60 years, Puakō has experienced extensive residential development, as well as improved access for tourists and fishing activities (reviewed by Minton et al. 2012). The residential and resort communities on the adjacent coast rely on several sewage treatment methods that vary in their efficacy to remediate eutrophication (reviewed by Minton et al. 2012), possibly explaining the unusually high $\delta^{15}N$ values (Dailer et al. 2013). At the colony level, this dramatic decline in coral cover may be partially attributed to the high

ALOG (second and third highest along the coast) as well as diseases PorGAs and PorTLS.

Another location of concern is the shallow zone within Ka‘ūpūlehu (Kahuwai Bay), as it has the highest PorGA prevalence (41.08%) and severity, elevated PorTLS, and 12% of all colonies were partially overgrown by algae. These conditions may also explain the high level of partial colony mortality observed within the Bay in previous studies (Stender et al. 1998). This reef is situated within an embayment whose watershed has undergone extensive resort development during the last 25 years, yet it is still unclear whether these activities have affected reef condition. Ka‘ūpūlehu’s deep habitat also experienced an 11.24% loss in coral cover between 2003 and 2011, which was primarily attributed to negligible recovery following strong winter storms in 2004. This site was also affected by a COTS outbreak of 59 individuals 200 m^{-2} in September 2012, predominately affecting *Porites* and *Montipora* colonies (Walsh et al. 2013).

Reef condition is also concerning in Hōnaunau Bay. Although coral cover appeared unchanged between 2008 (42.96%) and 2011 (42.26%) (Walsh unpublished data), 22.31% of all poritids had GAs, and perhaps more concerning was that this region had the highest level of ALOG (17.07%) and GastPRD (6.52%). In 2008, blooms of *Leptolyngbya crosbyana* were reported in the bay and was associated with widespread *P. compressa* mortality (Smith et al. 2008). While *L. crosbyana* density peaked during summer months, it was never fully eradicated during the winter. Small-scale agriculture, poor sewage treatment and an especially high level of tourism for

snorkeling, recreational diving and boating primarily affect the Hōnaunau watershed and adjacent coastal waters.

One of the common characteristics of all four regions is regular algal blooms, especially during the summer months, which are exacerbated due to the restricted water flow, particularly within the Ka‘ūpūlehu and Hōnaunau embayments (pers. obs.). Moreover, many of these regions also have shoreline access, which exposes them to significant public use. While disease levels in Puakō, Mauna Lani, Ka‘ūpūlehu and Hōnaunau are concerning, the synergistic effects of reduced top-down and unregulated bottom-up stressors, restricted water flow, and elevated terrestrial input render all of WHI particularly vulnerable to reef decline.

In conclusion, Pacific coral disease has become a major threat to reefs especially when acting synergistically with other global and local-scale stressors. One of the challenges facing coral reef managers is identifying reefs at risk and minimizing local stressors. While some regions of the MHI reefs have experienced degradation associated with anthropogenic disturbances, WHI has some of the most actively growing reefs in the state. Our study highlights that ongoing coral cover loss, especially in the Kohala District, and high disease prevalence may affect long-term WHI reef condition. The chronic diseases observed in this study generally do not result in rapid colony mortality, but can impair coral growth (Aeby 1991; Stimson 2010) and reproduction (Domart-Coulon et al. 2006; Work et al. 2008b), thus affecting long-term coral population demographics. The high prevalence and considerable spatial variation of disease and other biological interactions not only allowed us to target sites for future reef management (Puakō, Mauna Lani, Ka‘ūpūlehu and

Hōnaunau), but also highlights the importance of considering processes driving reef health and importance of incorporating other biological interactions into reef monitoring programs. Although we did not observe strong seasonal changes in disease, given the projected increase in global sea surface temperatures and the subsequent bleaching and disease outbreaks, future studies should continue to assess the seasonality of disease. This study advances our understanding of coral disease ecology and supports reef resilience planning by identifying vulnerable areas that would benefit most from targeted conservation and management efforts.

ACKNOWLEDGEMENTS

Special thanks to K. Gaab, N. Rozet, L. Kramer, G. Key, R. Martin, B. Carmen, K. Osada-D'Avella and Kona Diving Company for field support. We also thank G. Aeby, E. Weil, L. Raymundo, and M. Takabayashi for helpful feedback on project development. We are grateful to D. Ruiz Moreno, and B. Miner for assistance with statistical analyses. This study was generously supported by The Kohala Center, The NOAA Coral Reef Conservation Grant Program (grant # NA09NMF4630121 to C.D. Harvell & NA09NOS4260100 to Hawai‘i DAR), NSF Graduate Research Fellowship awarded to C. Couch and Cornell University. Thanks to C.D. Harvell, E. Peters, M. Mouchka, A. Tracy, C. Burge, I. Hewson, and J. Thaler for manuscript review.

REFERENCES

Aeby G (1991) Behavioral and ecological relationships of a parasite and its hosts within a coral reef system. Pacific Science 45:263-269

Aeby G, Williams GJ, Franklin EC, Haapkyla J, Harvell CD, Neale S, Page CA, Raymundo LJ, Vargas-Angel B, Willis BL, Work TM, Davy SK (2011a) Growth anomalies on the coral genera *Acropora* and *Porites* are strongly associated with host density and human population size across the Indo-Pacific PLoS ONE 6:e16887

Aeby GS (1998) A digenean metacercaria from the reef coral, *Porites compressa*, experimentally identified as *Podocotyloides stenometra*. Journal of Parasitology 84:1259-1261

Aeby GS (2007) Spatial and temporal patterns of infection of *Porites* trematodiasis on the reefs of Kaneohe Bay, Oahu, Hawaii. Bulletin of Marine Science 80:209-218

Aeby GS, Ross M, Williams GJ, Lewis TD, T.M. W (2010) Disease dynamics of *Montipora* white syndrome within Kaneohe Bay, Oahu, Hawaii: distribution, seasonality, virulence, and transmissibility. Diseases of Aquatic Organisms 91:1-8

Aeby GS, Williams GJ, Franklin EC, Kenyon J, Cox EF, Coles S, Work TM (2011b) Patterns of coral disease across the Hawaiian Archipelago: relating disease to environment. PLoS ONE 6:e20370

Al-Horani FA, Hamdi M, Al Rouson SA (2011) Prey selection and feeding rates of *Drupella cornus* (Gastropoda: Muricidae) on corals from the Jordanian Coast

of the Gulf of Aqaba, Red Sea. Jordan Journal of Biological Sciences 4:191-198

Aronson RB, Precht WF (2001) White-band disease and the changing face of Caribbean coral reefs. Hydrobiologia 460:25-38

Baayen RH, Davidson DJ, Bates DM (2008) Mixed-effects modeling with crossed random effects for subjects and items. Journal of Memory and Language 59:390-412

Battista TA, Costa BM, Anderson SM (2007) Shallow-Water Benthic Habitats of the Main Eight Hawaiian Islands (DVD). In: NOAA Technical Memorandum NOS NCCOS 61 BB (ed), Silver Spring, MD

Birkeland C (1997) Life and death of coral reefs. Chapman & Hall, New York

Bolker BM, Brooks ME, Clark CJ, Geange SW, Poulsen JR, Stevens MHH, White JSS (2009) Generalized linear mixed models: a practical guide for ecology and evolution. Trends in Ecology & Evolution 24:127-135

Boyett HV, Bourne DG, Willis BL (2007) Elevated temperature and light enhance progression and spread of black band disease on staghorn corals of the Great Barrier Reef. Marine Biology 151:1711-1720

Brown BE (1997) Disturbances to reefs in recent times. In: Birkeland C (ed) Life and death of coral reefs. Chapman & Hall, New York, pp 354-379

Bruno JF, Selig ER, Casey KS, Page CA, Willis BL, Harvell CD, Sweatman H, Melendy AM (2007) Thermal stress and coral cover as drivers of coral disease outbreaks. PLoS Biology 5:1220-1227

Burke LM, Reytar K, Spalding M, Perry A (2011) Reefs at risk revisited. World

Resources Institute Washington, DC

Burnham KP, Anderson DR (2002) Model selection and multi-model inference: a practical information-theoretic approach. Springer-Verlag, New York

Burns JHR, Rozet NK, Takabayashi M (2011) Morphology, severity, and distribution of growth anomalies in the coral, *Montipora capitata*, at Wai'opae, Hawai'i. Coral Reefs 30:819-826

Coles SL, Seapy DG (1998) Ultra-violet absorbing compounds and tumorous growths on acroporid corals from Bandar Khayran, Gulf of Oman, Indian Ocean. Coral Reefs 17:195-198

Connell JH (1997) Disturbance and recovery of coral assemblages. Coral Reefs 16:S101-S113

De'ath G, Fabricius KE, Sweatman H, Puotinen M (2012) The 27–year decline of coral cover on the Great Barrier Reef and its causes. Proceedings of the National Academy of Sciences 109:17995-17999

Domart-Coulon IJ, Traylor-Knowles N, Peters E, Elbert D, Downs CA, Price K, Stubbs J, McLaughlin S, Cox E, Aeby G, Brown PR, Ostrander GK (2006) Comprehensive characterization of skeletal tissue growth anomalies of the finger coral Porites compressa. Coral Reefs 25:531-543

Done TJ (1992) Phase shifts in coral reef communities and their ecological significance. In: Jaccarini V, Martens E (eds) The Ecology of Mangrove and Related Ecosystems. Springer, pp 121-132

Franklin EC, Jokiel PL, Donahue MJ (2013) Predictive modeling of coral distribution and abundance in the Hawaiian Islands. Marine Ecology Progress Series

481:121-132

Gateno D, Leon A, Barki Y, Cortes J, Rinkevich B (2003) Skeletal tumor formations in the massive coral *Pavona clavus*. Marine Ecology Progress Series 258:97-108

Guilherme Becker C, Dalziel BD, Kersch-Becker MF, Park MG, Mouchka M (2013) Indirect Effects of Human Development Along the Coast on Coral Health. Biotropica:401-407

Haapkylä J, Melbourne-Thomas J, Flavell M, Willis BL (2010) Spatiotemporal patterns of coral disease prevalence on Heron Island, Great Barrier Reef, Australia. Coral Reefs 29:1035-1045

Haapkylä J, Unsworth RKF, Seymour AS, Melbourne-Thomas J, Flavell M, Willis BL, Smith DJ (2009) Spatio-temporal coral disease dynamics in the Wakatobi Marine National Park, South-East Sulawesi, Indonesia. Diseases of Aquatic Organisms 87:105-115

Harvell CD, Jordán-Dahlgren E, Merkel S, Rosenberg E, Raymundo L, Smith GW, Weil E, Willis BL (2007) Coral disease, environmental drivers and the balance between coral and microbial associates. Oceanography 20:58-81

Hoegh-Guldberg O (1999) Climate change, coral bleaching and the future of the world's coral reefs. Marine and Freshwater Research 50:839-866

Hughes TP (1994) Catastrophes, phase shifts, and large scale degradation of a Caribbean coral reef. Science 265:1547-1551

Hunter CL, Evans CW (1995) Coral reefs in Kaneohe Bay, Hawaii: two centuries of western influence and two decades of data. Bulletin of Marine Science 57:501-

515

IPCC (2007) Climate Change 2007: The Physical Basis. Contribution of Working Group I to the Fourth Assessment Report of the Intergovernmental Panel on Climate Change, IPCC Geneva

Jokiel P, Coles S (1990) Response of Hawaiian and other Indo-Pacific reef corals to elevated temperature. Coral Reefs 8:155-162

Jokiel PL, Brown EK, Friedlander A, Rodgers K, Smith WR (2004) Hawai'i coral reef assessment and monitoring program: spatial patterns and temporal dynamics in reef coral communities. Pacific Science 58:159-174

Jompa J, McCook LJ (2003) Coral-algal competition: macroalgae with different properties have different effects on corals. Marine Ecology Progress Series 258:87-95

Kaczmarsky L, Richardson LL (2007) Transmission of growth anomalies between Indo-Pacific *Porites* corals. Journal of Invertebrate Pathology 94:218-221

Kaczmarsky L, Richardson LL (2010) Do elevated nutrients and organic carbon on Philippine reefs increase the prevalence of coral disease? Coral Reefs 30:253-257

Kim K, Harvell CD (2004) The rise and fall of a six-year coral-fungal epizootic. The American Naturalist 164:S52-S63

Kittinger JN, Pandolfi JM, Blodgett JH, Hunt TL, Jiang H, Maly K, McClenachan LE, Schultz JK, Wilcox BA (2011) Historical reconstruction reveals recovery in Hawaiian coral reefs. PLoS ONE 6:e25460

Kohler KE, Gill SM (2006) Coral Point Count with Excel extensions (CPCe): A

Visual Basic program for the determination of coral and substrate coverage using random point count methodology. Computers & Geosciences 32:1259-1269

Martinez JA, Smith CM, Richmond RH (2012) Invasive algal mats degrade coral reef physical habitat quality. Estuarine Coastal and Shelf Science 99:42-49

Minton D, Conklin E, Weiant P, Wiggins C (2012) 40 Years of Decline on Puako's Coral Reefs: A review of Historical and Current Data (1970-2010), The Nature Conservancy, Honolulu, pp140

Myers RL, Raymundo LJ (2009) Coral disease in Micronesian reefs: a link between disease prevalence and host abundance. Diseases of Aquatic Organisms 87:97-104

Nicolet K, Hoogenboom M, Gardiner N, Pratchett M, Willis B (2013) The corallivorous invertebrate *Drupella* aids in transmission of brown band disease on the Great Barrier Reef. Coral Reefs: 32:585–595

Nugues M, Bak R (2009) Brown-band syndrome on feeding scars of the crown-of-thorn starfish *Acanthaster planci*. Coral Reefs 28:507-510

Nystrom M, Folke C, Moberg F (2000) Coral reef disturbance and resilience in a human-dominated environment. Trends in Ecology & Evolution 15:413-417

Patterson KL, Porter JW, Ritchie KE, Polson SW, Mueller E, Peters EC, Santavy DL, Smith GW (2002) The etiology of white pox, a lethal disease of the Caribbean elkhorn coral, *Acropora palmata*. Proceedings of the National Academy of Sciences of the United States of America 99:8725-8730

Peters EC, Halas JC, McCarty HB (1986) Calicoblastic neoplasms in *Acropora*

palmata, with a review of reports on anomalies of growth and form in corals. Journal of the National Cancer Institute 76:895-912

Pinheiro JC, Bates DM (2000) Mixed-Effects Models in S and S-Plus. Springer, New York, NY

Ruiz-Moreno D, Willis BL, Page AC, Weil E, Croquer A, Vargas-Angel B, Jordan-Garza AG, Jordan-Dahlgren E, Raymundo L, Harvell CD (2012) Global coral disease prevalence associated with sea temperature anomalies and local factors. Dis Aquat Organ 100:249-261

Sato Y, Bourne DG, Willis BL (2009) Dynamics of seasonal outbreaks of black band disease in an assemblage of *Montipora* species at Pelorus Island (Great Barrier Reef, Australia). Proceedings of the Royal Society B-Biological Sciences 276:2795-2803

Schoepf V, Herler J, Zuschin M (2010) Microhabitat use and prey selection of the coral-feeding snail *Drupella cornus* in the northern Red Sea. Hydrobiologia 641:45-57

Smith JE, Runcie JW, Smith CM (2005) Characterization of a large-scale ephemeral bloom of the green alga *Cladophora sericea* on the coral reefs of West Maui, Hawai'i. Marine Ecology Progress Series 302:77-91

Smith JE, Shaw M, Edwards RA, Obura D, Pantos O, Sala E, Sandrin SA, Smirga SS, Hatay M, Rohwer FL (2006) Indirect effects of algae on coral: algae-mediated, microbe-induced coral mortality. Ecology Letters 9:835-845

Smith JE, Kuwabara J, Coney J, Flanagan K, Beets J, Brown D, Stanton F, Takabayashi M, Duplessis S, Griesemer B (2008) An unusual cyanobacterial

bloom in Hawaii. Coral Reefs 27:851-851

Stimson J (2010) Ecological characterization of coral growth anomalies on *Porites compressa* in Hawai`i. Coral Reefs 30:133-142

Street JH, Knee KL, Grossman EE, Paytan A (2008) Submarine groundwater discharge and nutrient addition to the coastal zone and coral reefs of leeward Hawai'i. Marine Chemistry 109:355-376

Sudek M, Work T, Aeby G, Davy S (2012) Histological observations in the Hawaiian reef coral, *Porites compressa*, affected by *Porites* bleaching with tissue loss. Journal of Invertebrate Pathology:121-125

Sussman M, Willis BL, Victor S, Bourne DG (2008) Coral pathogens identified for white syndrome (WS) epizootics in the Indo-Pacific. PLoS ONE 3:e2393

Takabayashi M, Gregg TM, Farah E, Burns J, Teves K, Cody NH (2008) The prevalence of skeletal growth anomaly and other afflictions in scleractinian corals in Waiopae, Hawaii. Proceedings of the 11th International Coral Reef Symposium:820-824

Tissot BN, Walsh WJ, Hallacher LE (2004) Evaluating effectiveness of a marine protected area network in West Hawai'i to increase productivity of an aquarium fishery. Pacific Science 58:175-188

Turner S (1994) Spatial variability in the abundance of the corallivorous gastropod *Drupella cornus*. Coral Reefs 13:41-48

US Census Bureau (2007) County Population Facts Hawaii Population Estimate: 2007

Ushijima B, Smith A, Aeby GS, Callahan SM (2012) *Vibrio owensii* induces the tissue loss disease *Montipora* white syndrome in the Hawaiian reef coral Montipora

capitata. PLoS ONE 7:e46717

Vargas-Angel B (2009) Coral health and disease assessment in the US Pacific Remote Island Areas. Bulletin of Marine Science 84:211-227

Vargas-Ángel B, Wheeler B (2009) Coral health and disease assessment in the US Pacific Territories and Affiliated States. Proceedings of 11th Int. Coral Reef Symp, Ft Lauderdale:175-179

Walsh WJ, Cotton S, Barnett C, Couch CS, Preskitt L, Tissot B, Osada-D'Avella K (2013) Long-term monitoring of coral reefs of the Main Hawaiian Islands. Final report 2009 NOAA Coral Reef Conservation Report; NA06NOS4260113 97

Williams GJ, Aeby GS, Cowie ROM, Davy SK (2010a) Predictive modeling of coral disease distribution within a reef system. PLoS ONE 5:e9264

Williams GJ, Work TM, Aeby GS, Knapp IS, Davy SK (2010b) Gross and microscopic morphology of lesions in Cnidaria from Palmyra Atoll, Central Pacific. Journal of Invertebrate Pathology 106:165-173

Willis BL, Page CA, Dinsdale EA (2004) Coral Disease on the Great Barrier Reef. In: Rosenberg E, Loya Y (eds) Coral Health and Disease. Springer-Verlag, Berlin, pp 69-104

Work T, Aeby G, Stanton F, Fenner D (2008a) Overgrowth of fungi (endolithic hypermycosis) associated with multifocal to diffuse distinct amorphous dark discoloration of corals in the Indo-Pacific. Coral Reefs 27:663-663

Work TM, Aeby GS (2011) Pathology of tissue loss (white syndrome) in Acropora sp corals from the Central Pacific. Journal of Invertebrate Pathology 107:127-131

Work TM, Aeby GS, Coles SL (2008b) Distribution and morphology of growth anomalies in *Acropora* from the Indo-Pacific. Diseases of Aquatic Organisms 78:255-264

Work TM, Russell R, Aeby GS (2012) Tissue loss (white syndrome) in the coral *Montipora capitata* is a dynamic disease with multiple host responses and potential causes. Proceedings of the Royal Society B: Biological Sciences 279:4334-4341

CHAPTER 2

WHAT CAN LOW DIVERSITY CORAL REEFS TELL US ABOUT THE ROLE OF POPULATION AND COMMUNITY-LEVEL PROCESSES IN DISEASE DYNAMICS?

ABSTRACT

The spatial extent of disease in communities is determined by an integrated series of population- and community-level processes. However, our understanding of the ecological processes mediating disease is largely based on terrestrial systems, with less focus on how these processes influence marine diseases. Here we investigate the effects of host demographics, coral species richness, predation and co-occurrence of the three most common diseases affecting the scleractinian coral *Porites* (growth anomalies (PorGAs), trematodiasis (PorTRM), and tissue loss syndrome (PorTLS)) on the Island of Hawai‘i. *Porites* disease prevalence was strongly driven by host demographics; PorGA and PorTLS were best-predicted in general linear models by a positive relationship with colony size and PorTRM driven by intermediate coral and butterflyfish abundance. We found weak evidence for a negative effect of coral diversity on PorTLS prevalence, likely due to an increase in other coral taxa with increasing species richness. PorTLS was also positively related to predation pressure (the proportion of colonies with predation scars), indicating that species interactions such as predation may indirectly facilitate disease. We found evidence that colonies were commonly affected by more than one disease (co-occurrence) and may affect disease dynamics. For example, PorTRM severity (number of lesions per colony) was significantly higher in colonies with PorGAs than without. With the increasing threat of disease, our study highlights the importance of considering multiple components of host demography as well as interrelated population and community-level factors when assessing disease risk.

INTRODUCTION

Disease outbreaks in terrestrial and marine environments present an increasing threat to biodiversity, ecosystem function, and organismal health (Daszak et al. 2000; Kilpatrick et al. 2010; Burge et al. 2013b). The extent to which communities are affected by diseases is determined by an integrated series of population- and community-level processes (Mitchell et al. 2002, Johnson et al. 2013, Collinge and Ray 2006). Disease is defined as "any impairment that interferes with or modifies the performance of normal function" and may be the result of biotic agents such as pathogenic microorganisms (e.g. viruses, bacteria, fungi and protozoans) and/or abiotic agents such as environmental disturbances (e.g. altered nutrition, temperature or exposure to toxicants) (Wobeser 1981). However, our understanding of the ecological processes mediating disease is largely based on infectious diseases in humans, livestock and agrosystems (Anderson et al. 1992; Mitchell et al. 2002; Pautasso et al. 2005; Keeling and Rohani 2011), with less focus on diseases affecting natural systems, particularly in the marine environment (Harvell et al. 2004). With the emergence of novel pathogenic microorganisms (Daszak et al. 2000; Woolhouse 2002) and disease outbreaks in previously unaffected regions (reviewed by Patz et al. 2008; Fisher et al. 2009; Burge et al. 2013b), it is imperative that we understand the complex population- and community-level processes driving disease in natural systems.

Dynamics of biotic diseases are ultimately mediated by the conflict between the host's immunocompetence and the pathogenic microorganism's ability to infect and spread between hosts (e.g. Anderson and May 1979). At the population scale,

within-host factors include the host's demographic structure. One of the theoretical predictions of disease ecology is that disease outbreaks occur after the host population density reaches a certain threshold necessary for infectious agents to encounter hosts, establish within them, and transmit between individuals (Anderson and May 1979; Burdon and Chilvers 1982; Anderson et al. 1986; Antonovics et al. 1995; Arneberg et al. 1998; Holt et al. 2003). In addition to abundance, host age and size can also influence disease susceptibility through several proposed mechanisms. Infection intensity may change with age or size as a function of altered age/size-related immunity (Anderson and Gordon 1982; Hudson and Dobson 1995; Dube et al. 2002). Older/larger hosts may also accumulate more of these pathogens due to repeated parasite exposure and/or represent larger targets for these pathogens to encounter (reviewed by Lafferty and Harvell in press). To date, studies on the role of host age and size in disease risk has been focused on vertebrate hosts (Anderson and Gordon 1982; Anderson and May 1985; Ferguson et al. 1999; Raffel et al. 2009; Raffel et al. 2011). The relative importance of these population processes also determines the variation in species-level susceptibility and ultimately community-level processes.

At the community-level, community composition and species interactions can also alter disease dynamics. Community composition directly affects disease patterns and spread as a result of variation in host species' ability to harbor and transmit pathogenic microorganisms (host competency). This concept provides the foundation for the diversity-disease hypothesis (Elton 1958). One mechanism by which diversity influences disease is the "dilution effect," which predicts that disease risk for

individuals will decrease with increasing host diversity. While this "dilution effect" has been detected in a variety of vertebrate (Ostfeld and Keesing 2000; Schmidt and Ostfeld 2001; Ezenwa et al. 2006; Keesing et al. 2006; Johnson et al. 2013) and plant systems (Haas et al. 2011, Mitchell et al. 2002, Knopps et al. 1999), the underlying mechanisms are highly dependent on pathogen specificity and abundance of the most competent hosts. Species-poor assemblages dominated by competent hosts can facilitate pathogen transmission (Johnson et al. 2013). In plant systems, the dilution effect is often solely driven by host abundance rather than pathogen transmission, whereby disease increases with increased density of competent hosts in species-poor systems (Mitchell et al. 2002). In light of declining biodiversity and increasing frequency of disease outbreaks, an increasing number of studies have tested the diversity-disease hypothesis, yet few have considered multiple levels of host demography alongside community composition.

In addition to host community composition, species interactions, such as predator-prey interactions, may also influence disease risk. Predators can exert top-down pressure on prey populations and thus reduce epidemic risk by reducing prey density or removing susceptible hosts (Lafferty 2004; Ostfeld and Holt 2004; Duffy et al. 2005). In modular organisms such as plants and corals, predators often do not kill the entire host and therefore influence infection dynamics by indirectly spreading pathogenic microorganisms (Costa 1976; Sussman et al. 2003; Sutherland et al. 2011; Nicolet et al. 2013). Herbivores/predators can also facilitate disease by wounding tissue, causing physiological stress, increasing susceptibility and providing an entry

site for opportunistic pathogens (Aeby and Santavy 2006; Page and Willis 2008; Nicolet et al. 2013).

Multiple diseases or pathogenic microorganisms often affect hosts simultaneously, which can influence within-host disease susceptibility, as well as population-level susceptibility and transmissibility (Abu-Raddad et al. 2006; Jolles et al. 2008; Telfer et al. 2010; Johnson and Hoverman 2012). For example, infection by one pathogenic microorganism can stimulate or suppress the host immune response to infection by another one (Graham et al. 2005; Graham et al. 2007; Ezenwa et al. 2010), or they can interact to modify each other's transmissibility and virulence (Back et al. 2002; Thomas et al. 2003; Wintermantel et al. 2008). In the absence of known pathogenic microorganisms, the co-occurrence (or co-morbidity) of diseases can often affect disease susceptibility such as in humans co-affected by rheumatoid arthritis and a cardiovascular disease (Turesson et al. 2008). This, in turn, can alter the geographic extent and spatial patterns of each disease (Abu-Raddad et al. 2006). While theoretical and empirical studies have addressed the underlying mechanisms of coinfection or co-occurrence of diseases, relatively few have investigated its role in disease risk in natural systems (but see Jolles et al. 2008; Telfer et al. 2010), especially in the marine environment.

Coral reefs provide an excellent opportunity to test the relative importance of these four prevailing hypotheses prevailing (host demography, community composition, species interactions, and disease co-occurrence) in disease dynamics in natural systems. Coral communities are affected by a variety of infectious and

noninfectious diseases (Sutherland et al. 2004), some of which are increasing spatially and temporally (Willis et al. 2004; Harvell et al. 2007; Ruiz-Moreno et al. 2012). As modular organisms, many corals have indeterminate growth and complex demography. Colony age/size, for example, may affect host abundance through space limitation and be especially important in disease patterns even though they are often ignored in favor of more easily measured demographic variables such as coral cover. While the diversity-disease hypothesis has not been widely tested (but see Ward et al. 2006; Aeby et al. 2010a), community composition is also likely important due to the host-specificity of many diseases, such as trematodiasis that only affects *Porites* spp. (Aeby 1998), or have a broad host range, such as black-band disease that affects 28 coral genera (Sutherland et al. 2004). Coral disease is also regulated by corallivorous predators. For example, the gastropod *Drupella* serves as the wounding agent and vector for the protozoan pathogen *Philaster guamensis*, which causes brown-band disease in acroporid corals (Nicolet et al. 2013). Finally, as long-lived colonial organisms, corals can be affected by multiple diseases simultaneously (Burge et al. 2013a), but to date, the co-occurrence of diseases has not been quantitatively assessed in coral communities.

The Hawaiian Islands is an ideal study system for investigating the role of complex population- and community-level processes in disease due to its low species diversity, and high level of genus-specific disease susceptibility, particularly in the dominant reef-builder, *Porites* (Aeby et al. 2011b). Using Hawaiian coral communities, we present one of the few studies to address the cumulative and interactive effects of host demographics, community structure, and predation in coral

disease dynamics. We use empirical data and generalized linear models to test the following hypotheses: (1) Disease prevalence is driven by interrelated host demographic variables and differential species-level susceptibility and increases with coral abundance and size. (2) Disease prevalence is dependent on community structure and decreases with increasing species diversity (*dilution effect*) due to genus-specific competency of coral hosts. (3) Disease prevalence is correlated with the proportion of corallivore scars (*Drupella* sp. and *Acanthaster planci*) and increases with predation pressure. (4) Disease prevalence and severity is affected by the co-occurrence of diseases and is expected to increase in ephemeral diseases when co-affected by chronic diseases.

METHODS

Study System:

Hawaiian corals are affected by twelve diseases ranging from chronic to acute and several of which are caused by known pathogenic microorganisms (Aeby et al. 2011b). While outbreaks of *Montipora* white syndrome have caused dramatic localized coral mortality (Aeby et al. 2010b), growth anomalies (PorGAs), trematodiasis (PorTRM), and tissue loss syndrome (PorTLS) on the dominant reef-building genus *Porites*, are the most widespread and prevalent diseases (Aeby et al. 2011b; Couch et al. in review). GA is a chronic disease that manifests as protuberant masses of the coral skeleton and can impair colony growth (Stimson 2010) and reproduction (Domart-Coulon et al. 2006; Work et al. 2008), as well as cause partial or complete colony mortality (Burns et al. 2011; Yasuda et al. 2011). GA etiology is still

unknown and there is conflicting evidence on GA transmissibility (Peters et al. 1986; Gateno et al. 2003; Kaczmarsky and Richardson 2007), but fungi (McClanahan et al. 2009), and genetic mutation (Work et al. 2008; Irikawa et al. 2011) have been proposed. PorTRM is one of the best-characterized diseases in Hawai‘i, which manifests as ephemeral pink nodules of coral tissue, caused by the digenetic trematode, *Podocotyloides stenometra* (Aeby 1998), and can reduce coral growth (Aeby 1991). The complex *P. stenometra* life cycle consists of a first intermediate molluscan host, which is yet to be identified, *Porites* as a second intermediate host, and the corallivorous butterflyfish (Chaetodontidae) as the final host that transmits the metacercariae by feeding on infected polyps (Aeby 1998). PorTLS is a subacute disease that comprises a broad range of lesions that progressively kill coral tissue, but whose etiology and transmissibility are still unknown.

Field Surveys:

Surveys were conducted at nine regions along the leeward coast of Hawai‘i Island, also known as West Hawai‘i, described in Couch et al. (in review). At each region, a shallow site was established by haphazardly choosing four coordinates within a 5,000 m^2 area between 3–6m of depth. At each coordinate, a 10-m transect was extended at a haphazard bearing parallel to shore and marked with GPS coordinates to relocate in future seasons. A deep site was also monitored at each region by surveying the first 10 m of the four WHAP permanent transects (10–15m depth) (Tissot et al. 2004).

Coral health surveys were conducted on each 10 x 2-m belt transect (80 m^2)

along which all *Porites* colonies were counted and identified to species. Each *Porites* colony was also inspected for signs of disease, but only the three most common diseases (PorGA, PorTRM, and PorTLS) are reported in this study (Fig. S2.1). Predation scars from three common invertebrate predators (*Drupella cornus, Coralliophila violacea*, and crown-of-thorns starfish (COTS)) were also recorded. Shallow and deep sites were surveyed between January–March 2011. Disease severity was estimated at all shallow sites by counting the number of lesions per colony. Due to time and weather restrictions during the winter months, population size structure was assessed in July 2010 at shallow sites only by measuring maximum diameter of each colony along one axis. Colonies were binned into the following size classes: 0-5 cm, 6-10 cm, 11-20 cm, 21-40 cm, 41-80 cm, 81-160 cm and > 160 cm. Average colony diameter estimates for deep sites were used from surveys conducted along the same transects in 2010 (Walsh et al. 2013).

Percent coral cover was estimated using photoquadrats at 1-m intervals along each transect with a Canon G9 digital camera elevated 0.75 m above the substrate during Winter 2010. Images were processed in CPCe v. 3.5 using 30 randomly generated points. Butterflyfish abundance was quantified by four observers along four 25m x 4m ($100m^2$) belt transects at each of the WHAP (deep) sites along the same coral health transects (Tissot et al. 2004). Surveys were conducted once in May, July, September, and November 2010.

Statistical Analyses:

Data were analyzed using generalized linear models (GLM) in R version

2.13.1. Disease prevalence was calculated for PorGA, PorTRM and PorTLS as the number of *Porites* colonies with lesions/total number of *Porites* colonies surveyed. Invertebrate predation prevalence was calculated as (number of colonies with *Drupella* + *Coralliophila* + COTS feeding scars)/total number of *Porites* colonies surveyed. Average butterflyfish density was calculated for deep sites only by averaging fish abundance for the four quarters by transect and site. Only primarily obligate corallivorous butterflyfish species were included in these analyses (*C. lunulatus, C. ornatissimus, C. multicinctus, C. unimaculatus, C. lineolatus*).

To test the role of *Porites* demography and determine which demographic variable(s) best predict disease prevalence, we conducted separate quasibinomial (due to overdispersion of mean and variance parameters) generalized linear models (GLMs) with logit link (Pinheiro and Bates 2000) for PorGA, PorTRM, and PorTLS. *Porites* percent cover, *Porites* colony density, and average maximum colony diameter were treated as fixed effects. After visually assessing the relationship between each disease and each demographic variable to check for non-linearity, colony density and *Porites* percent cover were fit with a quadratic term (colony density + colony density^2, *Porites* percent cover + *Porites* percent cover^2) for PorTRM prevalence. These quadratic models were compared to the linear model for each predictor to confirm non-linearity using Likelihood ratio tests (LRT) with chi-square test statistics and Akaike information criterion (AIC) (Burnham and Anderson 2002). An information theoretic approach, comparing quasi-corrected Akaike's information criterion (qAICc) and ΔqAICc values were used to determine which fixed effects best fit prevalence for each

disease (Burnham and Anderson 2002). The goodness of fit for each model was determined by calculating the percent deviance ((Null deviance - residual deviance)/null deviance * 100) (Mellin et al. 2010). To determine the relationship between PorTRM prevalence and butterflyfish abundance in deep zones, we used GLMs (quasibinomial errors with logit link) to fit the linear and quadratic effects of butterflyfish abundance, as well as the null model. We compared these models using sequential model selection with likelihood ratio test (LRTs) and chi square tests to find the best-fit model. Butterflyfish abundance was not included in the *Porites* demography model selection mentioned above, because we were unable to conduct fish assessments in shallow zones.

To determine which population (demography) or community-level predictors best explained disease prevalence, we conducted separate quasibinomial GLMs with the following fixed effects: average maximum colony diameter, *Porites* density, proportion of *Porites* colonies with invertebrate predation scars, and species richness. Percent cover of nonporitid coral genera was also considered as a fixed effect as an extension of the dilution effect, but was not included in the full model due to a positive correlation with species richness. We used a similar information theoretic approach for model selection described above. The goodness of fit for each model was determined by calculating the percent deviance.

Co-occurrence was defined as the presence of at least one lesion of more than one disease. Due to the ephemeral nature of PorTRM and PorTLS compared to PorGA, we predicted that PorTRM and PorTLS are more sensitive, e.g., more likely to

co-occur when a PorGA lesion is present on the colony. To determine whether PorTRM and PorTLS severity (number of lesions/colony) varied as a function of co-occurrence with another disease in shallow zones, we used GLMs (Poisson distribution and log link) with co-occurrence status (+ or -) as a fixed effect. We used generalized linear regressions to examine whether size drives the severity as a function of co-occurrence status. We used generalized linear regressions to examine whether prevalence of each disease was determined by prevalence of the other diseases.

RESULTS:

Effects of Host Population Demographics

Our results suggest that prevalence of the three most common poritid diseases are influenced by different demographic processes. While no single-factor model best predicted PorGA, prevalence was positively correlated and best predicted by a combination of host size (average maximum colony diameter) and abundance (percent *Porites* cover) (Table 2.1). Colony density was included in the top model, but was negatively correlated with PorGA prevalence and only increased percent deviance by 8.07%, suggesting that it is not an optimal predictor. Across all shallow sites, the size-frequency distribution of *Porites* colonies without GAs was significantly different from those with GAs (χ^2= 2337.01, df=6, p<0.0001), and more right skewed, indicating that larger colonies, especially greater than 40 cm in diameter are more affected by GAs (Fig. 2.1A). PorTRM prevalence at all sites was best predicated by a modal relationship with *Porites* colony density (Table 2.1, % deviance = 22.63%) with highest prevalence at 15–20 colonies m^{-2} (data not shown). PorTRM prevalence was

best predicted by host abundance and highest at intermediate colony density and *Porites* cover (Table 2.1). While both colony density and *Porites* cover were included as single-factor best-fit models (<10 ΔqAIC), colony density alone explained 26.18% of the variation in PorTRM compared to coral cover (4.96% deviance, Table 2.1). Similar to PorGA, no single-factor model best predicted PorTLS, but prevalence was positively correlated and best predicted by a combination of host size (average maximum colony diameter) and abundance (percent *Porites* cover), together explaining 54.31% of the variance (Table 2.1). Colony density was included in the top models, but was negatively correlated with prevalence and only increased percent deviance by 8.90%, suggesting that it is not an optimal predictor. The size-frequency distribution of *Porites* colonies without PorTLS was significantly different from those with PorTLS (χ^2= 894.81, df=6, p<0.0001), with colonies greater than 160cm in diameter more affected by PorTLS (Fig. 2.1B).

Table 2.1. Results of model selection of optimal host demographic factors for predicating PorGA, PorTRM and PorTLS prevalence (quasi-binomial GLMs). Values in parentheses are the standardized beta coefficients for variables included in models. Fixed effects = Average maximum colony diameter (Size), *Porites* % cover (Cover), and *Porites* colony density (Density). Note: PorTRM prevalence was fit to quadratic *Porites* colony density (colony density + colony density^2) and *Porites* % cover (% cover + % cover^2). Includes % deviance, degrees of freedom (df), corrected quasi-Akaike's Information Criteria qAICc, corrected delta quasi-AIC (ΔqAICc). Best-fit models (<10 ΔAIC) are indicated in bold.

Model Selection	df	% Deviance	AICc	ΔAICc
PorGA				
Size (0.04) + Cover (0.02) + Density (-0.05)	**4**	**63.21**	**58.63**	**0**
Size (0.07) + Cover (0.01)	**3**	**55.14**	**64.24**	**5.2**
Cover (0.03) + Density (-0.07)	3	59.34	69.78	10.8
Size (0.05) + Density (-0.03)	3	56.71	72.34	13.3
Size (0.08)	2	51.71	75.9	16.6
Density (-0.07)	2	45.22	95.58	36.3
Cover (0.04)	2	14.06	115.56	56.2
PorTRM				
Cover (0.15) + Cover^2 (-0.001) + Density (0.15) + Density^2 (-0.005)	**5**	**26.18**	**45.74**	**0**
Density (0.15) + Density^2 (-0.005)	**3**	**25.64**	**49.13**	**2.2**
Size (0.02) + Cover (0.14) + Cover^2 (-0.001) + Density (0.17) + Density^2 (-0.005)	**6**	**26.47**	**47.62**	**2.7**
Cover (0.17) + Cover^2 (-0.002)	**3**	**4.76**	**50.77**	**3.8**
Size (0.03) + Cover (0.17) + Cover^2 (-0.002)	**4**	**8.91**	**51.02**	**4.6**
Size (-0.01) + Density (0.14) + Density^2 (-0.005)	**4**	**25.82**	**51.04**	**4.6**
Size (0.02)	2	2.97	58.65	11.3
PorTLS				
Size (0.03) + Cover (0.02) + Density (-0.04)	**4**	**63.20**	**22.63**	**0**
Cover (0.03) + Density (-0.06)	**3**	**60.00**	**21.43**	**0.5**
Size (0.07) + Cover (0.01)	**3**	**54.31**	**22.9**	**6.1**
Size (0.05) + Density (-0.03)	3	56.66	24.56	13.6
Size (0.07)	2	50.97	24.87	17.6
Density (-0.07)	2	45.62	26.15	23.6
Cover (0.04)	2	20.00	29.66	36.9

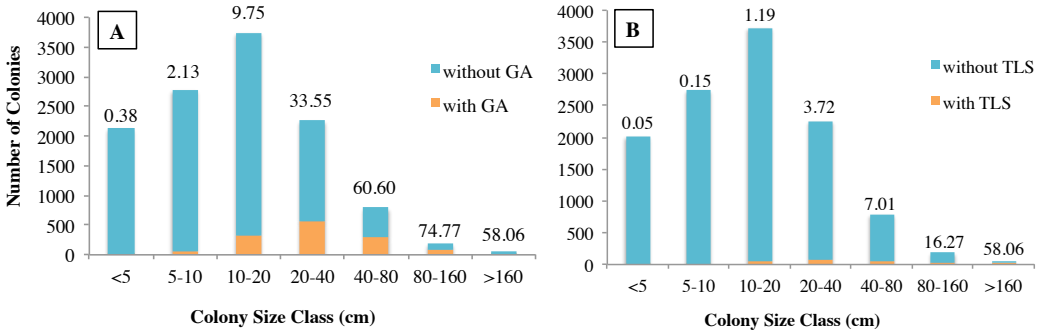

Figure 2.1. (A) Size frequency distributions of *Porites* colonies without growth anomalies (teal) and with GAs (orange). (B) Size frequency distributions of *Porites* colonies without tissue loss syndrome (teal) and with TLS (orange). Numbers indicate proportion of *Porites* colonies (%) with GA or TLS across all transects.

Although fish abundance was not measured in shallow habitats, mean abundance of obligate butterflyfish was a strong predictor of PorTRM prevalence in deep habitats, explaining 43.45% of the variance in prevalence and highest at intermediate butterflyfish abundance (6 fish/100m^{-2}) (Fig. 2.2, GLM $\beta \pm$ s.e. -0.05 $\pm$ 0.01, t=-3.109, p=0.00478).

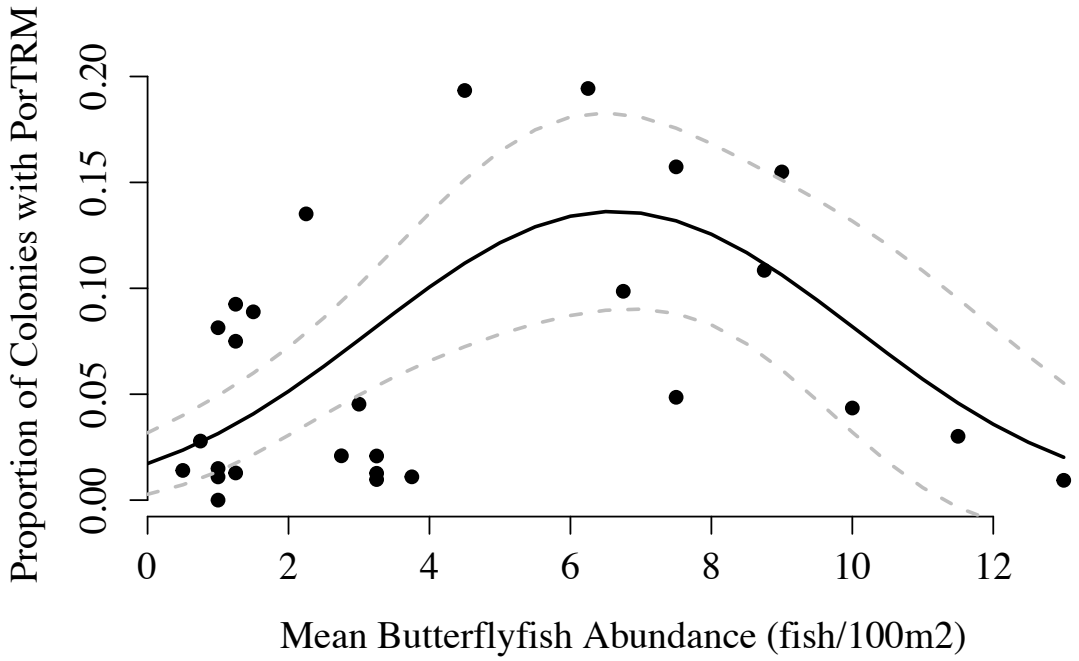

Figure 2.2. Relationship between the proportion of *Porites* colonies with TRM and mean obligate butterflyfish abundance. Solid line: quadratic logistic regression (with quasi-binomial errors). Grey dashed lines: upper and lower 95% confidence and prediction intervals.

Effects of Diversity and Predation

To test the diversity disease hypothesis (dilution effect) and role of community-level predation in the context of population demographics, we incorporated the optimal host demographic predictors into a GLM with community-level variables. Due to the strong predictive power and integrated nature of these population-level predictors in community structure and because we were interested in the effects of host demographics due to variation in species richness, we fit the demographic variable before species richness in the full models. Therefore, the effects of species richness were conditional on colony size or density. As the dominant genus, *Porites* demographics directly influence species composition and abundance of other genera. Due to the positive correlation between relative abundance (percent cover) of non-poritid species and species richness, we were unable to include it in the full models. Overall, host size and density were included as single-factor models for PorGA and PorTRM, suggesting that they remain the best predictors of these diseases (Table 2.2). Species richness was a poor predictor of PorGA and PorTRM prevalence (Table 2.2). Although species richness alone was positively correlated with PorTRM prevalence and included in the best-fit models, it only explained 3.83% of the variance (Table 2.2). Species richness was negatively correlated with PorTLS and together with colony size predicted 25.04% of the variance (Table 2.2).

The proportion of predation feeding scars was a poor predictor of PorGA and PorTRM, but was positively related to PorTLS prevalence. Colony size and the proportion of colonies with feeding scars together explained 23.72% of the variation in PorTLS, compared to the full model with 32.58%, suggesting that prevalence is driven

by multiple factors (Table 2.2).

Table 2.2. Best-fit models (<10 ΔqAIC) for predicting PorGA, PorTRM and PorTLS prevalence (quasibinomial GLMs). Values in parentheses are the standardized beta coefficients for variables included in models. Fixed effects = Average maximum colony diameter (Size), *Porites* Colony Density (Density), Proportion of *Porites* colonies with *Drupella* and COTS predation scars (Predation), and Species Richness. Note: PorTRM prevalence was fit to quadratic *Porites* colony density (colony density + colony density^2). Includes % deviance, degrees of freedom (df), corrected quasi-Akaike's Information Criteria qAICc, corrected delta quasi-AIC (ΔqAICc).

Best Fit Models	% Deviance	df	qAICc	ΔqAICc
PorGA				
Size (0.08)	51.71	2	60.65	0
Size (0.1) + Predation (-6.5)	53.12	3	61.42	1.1
Size (0.1) + Predation (-6.9) + Algal Overgrowth (-0.002)	53.25	4	63.30	3.3
Size (0.08) + Algal Overgrowth (-0.002) + Diversity (0.2)	52.11	4	64.30	4.3
Size (0.09) + Predation (-8.7) + Algal Overgrowth (-0.0) +Diversity (0.4)	54.38	5	64.31	4.8
PorTRM				
Density (0.2) + Density^2 (-0.005)	22.63	3	67.07	0
Density (0.1) + Density^2 (-0.005) + Algal Overgrowth (-0.006) + Diversity (-1.1)	28.76	5	66.88	0.7
Density (0.2) + Density^2 (-0.005) + Predation (-3.5)	22.98	4	68.85	2.2
Density (0.09) + Density^2 (-0.004), Predation (-5.8) + Algal Overgrowth (-0.006) + Diversity (-1.1)	29.47	6	68.40	2.8
Density (0.2) + Density^2 (-0.006) + Predation (-5.0) + Algal Overgrowth (-0.008)	26.53	5	69.10	2.9
PorTLS				
Size (0.03) + Predation (18.64) + Algal Overgrowth (-0.01)	28.9	4	83.88	0
Size (0.03) + Predation (19.92)	27.93	4	84.47	0.8
Size (0.02) + Predation (12.78) + Algal Overgrowth (-0.01) + Diversity (0.78)	30.39	3	84.96	1.1
Size (0.03) + Diversity (1.20)	20.78	5	84.99	1
Size (0.06)	16.58	2	87.31	3.6

Effects of Disease Co-occurrence

Due to the ephemeral nature of PorTRM and PorTLS compared to PorGA, we predicted that PorTRM and PorTLS are more sensitive to PorGA presence. PorTRM severity (number of lesions/colony) was significantly higher in colonies with PorGAs than without (Fig. 2.3, GLM, $\beta \pm$ s.e. -0.23 ± 0.0 t=-3.58, p=0.0004). While there was no significant interaction between co-occurrence status and colony size (LRT: χ^2=14.12, df= 7, p=0.828), PorTRM severity increased gradually with colony size, but was most pronounced in colonies larger than 40 cm and affected by PorGA (Fig. 2.3). PorGA severity was not, however, a strong predictor of PorTRM severity (GLM: % deviance= 3.9%, $\beta \pm$ s.e. 0.03 ± 0.01, t=3.69, p=0.0003). PorTLS severity (number of lesions/colony) did not vary significantly as a function of PorGA (GLM, $\beta \pm$ s.e. 0.31 ± 0.55, t=0.56, p=0.583) or PorTRM co-occurrence (GLM, $\beta \pm$ s.e. 0.42 ± 0.44, t=0.96, p=0.350). Overall, PorTRM and PorTLS prevalence was only weakly correlated with prevalence of other *Porites* diseases (Table 2.3).

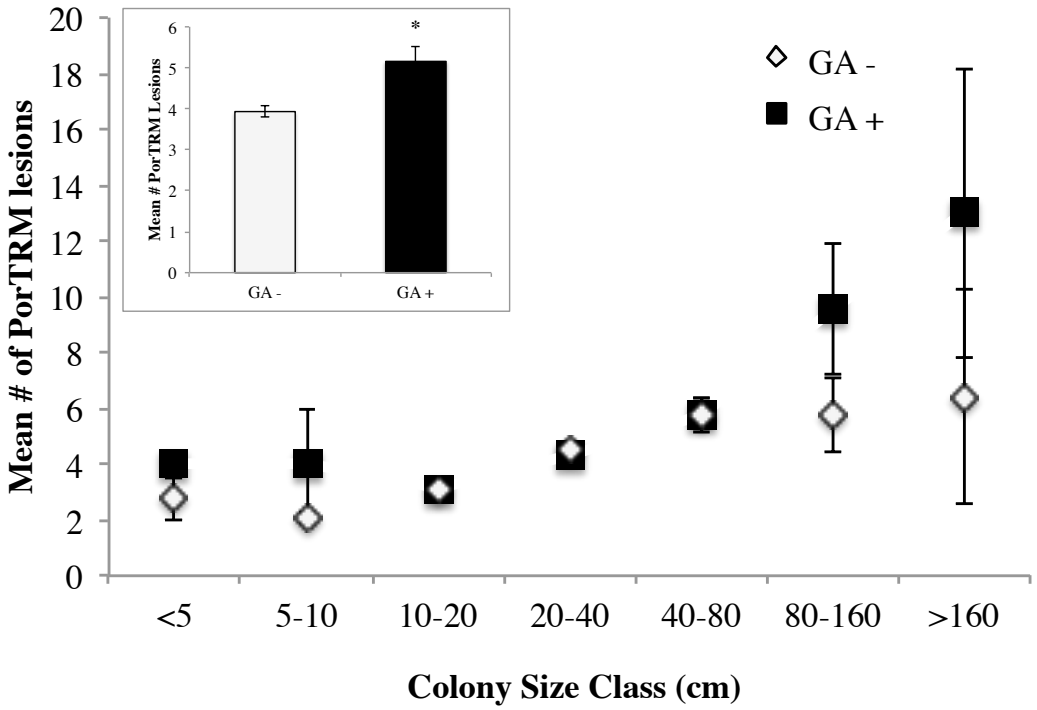

Figure 2.3. Host size-trematodiasis severity relationship for colonies with (grey diamonds) and without (black squares) growth anomalies averaged (± s.e.) for each size class and the entire population (inset map) in summer 2011 at shallow sites (n= 9 sites x 4 transects/site).

Table 2.3. Generalized linear regressions for PorTRM and PorTLS prevalence with PorGA, PorTLS and PorTRM prevalence as predictors and goodness of fit indicated as % of deviance explained by predictors.

	Coeffient (SE)	p-value	% Deviance
PorTRM			
PorGA prevalence	0.035 (0.01)	0.008	9.57
PorTLS prevalence	0.176 (0.14)	0.196	2.29
PorTLS			
PorGA prevalence	0.045 (0.01)	0.0004	18.42
PorTRM prevalence	0.022 (0.02)	0.214	2.10

DISCUSSION:

While traditional disease ecology focuses on single host-pathogen interactions, a more realistic view places host-pathogen interactions in a whole community context. Our results indicate that *Porites* disease dynamics are strongly determined by population-level processes specifically coral size and density, but unique for each disease. While disease prevalence was influenced by community-level factors such as coral diversity and corallivore predation, these factors were only important in the context of host demography. Finally, this study represents the first quantitative assessment of disease co-occurrence in corals, which was widespread, but did only mildly influenced disease dynamics.

Host abundance and size

Along WHI, host demography was the strongest driver of disease prevalence, accounting for 26.18 to 63.21 % of the variation in prevalence (Table 2.1), but was complicated by interrelated demographic factors. Average colony size together with *Porites* cover best-predicted PorGA and PorTLS prevalence, explaining 55.14 and 54.31% of the variance, respectively. PorGA and PorTLS prevalence was also highest in colonies > 40 cm in diameter. This size-specific disease pattern has been observed in small-scale case studies, where *Montipora capitata* GA severity increased three-fold in colonies > 1 m (Burns et al. 2011) and *Acropora cytherea* GA prevalence increased considerably in colonies > 2 m in diameter (Irikawa et al. 2011). Disease prevalence and severity also increased with colony size in diseases such as *Acropora* white syndrome (Roff et al. 2011) and aspergillosis in sea fan corals (Bruno et al.

2011). While the etiology of PorGA and PorTLS and mechanisms linking disease dynamics and size are unclear, based on known mechanisms in vertebrate systems, larger colonies have a longer time to come in contact with pathogens and/or are a larger target for pathogens. Larger colonies may also have reduced immune function compared to small colonies (Dube et al. 2002) and/or have accumulated more genetic mutations, which if occurring in genes regulating cell growth may lead to GA formation. Roff et al. (2011) also hypothesized that since small colonies experience faster rates of mortality (Hughes and Jackson 1980; Meesters et al. 1996), tissue loss diseases and GAs may be more persistent on larger colonies.

In most of the well-studied patho-systems, demographics are typically addressed with regards to density of susceptible and infected hosts as it relates to density- or frequency-dependent transmission. Coral cover is one of the most commonly used metrics of coral abundance, and has been positively associated with overall disease prevalence (Myers and Raymundo 2009), as well as white syndrome (Bruno et al. 2007). While percent *Porites* cover was included in many of the best-fit models, alone it only weakly predicted prevalence along WHI (Table 2.1). Roff et al. (2011) also found that coral cover was a poor predictor of the infectious disease white syndrome in acroporids, and suggested that this simple metric of host abundance is decoupled from density-dependent processes. Furthermore, unlike other regions of the Main Hawaiian Islands (Williams et al. 2010; Aeby et al. 2011b; Aeby et al. 2011a), PorGA and PorTLS prevalence along WHI was negatively correlated with colony density. These results, together with the uncorrelated nature of colony density and percent coral cover (linear regression, $R^2 = 0.0078$, $F = -1.15$, df = 39, p = 0.258),

suggests that coral colony size structure was not homogenous across all sites. Therefore, we hypothesize that colony density, along WHI, is an indirect predictor of colony size and percent coral cover may not capture small-scale processes shaping disease patterns, particularly on reefs dominated by one genus with variable size-structure.

Despite the strong role of colony size in PorGA and PorTLS, colony density was important in PorTRM prevalence. PorTRM prevalence increased with *Porites* colony density and cover (second intermediate host), peaking at 15–20 colonies m^{-2} and 50% cover, but decreased at high coral abundance. This modal pattern was also observed in obligate butterflyfish abundance (final host), which peaked at 6 fish 100 m^{-2} and explained as much as 43% of the PorTRM prevalence in deep habitats. A similar modal relationship between PorTRM and percent *Porites* cover has been observed on other Hawaiian Islands (Aeby 2007; Williams et al. 2010), suggesting that density-dependent transmission of the trematode *P. stenometra* is necessary for persistence of this disease, but only to intermediate host abundances. While it is still unclear why PorTRM prevalence decreases with high host abundance, there are several possible hypotheses. First, the relationship between PorTRM and butterflyfish density may indirectly reflect butterflyfish's preferences for habitats with intermediate coral density. This does not, however, appear to be the case, as butterflyfish density was not related to *Porites* colony density and did not show a curvelinear relationship with *Porites* percent cover. Second, the pattern may be driven by the distribution of the unknown molluscan host, which may preferentially inhibit reefs with intermediate colony density. Third, at high butterflyfish densities, parasites may be distributed

across a larger number of hosts, therefore diluting within-host parasite density.

Diversity-disease hypothesis

The relationship between host diversity and disease is inherently mediated by differential disease susceptibility, host abundance, and community composition, and therefore cannot be addressed without considering both population and community processes (e.g. Knops et al. 1999; Mitchell et al. 2002; Johnson et al. 2013). The role of species diversity in coral disease dynamics has not been well studied, but several studies have highlighted the importance of disease specificity at the genus level. For example, *Acropora* white syndrome was three times lower on the species-rich reefs of American Samoa compared to the monospecific reefs of the Northwestern Hawaiian Islands (Aeby et al. 2010a). However, Ward et al. (2006) found no relationship between prevalence of seven diseases and host diversity in Mexico, which may be attributed to the broad host range of the most common diseases. Due to high genus-level specificity, poritid disease prevalence, especially for the vector-borne diseases such as PorTRM, was predicted and indirectly related to species diversity due to an effect of non-competent hosts. However, our findings suggest that species richness was a poor predictor of PorGA and PorTRM. Species richness was, however, negatively correlated with PorTLS prevalence and explained as much as 25.04% of the variance together with colony size. This relationship, together with a positive relationship between species richness and percent cover of non-poritid hosts suggests a mild dilution effect of PorTLS by non-poritids. It is still unclear whether PorTLS is a vector-borne disease, but if this is true then it is possible that species diversity

decreases PorTLS transmission. Alternatively, as coral species richness and percent cover of non-poritids increases, *Porites* colony size decreases and so too does PorTLS prevalence. The lack of strong diversity effects for all three diseases may be to due to several factors. First, we did not detect significant variation in species richness across sites (LRT: χ^2= 2.28, df=7, p=0.9429), the spatial variation may have been too low or communities may be too dominated by *Porites* to detect a relationship with disease prevalence. Secondly, given the strong effects of colony size and density, diversity-mediated effects may have been masked by the host demographics. This scenario is often found in plant communities affected by vectored and non-vectored host-specific pathogens, where fungal disease severity decreases with species richness, but is primarily driven by host density, which decreases with increasing plant richness (Knops et al. 1999; Mitchell et al. 2002). While the mechanisms linking species diversity and disease are not well understood even in well-studied host-pathogen systems, our study and others emphasize the importance of considering multiple components of host demographics.

Indirect effects of predation

On coral reefs, invertebrate corallivores not only play an important role in structuring coral communities (reviewed by Turner 1994; Done 1999), but can also serve as a vector of pathogenic microorganisms and promote disease (Nugues and Bak 2009; Nicolet et al. 2013). While the proportion of *Porites* colonies with *Drupella* and COTS scars alone was not included in the subset of best-fit models, it was one of the best ecological predictors of PorTLS, and together with average colony size,

accounted for 23.72% of the variance in prevalence. As pathogen vectors, *Drupella* and COTS have been associated with transmission of ciliates such as *Philaster guamensis*, the causative agent of Acroporid brown band disease (Nicolet et al. 2013). While an etiological agent or agents have yet to be identified for PorTLS, lesions and necrosis have been associated with algae and helminths (Sudek et al. 2012, Work unpublished data). Therefore, invertebrate corallivores may enhance disease by wounding coral tissue, thus providing an entry site for these agents. Subacute tissue loss, such as PorTLS, can also occur in the absence of pathogens or other agents (Work and Aeby 2011, Work unpublished data). Since corallivore predation is also associated with physiological stress (Cole et al. 2012), these wounds may also be unable to heal and undergo tissue necrosis in the absence of an agent. Furthermore, Work and Aeby (2011) hypothesized that corallivore digestive enzymes that are actively secreted during feeding may promote tissue loss due to their toxic nature. In the absence of a pathogen, the role of predation may also be confounded by the ability of corals to heal tissue surrounding feeding scars. Tissue loss diseases, across coral taxa, have caused widespread mortality throughout the Pacific and given the role of corallivores in structuring coral communities and potential synergistic effects with disease. Future studies should track predation scars and lesion development through time to determine the extent to which corallivore predation facilitates disease.

Disease Co-occurrence

Disease co-occurrence and co-infection are important mediators of disease risk in a variety of terrestrial systems (Graham et al. 2005; Abu-Raddad et al. 2006; Jolles

et al. 2008; Turesson et al. 2008), but have been overlooked in most marine communities. Along WHI, 15.3 % of Porites colonies had some type of disease co-occurrence, with 2.13, 0.28, 0.17% of *Porites* colonies having PorTRM-PorGA, PorTRM-PorTLS, and PorTLS-PorTRM co-occurrences, respectively. Although disease co-occurrence is quite common in coral communities, it is less clear how the presence of one syndrome affects another. Of all the possible co-occurence scenarios, only PorTRM appeared sensitive to the presence of PorGAs, with significantly elevated severity in GA-affected colonies. It is reasonable to posit that GAs can increase susceptibility to other diseases. GAs are regions of accelerated growth and can drain a colony's energetic resources (Yamashiro et al. 2001), which depletes resources for growth and reproduction (Domart-Coulon et al. 2006; Work et al. 2008; Stimson 2010), and may also render them more susceptible to infectious or noninfectious diseases. Elevated PorTRM severity also appears to be at least partially due to increased severity in colonies above 81 cm in diameter with GAs compared to colonies only infected with PorTRM, further emphasizing the importance of colony size in disease. Interestingly, similar infection intensity-age relationships have been observed in rabbits where older animals co-infected by nematodes and poxviruses are unable to clear worm infections than those without viral infections due to modulation of the adaptive immune response (Cattadori et al. 2007). In addition to accumulated parasite density, host age and size may also have further implications for co-occurrence, whereby parasite diversity increases with age and size (reviewed by Lafferty and Harvell in press). Longitudinal studies that follow the progression of multiple diseases through time are needed to disentangle the processes operating in

disease co-occurrence scenarios. Despite the widespread nature and strong role of disease co-occurrence in disease susceptibility and host survival in other systems, our study provides the first quantitative assessment of this process on coral reefs.

In summary, while previous studies have investigated a variety of ecological factors in coral disease, our study indicates that the high spatial variation in WHI coral disease based on these data (Couch et al. in review) was determined primarily by host size and density, but was also influenced by community composition and top-down influences of corallivorous predators. We highlight the integrated nature of host demography in modular organisms and the importance of assessing size-specific disease patterns. While we did not observe strong effects of coral diversity on disease, it is possible that given the integrated nature of demography and community composition, diversity has a minimal effect on disease after accounting for host size or density in communities dominated by one taxon. Given these strong host-effects and the potential indirect effects of predation on disease, future studies should not only continue assessing the role of predation, but also consider the interactive effects of predator habitat and feeding preferences within host communities on disease. Finally, we provide the foundation for future studies of the role of disease co-occurrence in coral communities that should apply the theoretical framework developed for terrestrial communities to understand the consequences and mechanisms of disease co-occurrence in corals. While we provide unequivocal evidence of the importance of ecological processes in coral disease dynamics, a considerable amount of variance in disease is still unaccounted for. Similar to diseases such as cholera (Pascual et al. 2002) and amphibian chytridiomycosis (Bosch et al. 2007), where host-pathogen

interactions can be strongly mediated by the environment, coral diseases can be sensitive to fluctuations in temperature and water quality (e.g. Bruno et al. 2007; Kaczmarsky and Richardson 2010). Future studies should address the complex ecological factors in the context of environmental stress.

ACKNOWLEDGEMENTS

Special thanks to K. Gaab, N. Rozet, L. Kramer, G. Key, R. Martin, B. Carmen, K. Osada-D'Avella and Kona Diving Company for field support. We also thank G. Aeby, E. Weil, L. Raymundo, and M. Takabayashi for helpful feedback on project development. We are grateful to D. Ruiz Moreno, and B. Miner for assistance with statistical analyses. This study was generously supported by The Kohala Center, The NOAA Coral Reef Conservation Grant Program (grant # NA09NMF4630121 to C.D. Harvell & NA09NOS4260100 to Hawai'i DAR), NSF Graduate Research Fellowship awarded to C. Couch and Cornell University. Thanks to E. Peters, M. Mouchka, A. Tracy, C. Burge, I. Hewson, and J. Thaler for manuscript review.

REFERENCES

Abu-Raddad LJ, Patnaik P, Kublin JG (2006) Dual infection with HIV and malaria fuels the spread of both diseases in sub-Saharan Africa. Science 314:1603-1606

Aeby G (1991) Behavioral and ecological relationships of a parasite and its hosts within a coral reef system. Pacific Science 45:263-269

Aeby G, Bourne D, Wilson B, Work T (2010a) Coral diversity and the severity of disease outbreaks: A cross-regional comparison of *Acropora* white syndrome in a species-rich region (American Samoa) with a species-poor region (Northwestern Hawaiian Islands). Journal of Marine Biology 2011: doi:10.1155/2011/490198

Aeby G, Williams GJ, Franklin EC, Haapkyla J, Harvell CD, Neale S, Page CA, Raymundo LJ, Vargas-Angel B, Willis BL, Work TM, Davy SK (2011a) Growth anomalies on the coral genera *Acropora* and *Porites* are strongly associated with host density and human population size across the Indo-Pacific PLoS ONE 6:e16887

Aeby GS (1998) A digenean metacercaria from the reef coral, *Porites compressa*, experimentally identified as *Podocotyloides stenometra*. Journal of Parasitology 84:1259-1261

Aeby GS (2007) Spatial and temporal patterns of infection of *Porites* trematodiasis on the reefs of Kaneohe Bay, Oahu, Hawaii. Bulletin of Marine Science 80:209-218

Aeby GS, Santavy DL (2006) Factors affecting susceptibility of the coral *Montastraea*

faveolata to black-band disease. Marine Ecology-Progress Series 318:103-110

Aeby GS, Ross M, Williams GJ, Lewis TD, T.M. W (2010b) Disease dynamics of *Montipora* white syndrome within Kaneohe Bay, Oahu, Hawaii: distribution, seasonality, virulence, and transmissibility. Diseases of Aquatic Organisms 91:1-8

Aeby GS, Williams GJ, Franklin EC, Kenyon J, Cox EF, Coles S, Work TM (2011b) Patterns of coral disease across the Hawaiian Archipelago: relating disease to environment. PLoS ONE 6:e20370

Anderson R, May R (1985) Age-related changes in the rate of disease transmission: implications for the design of vaccination programmes. Joural of Hygeine Cambridge 94:365-436

Anderson R, May R, Joysey K, Mollison D, Conway G, Cartwell R, Thompson H, Dixon B, Anderson R, May R (1986) The invasion, persistence and spread of infectious diseases within animal and plant communities. Philosophical Transactions of the Royal Society of London. B, Biological Sciences 314:533-570

Anderson RM, May RM (1979) Population biology of infectious diseases: Part I. Nature 280:361

Anderson RM, Gordon DM (1982) Processes influencing the distribution of parasite numbers within host populations with special emphasis on parasite-induced host mortalities. Parasitology 85:373-398

Anderson RM, May RM, Anderson B (1992) Infectious diseases of humans: dynamics and control. Oxford university press, Oxford

Antonovics J, Iwasa Y, Hassell MP (1995) A generalized model of parasitoid, venereal, and vector-based transmission processes. American Naturalist 145:661-675

Arneberg P, Skorping A, Grenfell B, Read AF (1998) Host densities as determinants of abundance in parasite communities. Proceedings of the Royal Society of London. Series B: Biological Sciences 265:1283-1289

Back M, Haydock P, Jenkinson P (2002) Disease complexes involving plant parasitic nematodes and soilborne pathogens. Plant Pathology 51:683-697

Bosch J, Carrascal LM, Duran L, Walker S, Fisher MC (2007) Climate change and outbreaks of amphibian chytridiomycosis in a montane area of Central Spain; is there a link? Proceedings of the Royal Society B: Biological Sciences 274:253-260

Bruno JB, J. F., Ellner SP, Vu I, Kim K, Harvell CD (2011) Impacts of aspergillosis on sea fan coral demography: modeling a moving target. Ecological Monographs 81:123-139

Bruno JF, Selig ER, Casey KS, Page CA, Willis BL, Harvell CD, Sweatman H, Melendy AM (2007) Thermal stress and coral cover as drivers of coral disease outbreaks. PLoS Biology 5:1220-1227

Burdon J, Chilvers G (1982) Host density as a factor in plant disease ecology. Annual Review of Phytopathology 20:143-166

Burge CA, Kim CJ, Lyles JM, Harvell CD (2013a) Special issue oceans and humans health: the ecology of marine opportunists. Microbial Ecology 65:1-11

Burge CA, Eakin CM, Friedman CS, Froelich B, Hershberger PK, Hoffman EE,

Prager KC, Weil E, Willis B, Harvell CD (2013b) Climate change influences on marine infectious disease: implications for management and society. Annual Reviews in Marine Science 6: DOI: 10.1146/annurev-marine-010213-135029

Burnham KP, Anderson DR (2002) Model selection and multi-model inference: a practical information-theoretic approach. Springer-Verlag, New York

Burns JHR, Rozet NK, Takabayashi M (2011) Morphology, severity, and distribution of growth anomalies in the coral, *Montipora capitata*, at Wai'Opae, Hawai'i. Coral Reefs 30:819-826

Cattadori IM, Albert R, Boag B (2007) Variation in host susceptibility and infectiousness generated by co-infection: the myxoma–*Trichostrongylus retortaeformis* case in wild rabbits. Journal of the Royal Society Interface 4:831-840

Cole AJ, Lawton RJ, Wilson SK, Pratchett MS (2012) Consumption of tabular acroporid corals by reef fishes: a comparison with plant–herbivore interactions. Functional Ecology 26:307-316

Costa A (1976) Whitefly-transmitted plant diseases. Annual Review of Phytopathology 14:429-449

Couch CS, Garriques JD, Barnett C, Preskitt L, Cotton S, Giddens J, Walsh W (in review) Spatial and temporal patterns of coral health and disease along leeward Hawai‘i Island. Coral Reefs.

Daszak P, Cunningham AA, Hyatt AD (2000) Emerging infectious diseases of wildlife--threats to biodiversity and human health. Science 287:443-449

Domart-Coulon IJ, Traylor-Knowles N, Peters E, Elbert D, Downs CA, Price K, Stubbs J, McLaughlin S, Cox E, Aeby G, Brown PR, Ostrander GK (2006) Comprehensive characterization of skeletal tissue growth anomalies of the finger coral *Porites compressa*. Coral Reefs 25:531-543

Done TJ (1999) Coral community adaptability to environmental change at the scales of regions, reefs and reef zones. American Zoologist 39:66-79

Dube D, Kim K, Alker AP, Harvell CD (2002) Size structure and geographic variation in chemical resistance of sea fan corals *Gorgonia ventalina* to a fungal pathogen. Marine Ecology Progress Series 231:139-150

Duffy MA, Hall SR, Tessier AJ, Huebner M (2005) Selective predators and their parasitized prey: Are epidemics in zooplankton under top-down control? Limnology and Oceanography 50:412-420

Elton CS (1958) The Ecology of Invasions by Animals and Plants. Methuen & Co., London.

Ezenwa VO, Godsey MS, King RJ, Guptill SC (2006) Avian diversity and West Nile virus: testing associations between biodiversity and infectious disease risk. Proceedings of the Royal Society B: Biological Sciences 273:109-117

Ezenwa VO, Etienne RS, Luikart G, Beja-Pereira A, Jolles AE (2010) Hidden consequences of living in a wormy world: nematode-induced immune suppression facilitates tuberculosis invasion in African buffalo. The American Naturalist 176:613-624

Ferguson NM, Donnelly CA, Anderson RM (1999) Transmission dynamics and epidemiology of dengue: insights from age–stratified sero–prevalence surveys.

Philosophical Transactions of the Royal Society of London. Series B: Biological Sciences 354:757-768

Fisher MC, Garner TW, Walker SF (2009) Global emergence of *Batrachochytrium dendrobatidis* and amphibian chytridiomycosis in space, time, and host. Annual Review of Microbiology 63:291-310

Gateno D, Leon A, Barki Y, Cortes J, Rinkevich B (2003) Skeletal tumor formations in the massive coral *Pavona clavus*. Marine Ecology Progress Series 258:97-108

Graham AL, Lamb TJ, Read AF, Allen JE (2005) Malaria-filaria coinfection in mice makes malarial disease more severe unless filarial infection achieves patency. Journal of Infectious Diseases 191:410-421

Graham AL, Cattadori IM, Lloyd-Smith JO, Ferrari MJ, Bjørnstad ON (2007) Transmission consequences of coinfection: cytokines writ large? Trends in Parasitology 23:284-291

Harvell CD, Jordán-Dahlgren E, Merkel S, Rosenberg E, Raymundo L, Smith GW, Weil E, Willis BL (2007) Coral disease, environmental drivers and the balance between coral and microbial associates. Oceanography 20:58-81

Harvell CD, Aronson R, Baron N, Connell J, Dobson A, Ellner S, Gerber L, Kim K, Kuris A, McCallum H, Lafferty K, McKay B, Porter J, Pascual M, Smith G, Sutherland K, Ward J (2004) The rising tide of ocean diseases: unsolved problems and research priorities. Frontiers in Ecology and the Environment 2:375-382

Holt RD, Dobson AP, Begon M, Bowers RG, Schauber EM (2003) Parasite

establishment in host communities. Ecology Letters 6:837-842

Hudson P, Dobson A (1995) Macroparasites: observed patterns in naturally fluctuating animal populations. In: Grenfell BT, Dobson A (eds) Ecology of infectious diseases in natural populations. Cambridge University Press, Cambridge, pp 144-176

Hughes T, Jackson J (1980) Do corals lie about their age? Some demographic consequences of partial mortality, fission, and fusion. Science 209:713-715

Irikawa A, Casareto BE, Suzuki Y, Agostini S, Hidaka M, van Woesik R (2011) Growth anomalies on *Acropora cytherea* corals. Marine Pollution Bulletin 62:1702-1707

Johnson PT, Hoverman JT (2012) Parasite diversity and coinfection determine pathogen infection success and host fitness. Proceedings of the National Academy of Sciences 109:9006-9011

Johnson PT, Preston DL, Hoverman JT, Richgels KL (2013) Biodiversity decreases disease through predictable changes in host community competence. Nature 494:230-233

Jolles AE, Ezenwa VO, Etienne RS, Turner WC, Olff H (2008) Interactions between macroparasites and microparasites drive infection patterns in free-ranging African buffalo. Ecology 89:2239-2250

Kaczmarsky L, Richardson LL (2007) Transmission of growth anomalies between Indo-Pacific *Porites* corals. Journal of Invertebrate Pathology 94:218-221

Kaczmarsky L, Richardson LL (2010) Do elevated nutrients and organic carbon on Philippine reefs increase the prevalence of coral disease? Coral Reefs 30:253-

257

Keeling MJ, Rohani P (2011) Modeling infectious diseases in humans and animals. Princeton University Press

Keesing F, Holt RD, Ostfeld RS (2006) Effects of species diversity on disease risk. Ecology Letters 9:485-498

Kilpatrick AM, Briggs CJ, Daszak P (2010) The ecology and impact of chytridiomycosis: an emerging disease of amphibians. Trends in Ecology & Evolution 25:109-118

Knops JM, Tilman D, Haddad dN, Naeem S, Mitchell C, Haarstad J, Ritchie M, Howe K, Reich P, Siemann E (1999) Effects of plant species richness on invasion dynamics, disease outbreaks, insect abundances and diversity. Ecology Letters 2:286-293

Lafferty KD (2004) Fishing for lobsters indirectly increases epidemics in sea urchins. Ecological Applications 14:1566-1573

Lafferty KD, Harvell CD (in press) The Role of Infectious Diseases in Marine Communities. In: Bertness MD, Bruno JF (eds) Marine Community Ecology

McClanahan TR, Weil E, Maina J (2009) Strong relationship between coral bleaching and growth anomalies in massive *Porites*. Global Change Biology 15:1804-1816

Meesters EH, Wesseling I, Bak RP (1996) Partial mortality in three species of reef-building corals and the relation with colony morphology. Bulletin of Marine Science 58:838-852

Mellin C, Bradshaw CJA, Meekan MG, Caley MJ (2010) Environmental and spatial

predictors of species richness and abundance in coral reef fishes. Global Ecology and Biogeography 19:212-222

Mitchell CE, Tilman D, Groth JV (2002) Effects of grassland plant species diversity, abundance, and composition on foliar fungal disease. Ecology 83:1713-1726

Myers RL, Raymundo LJ (2009) Coral disease in Micronesian reefs: a link between disease prevalence and host abundance. Diseases of Aquatic Organisms 87:97-104

Nicolet K, Hoogenboom M, Gardiner N, Pratchett M, Willis B (2013) The corallivorous invertebrate *Drupella* aids in transmission of brown band disease on the Great Barrier Reef. Coral Reefs 32:585–595

Nugues M, Bak R (2009) Brown-band syndrome on feeding scars of the crown-of-thorn starfish *Acanthaster planci*. Coral Reefs 28:507-510

Ostfeld RS, Keesing F (2000) Biodiversity and disease risk: the case of Lyme disease. Conservation Biology 14:722-728

Ostfeld RS, Holt RD (2004) Are predators good for your health? Evaluating evidence for top-down regulation of zoonotic disease reservoirs. Frontiers in Ecology and the Environment 2:13-20

Page CA, Willis BL (2008) Epidemiology of skeletal eroding band on the Great Barrier Reef and the role of injury in the initiation of this widespread coral disease. Coral Reefs 27:257-272

Pascual M, Bouma MJ, Dobson AP (2002) Cholera and climate: revisiting the quantitative evidence. Microbes and Infection 4:237-245

Patz JA, Olson SH, Uejio CK, Gibbs HK (2008) Disease emergence from global

climate and land use change. Medical Clinics of North America 92:1473-1491

Pautasso M, Holdenrieder O, Stenlid J (2005) Susceptibility to fungal pathogens of forests differing in tree diversity Forest diversity and function. Springer, pp 263-289

Peters EC, Halas JC, McCarty HB (1986) Calicoblastic neoplasms in *Acropora palmata*, with a review of reports on anomalies of growth and form in corals. Journal of the National Cancer Institute 76:895-912

Pinheiro JC, Bates DM (2000) Mixed-Effects Models in S and S-Plus. Springer, New York, NY

Raffel TR, LeGros RP, Love BC, Rohr JR, Hudson PJ (2009) Parasite age-intensity relationships in red-spotted newts: does immune memory influence salamander disease dynamics? International Journal for Parasitology 39:231-241

Raffel TR, Lloyd-Smith JO, Sessions SK, Hudson PJ, Rohr JR (2011) Does the early frog catch the worm? Disentangling potential drivers of a parasite age–intensity relationship in tadpoles. Oecologia 165:1031-1042

Roff G, Kvennefors ECE, Fine M, Ortiz J, Davy JE, Hoegh-Guldberg O (2011) The ecology of ‘acroporid white syndrome', a coral disease from the southern Great Barrier Reef. PLoS ONE 6:e26829

Ruiz-Moreno D, Willis BL, Page AC, Weil E, Croquer A, Vargas-Angel B, Jordan-Garza AG, Jordan-Dahlgren E, Raymundo L, Harvell CD (2012) Global coral disease prevalence associated with sea temperature anomalies and local factors. Dis Aquat Organ 100:249-261

Schmidt KA, Ostfeld RS (2001) Biodiversity and the dilution effect in disease

ecology. Ecology 82:609-619

Stimson J (2010) Ecological characterization of coral growth anomalies on *Porites compressa* in Hawai`i. Coral Reefs 30:133-142

Sudek M, Work T, Aeby G, Davy S (2012) Histological observations in the Hawaiian reef coral, *Porites compressa*, affected by *Porites* bleaching with tissue loss. Journal of Invertebrate Pathology 111:121-125

Sussman M, Loya Y, Fine M, Rosenberg E (2003) The marine fireworm *Hermodice carunculata* is a winter reservoir and spring-summer vector for the coral-bleaching pathogen *Vibrio shiloi*. Environmental Microbiology 5:250-255

Sutherland KP, Porter JW, Torres C (2004) Disease and immunity in Caribbean and Indo-Pacific zooxanthellate corals. Marine Ecology-Progress Series 266:273-302

Sutherland KP, Shaban S, Joyner JL, Porter JW, Lipp EK (2011) Human pathogen shown to cause disease in the threatened eklhorn coral *Acropora palmata*. PLoS ONE 6(8): e23468.

Telfer S, Lambin X, Birtles R, Beldomenico P, Burthe S, Paterson S, Begon M (2010) Species interactions in a parasite community drive infection risk in a wildlife population. Science 330:243-246

Thomas MB, Watson EL, Valverde-Garcia P (2003) Mixed infections and insect–pathogen interactions. Ecology Letters 6:183-188

Tissot BN, Walsh WJ, Hallacher LE (2004) Evaluating effectiveness of a marine protected area network in West Hawai'i to increase productivity of an aquarium fishery. Pacific Science 58:175-188

Turesson C, Jacobsson LT, Matteson EL (2008) Cardiovascular co-morbidity in rheumatic diseases. Vascular health and risk management 4:605

Turner SJ (1994) The biology and population outbreaks of the corallivorous gastropod *Drupella* on Indo-Pacific reefs. Oceanography and Marine Biology, Vol 32 32:461-530

Ward J, Rypien K, Bruno J, Harvell C, Jordan-Dahlgren E, Mullen K, Rodriguez-Martinez R, Sanchez J, Smith G (2006) Coral diversity and disease in Mexico. Diseases of Aquatic Organisms 69:23-31

Williams GJ, Aeby GS, Cowie ROM, Davy SK (2010) Predictive Modeling of Coral Disease Distribution within a Reef System. PLoS ONE 5:e9264

Willis BL, Page CA, Dinsdale EA (2004) Coral Disease on the Great Barrier Reef. In: Rosenberg E, Loya Y (eds) Coral Health and Disease. Springer-Verlag, Berlin, pp 69-104

Wintermantel WM, Cortez AA, Anchieta AG, Gulati-Sakhuja A, Hladky LL (2008) Co-infection by two criniviruses alters accumulation of each virus in a host-specific manner and influences efficiency of virus transmission. Phytopathology 98:1340-1345

Wobeser GA (1981) Diseases of Wild Waterfowl. Plenum Press, New York, pp 324

Woolhouse ME (2002) Population biology of emerging and re-emerging pathogens. Trends in Microbiology 10:s3-s7

Work TM, Aeby GS (2011) Pathology of tissue loss (white syndrome) in *Acropora* sp corals from the Central Pacific. Journal of Invertebrate Pathology 107:127-131

Work TM, Aeby GS, Coles SL (2008) Distribution and morphology of growth

anomalies in *Acropora* from the Indo-Pacific. Diseases of Aquatic Organisms 78:255-264

Yamashiro H, Oku H, Onaga K, Iwasaki H, Takara H (2001) Coral tumors store reduced levels of lipids. Journal of Experimental Marine Biology and Ecology 265:171-179

Yasuda N, Nakano Y, Yamashiro H, Hidaka M (2011) Skeletal structure and progression of growth anomalies in *Porites australiensis* in Okinawa, Japan. Diseases of Aquatic Organisms 97:237

CHAPTER 3

THE ROLE OF LOCAL HYDROLOGY AND HOST DEMOGRAPHICS IN *PORITES LOBATA* GROWTH ANOMALIES

ABSTRACT:

Coral disease, often acting synergistically with other environmental stressors, is among the leading contributors to global coral reef decline. Growth anomalies (GAs) are the most widespread coral disease in the Pacific, with one of the highest reported prevalence levels along the western/leeward coast of the island of Hawai‘i (WHI). Hawai‘i’s coastal ecosystem is especially susceptible to land-based pollution due to its porous basaltic rock that exports terrestrial input directly to adjacent reefs through submarine groundwater discharge (SGD). To identify factors facilitating GA development in the dominant reef-building species *Porites lobata* (PorGA), we tested the correlation between prevalence, severity and rate of linear extension and a suite of ecological and environmental parameters at eleven sites with increasing distance from SGD plumes. Longitudinal studies of individual colonies revealed that PorGAs are progressive and increase susceptibility to partial mortality. While PorGA prevalence and severity declined significantly with distance from SGD, overall prevalence and severity were primarily driven by colony size and degree of water motion, whereby more GAs were found on reefs dominated by large colonies with low water motion. This study demonstrates that coral populations within sheltered embayments with low water circulation comprised of larger/older colonies are likely at increased risk of this chronic yet deleterious disease.

INTRODUCTION:

Disease can result from the outcome of host-pathogen interactions, but can also be the result of or mediated by extrinsic (environment) factors (Pascual et al. 2002; Koelle et al. 2005; Pascual et al. 2008; Harvell et al. 2009; Burge et al. 2013). Environmental change can alter disease dynamics from the organismal to community scale by increasing pathogenicity and/or

impairing host resistance or immunocompetence (reviewed by Harvell et al. 2002; Altizer et al. 2013; Burge et al. 2013), as well as shifting pathogen and host ranges (reviewed by Harvell et al. 2009; Lafferty 2009). When these changes do occur, the resulting increase in disease can have far reaching effects on host populations and communities. For example, increasing climate variability has been associated with the spread of infectious diseases and precipitous declines in oyster, abalone, coral, reindeer and amphibian populations (reviewed by Altizer et al. 2013). The evidence for the role of environment in disease patterns is mounting with the expanding scale of anthropogenic disturbances (Harvell et al. 2002; Pascual et al. 2002; Patz et al. 2008). The degree to which the environment affects disease dynamics is often highly dependent on intrinsic factors such as host density, host susceptibility, and pathogen virulence (Bruno et al. 2007; Doddington et al. 2013). While most studies of the intrinsic and extrinsic factors of disease have focused on terrestrial ecosystems where disease affects humans and economically important crops and livestock, an important knowledge gap in marine systems is the interaction of intrinsic and extrinsic factors in disease risk (Burge et al. 2013).

The complex interaction between environmental (extrinsic) and ecological (intrinsic) factors in disease dynamics is especially apparent in coral communities where disease has become a major threat and hosts are unable to escape environmental disturbances due to their sessile and ecotothermic nature. During the last four decades, coral disease has steadily increased both spatially and temporally, altering coral health from the physiological to ecosystem-level (reviewed by Sutherland et al. 2004; Harvell et al. 2007). Originally restricted to the Caribbean basin, the ecosystem-wide effects of disease, acting synergistically with other environmental stressors, are now threatening Pacific reefs (Willis et al. 2004; Ruiz-Moreno et al. 2012). While the underlying mechanisms are still unclear, environmental stress has been linked to several

global and local factors. For example, disease outbreaks have been associated with seasonal increases in temperature and light irradiance (Boyett et al. 2007; Sato et al. 2009), as well as climate-linked thermal stress (Bruno et al. 2007; Heron et al. 2010; Ruiz-Moreno et al. 2012). On the local scale, disease risk as also been associated with elevated nutrient concentrations (Kuta and Richardson 2002; Kaczmarsky and Richardson 2010; Williams et al. 2010), sedimentation, and low salinity accompanying seasonal rain events (Haapkylä et al. 2011). During *in situ* experimental studies, elevated nutrients exacerbated disease severity (Bruno et al. 2003; Voss and Richardson 2006), and altered coral-associated microbial dynamics (Klaus et al. 2005; Kline et al. 2006; Thurber et al. 2009). Land-based pollution may also transport novel pathogens into the marine environments, such as in the case of the human fecal bacterium *Serratia marcescens,* the causative agent of white pox disease in the Caribbean coral, *Acropora palmata* (Sutherland et al. 2010). Environmental stress associated with reduced water circulation may also exacerbate disease (Burns et al. 2011). However, the degree to which coral disease is influenced by environmental stress is also highly dependent on host population structure, such as coral abundance and colony sizes. For instance, Bruno et al. (2007) found that white syndrome on the Great Barrier Reef was only affected by temperature on reefs with high host abundance (coral cover >50%). While disease prevalence has been positively linked with coral abundance (Myers and Raymundo 2009; Aeby et al. 2010; Aeby et al. 2011b; Aeby et al. 2011a), and other demographic factors such as colony size (e.g., Loya et al. 1984; Bruno et al. 2011), no studies have examined the synergism between point source environmental stressors, water circulation, and population size structure in determining local-level disease risk.

Outbreaks of acute, rapidly spreading diseases such as white syndrome and white band disease have resulted in visible reef decline (Aronson and Precht 2001; Willis et al. 2004; Miller

et al. 2009), but regionally high prevalence of chronic diseases such as growth anomalies (GAs) also have potential long-term effects on reef condition (e.g. Work et al. 2008; Stimson 2010). Also identified in the early literature "tumors," coral GAs are areas of tissue and supporting skeleton that differ morphologically from the surrounding tissue and skeleton on a colony. They may be the result of hyperplasia or cellular proliferation accompanying injury or parasites (Domart-Coulon et al. 2006; Kaczmarsky 2009; Burns and Takabayashi 2011) or neoplasia, abnormal growth of cells that persists after the removal of a stimulus (Peters et al. 1986; Kaczmarsky 2009). GA lesion morphology is highly variable, owing to its broad host range (Sutherland et al. 2004). In addition to skeletal changes, GA formation also causes tissue-level changes, such as proliferation of epithelial cells, loss of mucocytes and nematocysts, fewer polyps and lack of endosymbiotic dinoflagellates, and degraded gametes (Sutherland et al. 2004). To facilitate sustained anomalous growth, corals translocate nutrients from surrounding tissue (Yamashiro et al. 2001). GAs can also reduce colony growth (Cheney 1975; Bak 1983; Stimson 2010), impair fecundity (Domart-Coulon et al. 2006; Work et al. 2008; Yasuda et al. 2011), and cause partial or complete mortality (Stimson 2010; Yasuda et al. 2011). "While virus-like particles (Kaczmarsky 2009) and fungi (Coles and Seapy 1998) have been associated with GAs, it is unclear whether they are primary or secondary opportunistic pathogens because they have also been found in apparently healthy tissues. Furthermore, there is conflicting evidence on GA transmissibility in experiments where healthy colonies are exposed to GA tissue or tissue homogenate (Peters et al. 1986; Gateno et al. 2003; Kaczmarsky and Richardson 2007). Alternatively, others have hypothesized that GAs are the result of genetic mutations, possibly related to the loss of UV-absorbing compounds from affected tissues (Peters et al. 1986; Work et al. 2008; Irikawa et al. 2011).

First reported in 1901 (Whitfield 1901), GAs are now one of the most widespread diseases in the Indo-Pacific (Vargas-Angel 2009; Aeby et al. 2011b; Aeby et al. 2011a), affecting 13 scleractinian genera (Sutherland et al. 2004). GA prevalence is low on the Pacific-wide scale (Aeby et al. 2011a), but can be anomalously high on the regional and local scale (Kaczmarsky 2006; Burns et al. 2011). In the Main Hawaiian Islands, *Porites,* the dominant reef-building genus, is the most susceptible to GAs (Domart-Coulon et al. 2006; Stimson 2010; Aeby et al. 2011a) and were first reported on *Porites lobata* in 1990 (Hunter 1999). *Porites* growth anomaly (PorGA- Fig. 3.1) prevalence along the leeward coast of the island of Hawai‘i (also known as West Hawai‘i, WHI) is especially high with an overall PorGA prevalence 25 higher than the Main Hawaiian Islands and over 300 times higher than American Samoa (Aeby et al. 2011a; Couch et al. in review).

In addition to its high PorGA prevalence, WHI is unique for its reef development and geohydrology, both of which render WHI reefs vulnerable to environmental disturbances. As the youngest of the Hawaiian Islands (0-0.5 Ma BP), Hawai‘i Island’s reefs developed on recent lava flows, directly adjacent to the coast and terrestrial inputs (Grigg and Maragos 1974). WHI is also highly sheltered, which has facilitated extensive reef development and makes it one of the most intact reef systems in the state (Battista et al. 2007; Franklin et al. 2013). With its young geology, Hawai‘i’s terrestrial and coastal regions are comprised of highly porous basaltic bedrock, especially along WHI. Consequently, most of WHI’s terrestrial input is delivered through submarine groundwater discharge (SGD) (Bienfang 1980; Oki 1999), with an estimated 42 known plumes delivering 260,000 m^3 of ground water per day (Johnson 2008). SGD is formed when fresh and oceanic water mixes in underground aquifers and is discharged as cooler (19.4-29.1°C), brackish water (7.3-34.8 ppt), and is the primary source of nutrients into oligotrophic

coastal habitats (Street et al. 2008; Knee et al. 2010). While nutrient levels are naturally elevated in SGD (Street et al. 2008), the island's highly porous rock also makes SGD especially likely to receive anthropogenic-related contamination (Knee et al. 2010). Furthermore, coastal pollution is predicted to increase on Hawai'i Island given the rapid human population growth rate (24% between 2000 and 2010) (CensusScope 2010; US Department of Commerce 2010), and ongoing land use changes to accommodate residential and commercial development (Friedlander et al. 2008; Parsons et al. 2008).

On a Pacific-wide scale, GA prevalence is highly correlated with human population density and percent coral cover (Aeby et al. 2011a). In small-scale case studies, GA spatial patterns are also positively correlated with colony size (Burns et al. 2011; Irikawa et al. 2011), light irradiation (Aeby et al. 2011b), bleaching stress (McClanahan et al. 2009), and nutrients (Kaczmarsky and Richardson 2010). However, very few studies have assessed the interactions between ecological and environmental factors in driving reef-level GA dynamics along environmental gradients (but see Kaczmarsky and Richardson 2010). Furthermore, it is unclear whether environmental stress enhances GA progression and partial mortality. This study was designed to test three hypotheses: (1) PorGAs along WHI are progressive and contribute to partial mortality, (2) PorGA prevalence, severity, linear extension, and partial mortality vary spatially, and (3) PorGA dynamics are correlated with host demography (colony abundance and size), local hydrology, and exposure to terrestrial input via SGD. Thus we expect PorGA prevalence, severity, and progression (linear extension) to increase with colony size and proximity to SGD, but decrease with elevated water motion.

METHODS:

Study Sites

Surveys were conducted in Kailua Bay (Fig. 3.2A) and Kaloko-Honokōahu National Historical Park (Fig. 3.3A), located near Kailua-Kona on the leeward/western coast of the island of Hawai‘i (WHI). These regions were chosen based on the presence of chronic SGD and robust *P. lobata* populations (mean percent cover = Kailua: 66.30 ± 3.58, Kaloko: 66.57 ± 4.01), as well as year-round accessibility. Kailua Bay (Kailua) experiences persistent SGD, with fresh SGD fluxes measuring between 14 and 41 L m^{-1} min^{-1} (Peterson et al. 2009; Knee et al. 2010). This region is also directly adjacent to the town of Kailua-Kona, which has substantial commercial and residential development within the Kailua Bay watershed. Kaloko-Honokōhau National Park (Kaloko) has one of the largest SGD fluxes along WHI, with the northern sector of the Park experiencing 3–40 L m^{-1} min^{-1} of SGD alone (Knee et al. 2010). This region's watershed is also exposed to terrestrial inputs from commercial development 1.3 km from the coastline, the Honokōhau Harbor, and recent residential development directly adjacent to the coastline (Knee et al. 2008; SCD-TSA Kaloko Makai 2010). Using aerial infrared images of WHI that track SGD input (Johnson 2008) and *in situ* reconnaissance surveys, we identified one SGD plume in each region and then haphazardly chose five and six sites (Kaloko and Kailua, respectively), 100–300 m apart, extending away from the SGD plume. At each site, we established two 15-m transects at a haphazard bearing parallel to shore (4–7 m depth). All transects were mapped and marked with GPS coordinates to relocate in future surveys.

Field Surveys

In July 2010, growth anomaly surveys were conducted on each 15 x 2-m belt transect along which all *P. lobata* colonies were counted, sized using maximum diameter, and inspected for signs of GAs (Fig. 3.1). All GAs were enumerated and measured along the two maximum diameters. Colony size was also estimated by measuring the maximum diameter and binning into the following size classes: 0-5 cm, 6-10 cm, 11-20 cm, 21-40 cm, 41-80 cm, 81-160 cm and > 160 cm. To estimate the rate of GA linear extension and GA-related partial mortality, we photographed 10 small (0–30 cm), 10 medium (31–70 cm) and 10 large (>71 cm) *P. lobata* colonies/transect with GAs (total = 602 colonies) in February–March 2011. These colonies were visually mapped along our pre-established transects at each site and GAs were photographed at a 90° angle from the colony surface with a ruler in the field of view for scale.

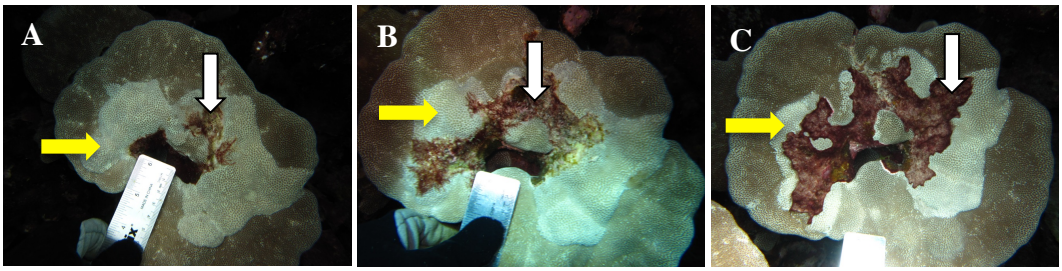

Figure 3.1. *Porites lobata* growth anomalies (GA) on a colony monitored between 2011 and 2012. (A) GA surrounded by healthy tissue (January 2011). (B) Same GA region observed six months later (July 2011) with partial mortality (white arrow). (C) Same colonies six months later (January 2012) increased partial mortality (white arrow). Ruler in field-of-view for scale.

These colonies and their GAs were re-photographed in August 2011 and February 2012. *P. lobata* GA prevalence was calculated as the number of *P. lobata* colonies with GAs/total number of *P. lobata* colonies x 100. Due to the spatial extent and number of colonies (total = 8482) surveyed in July 2010 we estimated GA severity by calculating the total GA area per colony as follows using the area of an ellipse:

$$A = \Sigma(\pi a_i b_i)$$

where a_i is the first GA axis and b_i is the second GA axis.

Water Quality Assessments

We conducted water quality assessments on March 30, 2010, August 29, 2010, and August 15, 2011. We collected triplicate 1000-ml water samples in acid-washed Nalgene bottles just below the surface and just above the substrate to measure inorganic nutrient (nitrate plus nitrite, ammonium, orthophosphate) concentrations. These samples were transported to the Natural Energy Laboratory of Hawai'i Authority in Kailua-Kona, Hawai'i for processing. At the lab, each sample was filtered through a 0.45 μm GF/F Whatman filter into triple-rinsed, acid-cleaned, 125-ml polyethylene bottles and kept frozen prior to nutrient analysis. Nitrate plus nitrite, ammonium, soluble reactive phosphorus (SRP), and silicate were analyzed using flow-injection analysis on an Astoria Pacific Instruments autoanalyzer. Silicate was included as a commonly used indicator of groundwater input (e.g. Street et al. 2008). Temperature, salinity, and nutrient concentrations were averaged across seasons and surface and benthic samplings.

To assess the role of local hydrology in GA dynamics, we assayed water motion on September 15, 2012, using slow-dissolving (S-type) clod cards to compare dissolution rates between sites (e.g., Jokiel and Morrissey 1993; Burns et al. 2011). Clod cards were composed of

1 part powdered resin glue (Weldwood Brand, Weldwood Packaged Product, Champion International Corporation), 10.5 parts wall patching compound (Fixall Brand, Dowman Products Inc.), and 5.1 parts water. 60 mL of plaster was poured into 88 mL paper cups, dried for 48 h in an air-conditioned room and weighed to the nearest 0.01 g prior to deployment. The deployed clod cards were attached to the dead substrate with galvanized steel wire embedded in the plaster during casting. A total of 132 clod cards were deployed across all 11 sites for 24 h. Four clod cards were haphazardly placed in each of three randomly delineated sectors (12 clod cards total) at each site to account for heterogeneity of water flow. Following retrieval, the clod cards were dried for 48 h in an air-conditioned room and then weighed to the nearest 0.01 g. A total of three clod cards were kept in a shaded container of seawater for the same duration to serve as the control for all deployed clod cards (Jokiel and Morrissey 1993). The dissolution rate for each clod card was calculated as the final minus initial weight divided by initial weight. The mean dissolution rate of the control clod cards was subtracted from the dissolution rate of each experimental card to obtain a dissolution rate due to water motion. This final value of dissolution rate due to water motion over 24 h is referred to as clod card dissolution.

Image Analysis

To investigate the morphological difference of PorGA tissue and healthy tissue, polyp density was measured in a subset of 30 PorGAs and adjacent healthy tissue (0.5 to 1 cm away from GA). Fifteen PorGAs were randomly selected from a subset of PorGAs from each Kailua 2 and Kaloko 3 with initial areas less than five cm^2 to limit variation due to size-dependent factors. The number of polyps were counted in both the PorGA and apparently healthy tissue using the cell counter tool and calculated as the number of polyps per area.

To determine the rate of PorGA linear extension and partial mortality, we first matched GAs across seasons and only measured/included PorGAs that could be found in all three seasons (Kailua: 197 colonies and 447 PorGAs; Kaloko: 122 colonies and 204 PorGAs). Using Image *J*, we measured the area of each GA and GA-related mortality with the freeform tool. PorGAs were omitted from analyses in the rare cases they were photographed less than 90° from the colony surface. In cases where other sources of partial mortality (e.g., predation) confounded measurements of PorGA-related partial mortality, the mortality was noted but not measured. PorGA linear extension rate for each PorGA was calculated in cm^2 mo^{-1} using the following formula:

$$LE = (A_{W'12}-A_{W'11})/(t_{W'12}-t_{W'11})$$

where $A_{W'12}$ and $A_{W'11}$ are the PorGA area in winter 2012 and winter 2011, respectively and $t_{W'12}$ and $t_{W'11}$ are the dates each image was taken.

We calculated the rate of measurable PorGA-related partial mortality for each GA as:

$$\text{Partial mortality} = (A_{W'12}-A_{W'11})/(t_{W'12}-t_{W'11})$$

where $A_{W'12}$ and $A_{W'11}$ are the area of PorGA-related partial in winter 2012 and winter 2011, respectively and $t_{W'12}$ and $t_{W'11}$ are the dates each image was taken.

We calculated the proportion of colonies with any type of PorGA-related partial mortality by dividing the number of colonies with PorGA-related partial mortality by the total number of colonies measured.

Statistical Analyses

GA Temporal Dynamics

All data were analyzed in R version 2.13.1. To confirm that PorGA tissue is morphologically distinct from apparently healthy tissue (polyp density) and determine whether polyp density and PorGA area increased significantly from winter 2011 to winter 2012, data were power transformed and analyzed using linear mixed-effect models (LMEM) with helmert contrasts and maximum likelihood estimation using the lme4 package (Bates and Maechler 2009). We used the Markov chain Monte Carlo simulation (MCMC) to detect differences between treatments at specific time points (see Baayen et al. 2008). MCMC generates random samples from a posterior distribution of parameter values for fixed and random effects (Bolker et al. 2009). We conducted 50,000 iterations to estimate the highest posterior density (HPD) interval for each parameter, using 95% of the probability distribution (credible intervals). HPD intervals that did not overlap zero indicated conservative significant effects of the specified parameters at $\alpha = 0.05$ (Pinheiro and Bates 2000). To determine whether PorGA-related partial mortality varied temporally, we use an analysis of variance (ANOVA) with Tukey's *post hoc* tests for partial mortality area per PorGA and a generalized linear model (binomial errors with logit link) and generalized linear hypothesis tests (glht function in the multcomp package in R) for the proportion of colonies with any type of PorGA-related partial mortality.

Spatial Dynamics of PorGA Prevalence, Severity, and Linear Extension

Generalized linear models (GLMs-quasibinomial errors with logit link) were used to determine whether PorGA prevalence varied between sites (fixed effect) for each region. We compared the fixed-effect to the null model using likelihood ratio tests (LRT) with chi-square

test statistics (Burnham and Anderson 2002). Generalized linear hypothesis tests were used to identify significant differences between sites. Severity and linear extension rate data were power transformed with box-cox transformation and then site-level variation was tested using an ANOVA with Tukey *post hoc* tests.

Demographic and Environmental Drivers of PorGA Prevalence and Severity

To determine which demographic variable was the best predictor of disease prevalence, we used mixed-effect models. Due to the potential issues of multicollinearity in the predictor variables, we calculated the variance inflation factors (VIF) prior to running the models. VIF indicate the inflation in the variance of each regression coefficient compared with the situation of orthogonality. VIF values >5 suggest the existence of multicollinearity (Zuur et al. 2009). Due to issues with multicollinearity when all demographic and environmental variables were included in the model, we used one set of mixed-effect models to identify the best demographic predictor of prevalence and severity and then used that optimal predictor in a second set of models including the environmental predictors.

We fit PorGA prevalence generalized linear mixed-effect models (GLMM) using maximum likelihood estimation (glmer function in lme4 package), with PorGA prevalence as the response, and *P. lobata* % cover, colony density, and average maximum colony diameter as fixed effects (binomial distribution; parameter estimates $\beta \pm$ s.e. given in logit form). We built eight hierarchical or single-factor models. Due to the interaction between colony size and abundance (Chapter 3), we also included a size x coral cover interaction model. We used an information theoretic approach, comparing corrected Akaike's information criterion (AICc, ΔAICc and AIC weight) to determine which demographic variable(s) best fit prevalence (Burnham and Anderson

2002). We power transformed the total PorGA area/colony (severity) to meet assumptions of normality and equal variances and then used linear mixed-effect modeling with the same framework for parameter estimation and model selection described for the prevalence GLMMs

To determine the relationship between PorGAs and the optimal demographic variable and the environment, we used a second set of mixed models. Due to high correlation between the nutrient parameters, we used a principle components analysis (PCA) to condense the nutrient parameter into one principle component to include in the mixed-effect models. The nutrient principle component accounted for 74% of the variance in nutrient concentration (data not shown). We constructed two sets of models with either prevalence or severity as the response variable and the optimal predictor variable, temperature, salinity, nutrient concentration, water motion, and distance from ground water input as fixed effects. We built 30 hierarchical or single-factor models. Given that water motion is also known to affect coral demography (Dollar 1982; Storlazzi et al. 2005), we also included a size x water motion interaction model. We used the same model selection approach discussed above.

To ensure spatial patterns were not solely driven by variation in colony size, we standardized total GA area per colony by dividing by the maximum colony diameter. These size-corrected data were power transformed and then regressed against water motion.

RESULTS:

GA Temporal Dynamics

P. lobata GAs were morphologically distinct from adjacent apparently healthy tissue and temporally dynamic. Mean polyp density was significantly higher in PorGA tissue compared to

adjacent apparently healthy tissue at both Kailua 2 (Table 3.1, HPD intervals 11.56, 13.12) and Kaloko 3 (Table 3.1, HPD intervals 13.79, 15.00). At Kailua 2, polyp density increased significantly from winter 2011 to winter 2012 in both GA and healthy tissue (Table 3.1, HPD intervals: GA 1.15, 4.44; H 3.23, 7.52), but did not change significantly over time at Kaloko 3 (Table 1, HPD intervals: GA 2.11, 5.48; H -2.59, 0.26). Mean PorGA area, however, did increase significantly over time (Table 3.1). Mean PorGA area increased significantly and by 2 cm^2 between winter 2011 and winter 2012 at Kailua (Table 3.1, HPD interval: 0.59, 1.16) and by 3.4 cm^2 in Kaloko (Table 3.1, HPD interval: 0.74, 1.43). PorGA area in Kailua and Kaloko increased at a mean rate of 0.19 ± 0.02 cm^2 mo^{-1} and 0.27 ± 0.04 cm^2 mo^{-1}, respectively. Despite the mean overall increase in area, 85% of the PorGAs increased in size while 15% of PorGAs decreased in size, highlighting PorGAs dynamic nature (data not shown). We observed considerable PorGA-related partial mortality, with the mean partial mortality area/GA increasing significantly in both regions (Table 3.1, ANOVA with *post hoc* test $p<0.05$). Overall, 48 ± 3.0% of the colonies also experienced PorGA-related partial mortality, but mortality did not vary significantly over time (Table 3.1, GLM with *post hoc* test $p<0.05$).

Table 3.1. Seasonal estimates of mean GA area, partial mortality area, GA-related partial mortality prevalence, and polyp density by region. Parentheses indicate ± standard error and asterisks indicate significant difference between winter 2011 and winter 2012. Polyp density and GA area were analyzed with LMEMs and MCMC simulation (HPD intervals that do not overlap 0, $\alpha = 0.05$). Partial morality estimates were analyzed with ANOVA and binomial GLM with *post hoc* tests ($p<0.05$).

	GA polyp density (polyps cm^{-2})	**Healthy tissue polyp density (polyps cm^{-2})**	**GA area (cm^2)**	**Partial mortality area (cm^2) per GA**	**Proportion of colonies with GA-related partial morality**
Kailua					
Winter 2011	50.9 (1.8)	71.1 (1.9)	7.8 (1.0)	1.4 (0.6)	0.54 (-0.04)
Summer 2011	52.3 (2.0)	76.1 (2.2)	8.9 (1.0)	2.1 (0.6)	0.59 (-0.04)
Winter 2012	**55.9 (2.0)***	**88.2 (2.9)***	**10.0 (1.0)***	**2.7 (0.8)***	0.65 (-0.04)
Kaloko					
Winter 2011	54.6 (1.4)	90.0 (2.5)	5.2 (0.7)	0.7 (0.1)	0.40 (-0.05)
Summer 2011	58.7 (1.3)	85.8 (1.1)	6.9 (1.2)	1.2 (0.3)	0.48 (-0.05)
Winter 2012	**58.4 (1.3)***	83.8 (1.4)	**8.6 (1.1)***	**1.9 (0.4)***	0.56 (-0.05)

Spatial Dynamics of GA Prevalence, Severity, and Linear Extension

Within Kailua (Fig. 3.2A), PorGA prevalence varied between sites (LRT: χ^2= 183.53, df=5, p<0.0001) and decreased significantly with distance from SGD input (near Kailua 1). Kailua 1, 2, and 3 (Table 3.2, within the bay) were significantly lower than Kailua 4, 5 and 6 (Table 3.2, outside the bay) (Fig. 2B, *post hoc* tests, p<0.01). These patterns were also consistent for PorGA severity (total GA area/colony), which decreased significantly with distance from SGD (Fig. 3.2C, ANOVA, df=5, F=11.613, p<0.00001, *post hoc* tests p<0.05). GA linear extension rates did not vary significantly between sites (Fig. 3.2D, ANOVA, df=5, F=0.666, p=0.65).

Within Kaloko-Honokōhau (Fig. 3A), PorGA prevalence varied between sites (LRT: χ^2= 142.05, df=4, p=0.0048), decreasing significantly with distance from SGD input (Kaloko 3) (Fig. 3.3B, post hoc HSD p<0.0001). PorGA severity (total GA area/colony) also decreased significantly with distance from Kaloko 3 (Fig. 3.3C, ANOVA, df=4, F=3.77, Tukey HSD p=0.005). While PorGA linear extension rate followed similar spatial patterns, it did not vary significantly between sites (Fig. 3.3D, ANOVA, df=4, F=0.858, p=0.49).

Table 3.2. Mean values (± standard error) for response and predictor variables at each site.

Site	GA Prevalence	GA severity (total GA area colony^{-1})	GA linear extension rate (cm^2 mo^{-1})	*P. lobata* % cover	# of *P. lobata* colonies m^{-2}	Maximum Colony Diameter (cm)	NH_3 (µg/l)	SRP (µg/l)	NO_3 + NO_2 (µg/l)	Si (µg/l)	Temperature (°C)	Salinity (ppt)	Water motion (% dissolution of cards)	Distance (m)
Kailua 1	24.70 (0.63)	37.69 (11.7)	0.18 (0.05)	57.12 (6.1)	8.43 (3.0)	41.83 (2.9)	4.82 (0.71)	3.40 (1.4)	30.93 (9.4)	625.49 (208.0)	25.88 (0.36)	35.00 (0.44)	14.73 (0.60)	55
Kailua 2	36.08 (11.8)	24.11 (3.8)	0.16 (0.04)	61.88 (7.5)	11.03 (3.8)	37.49 (0.81)	2.57 (0.61)	1.75 (0.17)	6.14 (0.63)	152.08 (24.7)	25.83 (0.47)	35.24 (0.27)	10.64 (0.80)	156
Kailua 3	33.79 (2.2)	31.87 (4.8)	0.25 (0.03)	55.62 (5.0)	10.22 (0.90)	38.95 (2.9)	2.40 (0.50)	1.56 (0.15)	4.92 (0.65)	144.41 (20.8)	25.97 (0.48)	35.38 (0.28)	13.96 (1.6)	317
Kailua 4	11.17 (0.03)	9.24 (1.7)	0.16 (0.03)	50.39 (6.4)	24.85 (0.15)	23.13 (2.6)	2.14 (0.38)	1.45 (0.13)	3.76 (0.67)	190.66 (34.0)	26.03 (0.47)	35.47 (0.27)	22.62 (1.5)	378
Kailua 5	11.07 (1.3)	9.10 (1.5)	0.20 (0.05)	58.57 (9.5)	16.93 (2.0)	23.46 (0.60)	1.99 (0.46)	1.27 (0.20)	3.18 (0.46)	208.23 (56.7)	26.02 (0.48)	35.49 (0.28)	16.62 (1.2)	781
Kailua 6	13.97 (1.3)	9.97 (2.4)	0.21 (0.04)	46.02 (3.4)	11.98 (0.13)	26.56 (2.6)	2.57 (0.39)	1.54 (0.20)	9.03 (0.91)	167.35 (23.6)	25.99 (0.41)	35.33 (0.28)	19.69 (1.7)	1226
Kaloko 1	6.33 (0.40)	7.82 (1.07)	0.16 (0.06)	46.43 (3.1)	27.25 (0.25)	20.12 (0.30)	4.07 (0.79)	1.56 (0.40)	7.45 (2.7)	242.51 (84.1)	25.70 (0.43)	35.28 (0.41)	13.43 (1.5)	248
Kaloko 2	9.41 (4.5)	19.19 (3.0)	0.23 (0.06)	66.92 (0.40)	28.60 (3.1)	23.55 (3.1)	5.09 (0.58)	2.36 (0.64)	12.36 (4.4)	392.01 (149.0)	25.77 (0.41)	35.26 (0.44)	9.54 (1.4)	168
Kaloko 3	20.3 (0.83)	21.94 (3.6)	0.34 (0.08)	73.72 (5.02)	25.08 (3.5)	25.67 (0.19)	5.07 (0.72)	3.27 (0.89)	20.79 (6.9)	609.51 (199.7)	25.61 (0.46)	35.07 (0.48)	9.19 (0.83)	83
Kaloko 4	8.15 (1.9)	11.32 (1.2)	0.24 (0.04)	66.10 (0.6)	25.35 (0.85)	25.09 (0.82)	6.29 (1.29)	3.32 (0.83)	21.52 (6.4)	1074.45 (282.7)	25.82 (0.46)	34.88 (0.58)	12.98 (1.4)	180
Kaloko 5	5.63 (2.9)	8.68 (1.7)	0.19 (0.04)	59.05 (5.1)	22.35 (0.55)	23.72 (1.5)	5.33 (0.83)	3.05 (0.72)	16.08 (5.0)	812.72 (277.2)	25.71 (0.42)	34.46 (0.66)	13.31 (1.7)	246

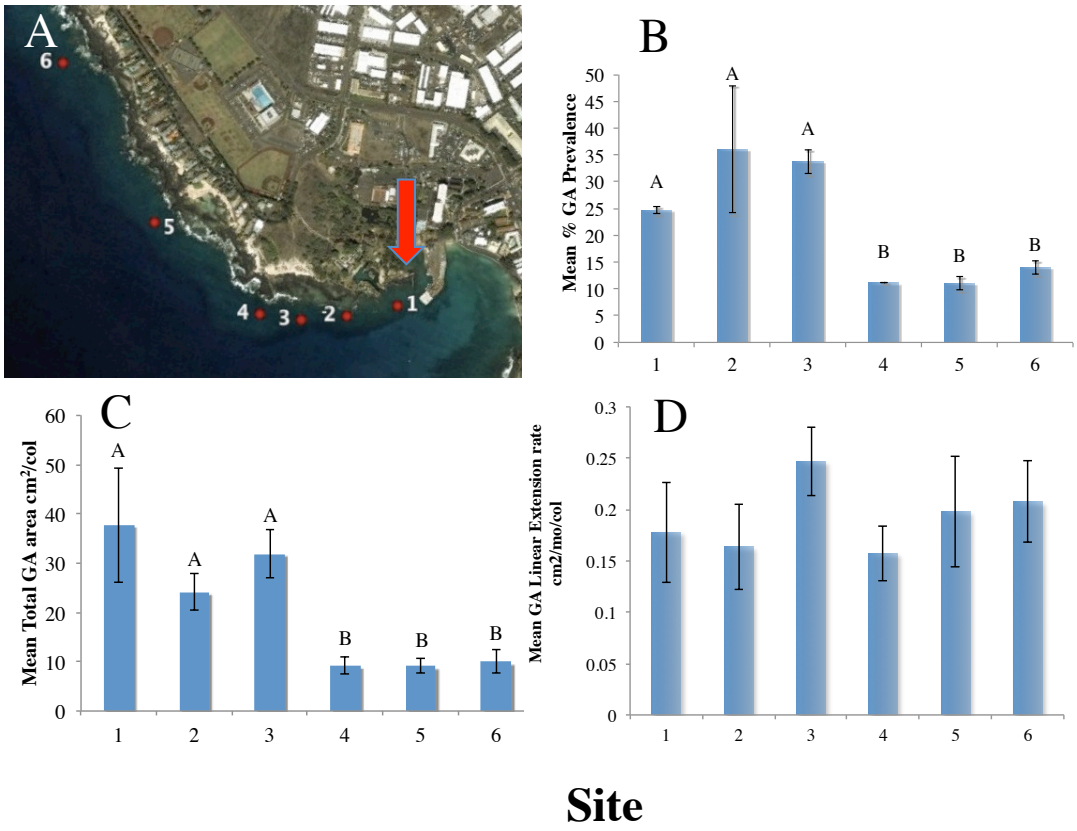

Figure 3.2. A) Map of Kailua Bay sites (B) Mean % ± SE *P. lobata* GA prevalence n=2 transects/sites, (C) Mean ± SE total GA tissue area/colony (severity) n=2 transects/sites (D) Mean rate of GA linear extension (n=447 GAs). Note: Sites situated with increasing distance from strongest submarine groundwater input (red arrow); letters indicate significant differences (post hoc HSD tests $p<0.05$).

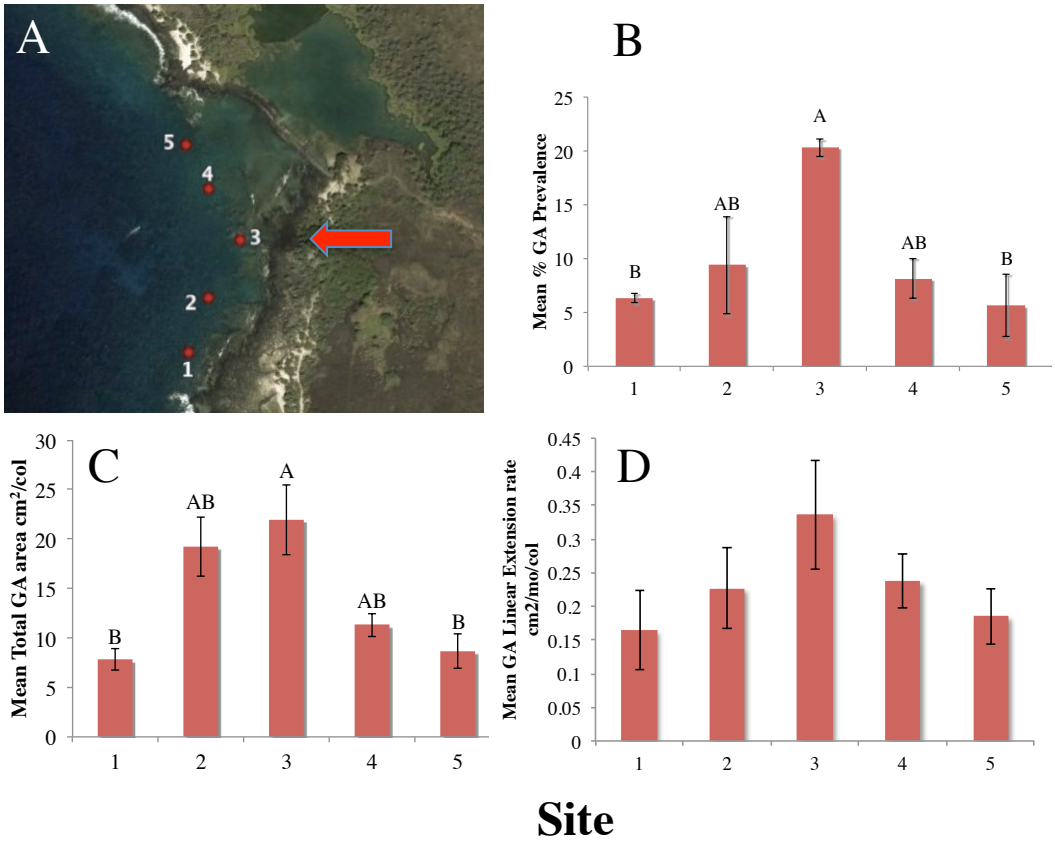

Figure 3.3. A) Map of Kaloko-Honokōhau sites (B) Mean % ± SE *P. lobata* GA prevalence n=2 transects/sites, (C) Mean ± SE total GA tissue area/colony (severity) n=2 transects/sites (D) Mean rate of GA linear extension (n=204 GAs). Note: Sites situated with increasing distance from strongest submarine groundwater input (red arrow); letters indicate significant differences (post hoc HSD tests $p<0.05$).

Host Demographic Drivers of P. lobata GA Prevalence and Severity

Our mixed effects models and model selection highlights *P. lobata*'s integrated demography and suggests that GAs are predominantly driven by colony size. When accounting for regional variation, colony size, coral cover, and colony density were included in the subset of 'best-fit' (ΔAICc < 10) single factor models, but colony size and coral cover accounted for 0.67 and 0.17 of the AICc weight (Table 3.3, Fig. S3.1). GA prevalence was positively correlated with percent coral cover, but negatively correlated with colony density, which only accounted for 0.17 and 0.08 of the AICc weight, respectively (Table 3.3, Fig S3.1), suggesting that while prevalence was density-dependent, it was primarily driven by host size.

Colony size was also positively correlated with severity, was included in both the 'best-fit' models, and accounted for all of the AICc weight, implying that size is the best predictor of severity (Table 3.3, Fig. S3.2). While colony density was included in the top model, its negative correlation with prevalence and severity implies that it is not the primary mechanism driving GAs dynamics. Across both regions, the size-frequency distribution of *P. lobata* colonies without GAs was significantly different from those with GAs (χ^2= 1181.52, *d.f.* = 6, p<0.0001), and more right skewed, indicating that larger colonies, especially greater than 40 cm in diameter are more affected by GAs (Fig. S3.3). GA linear extension rate was not correlated with colony size (Kailua: Linear regression, R^2 = -0.002, F = 0.010, *d.f.* = 445, p = 0.92; Kaloko: R^2= -0.003, F=0.32, *d.f.* = 202, p = 0.57) and was not modeled since it did not vary significantly between sites at either region.

Table 3.3. GA prevalence GLMMs and severity LMEMs with host demographic predictors as fixed effects and region as random effect.

	K	AICc	ΔAICc	w_i
Prevalence GLMMs				
Size	4	124.07	0.00	0.67
Cover	4	126.77	2.69	0.17
Density	4	128.38	4.31	0.08
Size + Cover	5	129.94	5.87	0.04
Size + Density	5	130.73	6.66	0.02
Cover + Density	5	130.93	6.86	0.02
Size * Density	6	137.55	13.48	0.00
Size + Cover + Density	6	140.30	16.23	0.00
Severity LMEMs				
Size * Density	6	66.20	0.00	0.87
Size + Cover	5	70.13	3.93	0.12
Size * Density	5	77.13	10.93	0.00
Size	4	77.60	11.40	0.00
Size + Cover + Density	6	79.17	12.97	0.00
Cover + Density	5	84.72	18.51	0.00
Cover	4	86.16	19.96	0.00
Density	4	89.09	22.89	0.00

Demographic and Environmental Drivers of GAs

To establish the best predictors of GA prevalence, we used a combination of principal component analysis, mixed-effect models and model selection. Following model selection of 30 GLMMs (accounting for regional variation as a random effect), we found that prevalence was best predicted by the interaction of *P. lobata* colony size and water motion, which also accounted for 0.94 of the AICc weight (Table 3.4). Water motion was negatively correlated with prevalence and included in both the 'best-fit' models (Tables 3.4 and S3.1), suggesting the importance of local hydrology in addition to host size. Temperature was also included in the second 'best-fit' model and positively correlated with prevalence, but was a less important predictor since this model only accounted for 0.05 of the AICc weight (Tables 3.1, 3.4 and S3.1).

Table 3.4. GA prevalence GLMMs with optimal demographic predictor and environmental predictors as fixed effects and region as random effect.

GA Prevalence GLMMs	K	AICc	ΔAICc	w_i
Size * Water Motion	5	114.86	0.00	0.94
Temperature + Water Motion	4	120.62	5.75	0.05
Size + Temperature + Water Motion	5	126.12	11.26	0.00
Distance + Water Motion	4	131.84	16.98	0.00
Size + Distanct + Water Motion	5	131.88	17.01	0.00
Size + Water Motion	4	136.06	21.20	0.00
Size + Temperature + Salinity + Water Motion	6	136.39	21.53	0.00
Nutrients + Distance + Water Motion	5	139.06	24.19	0.00
Water Motion	3	140.30	25.44	0.00
Salinity + Water Motion	4	142.12	27.25	0.00
Nutrients + Water Motion	4	144.37	29.50	0.00
Size + Temperature + Salinity + Nutrients + Water Motion	7	154.64	39.78	0.00
Size + Distance	4	177.16	62.29	0.00
Temperature + Distance	4	179.48	64.62	0.00
Size + Temperature	4	199.21	84.35	0.00
Size	3	202.76	87.90	0.00
Distance * Salinity	5	203.25	88.38	0.00
Size + Temperature + Salinity	5	205.69	90.82	0.00
Distance * Temperature	5	209.40	94.54	0.00
Distance * Nutrients	5	227.61	112.75	0.00
Salinity + Distance	4	243.77	128.91	0.00
Nutrients + Distance	4	250.94	136.07	0.00
Distance	3	252.90	138.04	0.00
Temperate + Salinity + Nutrients	5	261.06	146.20	0.00
Temperature + Salinity	4	270.42	155.56	0.00
Nutrients + Temperature	4	298.70	183.84	0.00
Temperature	3	302.76	187.89	0.00
Salinity + Nutrients	4	319.18	204.31	0.00
Nutrients	3	321.90	207.04	0.00
Salinity	3	343.83	228.96	0.00

Using a similar modeling approach to identify drivers of GA severity, we found that colony size remained the best predictor of GA severity since it was included as a single-factor model accounting for 0.71 of the AICc weight (Tables 3.5, S3.2). Water motion was negatively correlated with severity and was included as a single factor model (Tables 3.5 and S3.2, AICc weight = 0.20). While temperature and distance from SGD were included in the 'best-fit' models, they accounted for little of the AICc weight (Table 3.5). Nutrient concentration and salinity did not appear to be important predictors of either prevalence or severity.

Table 3.5. GA severity LMEMs with optimal demographic predictor and environmental predictors as fixed effects and region as random effect.

GA Severity LMEMs	K	AICc	ΔAICc	w_i
Size	4	77.60	0.00	0.71
Size + Water Motion	5	80.18	2.58	0.19
Size + Distance	5	83.03	5.43	0.05
Size + Temperature	5	84.36	6.76	0.02
Water Motion	4	86.53	8.93	0.01
Temperature + Distance	5	87.50	9.90	0.01
Size + Temperature + Water Motion	6	88.49	10.88	0.00
Distance	4	89.17	11.56	0.00
Nutrients	4	89.72	12.12	0.00
Temperature + Water Motion	5	89.99	12.39	0.00
Temperature	4	90.31	12.71	0.00
Size * Water Motion	6	90.96	13.36	0.00
Size + Distance + Water Motion	6	91.14	13.54	0.00
Salinity	4	91.61	14.01	0.00
Nutrients + Water Motion	5	92.15	14.54	0.00
Distance + Water Motion	5	92.51	14.91	0.00
Salinity + Water Motion	5	92.88	15.28	0.00
Size + Temperature + Salinity	6	94.69	17.08	0.00
Nutrients + Distance	5	95.17	17.56	0.00
Nutrients + Temperature	5	95.82	18.21	0.00
Salinity + Distance	5	96.50	18.90	0.00
Salinity + Nutrients	5	96.89	19.28	0.00
Temperature + Salinity	5	97.59	19.98	0.00
Distance * Temperature	6	98.38	20.78	0.00
Nutrients + Distance + Water Motion	6	101.97	24.36	0.00
Distance * Temperature	6	105.96	28.36	0.00
Temperature + Salinity + Nutrients	6	106.25	28.64	0.00
Distance * Salinity	6	106.50	28.89	0.00
Size + Temperature + Salinity + Water Motion	7	106.81	29.21	0.00
Size + Temperature + Salinity + Nutrients + Water Motion	8	143.47	65.86	0.00

To confirm the role of water motion in GA dynamics and address the influence of water motion on colony size, we applied a size correction to prevalence and severity, and then regressed these data against water motion. When analyzed by region, we found that prevalence and severity were still strongly negatively correlated with water motion even after correcting for host demography, but not significantly in the case of size-corrected prevalence in Kaloko-Honokōhau (Fig. 3.4).

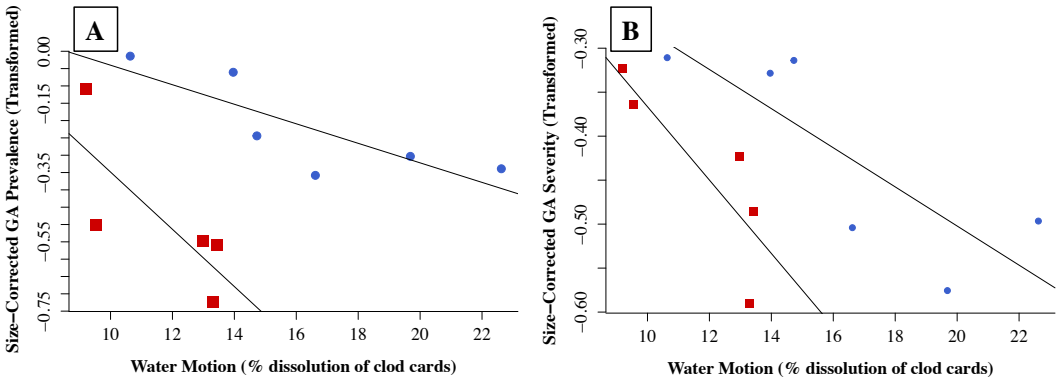

Figure 3.4. (A) Size-corrected PorGA prevalence (prevalence/average maximum colony diameter) as a function of clod card dissolution (Linear Regression, Kailua: $R^2 = 0.58$, $F = 8.10$, $d.f. = 5$, $p = 0.046$; Kaloko: $R^2 = 0.46$, $F = 4.39$, $d.f. = 4$, $p = 0.12$). (B) Size-corrected PorGA severity (total GA area per colony/maximum colony diameter) as a function of clod card dissolution (Linear Regression, Kailua: $R^2 = 0.57$, $F = 7.74$, $d.f. = 5$, $p = 0.05$; Kaloko: $R^2 = 0.61$, $F = 7.38$, $d.f. = 4$, $p = 0.07$). Blue= Kailua Bay, Red=Kaloko.

DISCUSSION:

Disease dynamics are often modulated by the environment, yet the integration of intrinsic and extrinsic factors is poorly understood, inhibiting our ability to predict disease risk during ongoing environmental change (Lafferty 2009; Burge et al. 2013). Since disease risk is strongly dependent on host-pathogen-environment interactions (e.g. Burge et al. 2013), it is important to understand how these organismal-level interactions scale up to the population level and interact with the environment to facilitate disease. Growth anomalies in Hawai'i provide an ideal study system for disentangling complex demographic and environmental factors due to their high prevalence on the structurally simple reefs of Hawai'i and widespread distribution (Vargas-Ángel and Wheeler 2009; Aeby et al. 2011a; Couch et al. in review). West Hawai'i has one of the highest levels of *Porites* GAs (Hawai'i's dominant reef-building genus) in the Pacific, including other MHI (Aeby et al. 2011a; Couch et al. in review). Using longitudinal colony monitoring and a gradient design, we found that *P. lobata* GAs increased in size over time and contributed to colony-level mortality. PorGA prevalence and severity were also strongly driven by synergistic interactions between host demography and local hydrology.

Our study highlights the high degree of spatial variation of this disease on a relatively small spatial scale. On the Pacific-wide scale, PorGA prevalence can vary considerably from 0% in regions such as the Marianas Islands (Aeby et al. 2011) to as high as 41% along WHI (Couch et al. in review). While PorGA prevalence is anomalously high compared to other Pacific reefs, it was highly variable at both the coast-wide (range = 0.49 - 41.08%, Couch et al. in review) and within-reef scale (range = 5.63 - 36.08%, this study). Despite their relatively close proximity (7 km), average GA prevalence and severity in Kailua was 2.2 and 1.5 times higher than in Kaloko. Few studies have assessed multiple components of GA dynamics across space, but our study

indicates that the degree to which colonies are affected (severity), is far more variable than the rate of progression.

GA Temporal Dynamics

Our study highlights the GAs' dynamic nature and role in coral mortality. GA-affected tissue had significantly fewer polyps compared to adjacent apparently healthy tissue. In addition to the reduced polyp density, *P. lobata* GAs have enlarged corallites, increased gastrovascular canals, hyperplasia of mucocytes and fewer zooxanthellae (Couch et al. 2012), suggesting that WHI *P. lobata* GAs are morphologically similar to previously characterized PorGAs (Domart-Coulon et al. 2006; Kaczmarsky 2009). Our longitudinal study showed that while 85% of all GAs increased in size over our year-long study, 15% of GAs also decreased in size. Overall, *P. lobata* GAs grew at a rate of 0.22 cm^2 mo^{-1}, which was slower than rates in other poritids (0.44 cm^2 mo^{-1}, Yasuda et al. 2012). In other corals, GAs linear extension rates can be highly variable: 0.36 cm^2 mo^{-1} in *Acropora palmata* (Peters et al. 1986) and 0.13 cm^2 mo^{-1} in *Acropora cytherea* (Irikawa et al. 2011), highlighting that GA dynamics differ across coral taxa and are likely shaped by genetic and regional factors. Growth rates may also be affected by inherent seasonal changes in growth and calcification attributed to temperature and light fluctuations (Lough and Barnes 2000). While we do not have the temporal resolution to address GA seasonality, Stimson (2010) found that *P. compressa* GAs in Kaneohe Bay, Hawai'i, develop in early spring and peak in the summer. WHI GAs growth rates were also likely affected by other colony-level factors such as colony investment in growth compared to other life-history traits.

As a chronic disease, GA contribution to colony mortality is often underestimated or unaccounted for, but our results suggest a large impact, with 48% of the *P. lobata* colonies with GAs experienced partial mortality associated with these lesions. Consistent with previous GA

case studies (Peters et al. 1986; Yamashiro et al. 2000; Irikawa et al. 2011; Yasuda et al. 2011), GA mortality often originated in the center of the GA lesion (Fig 3.1). This type of partial mortality has been attributed to reduced mucocyte and nematocyte counts as well as disruption of the epidermis within GA tissue, thus inhibiting GAs ability to remove debris and algae, ultimately leading to tissue mortality (Bak 1983; Kaczmarsky 2009). However, we underestimated the relative contribution of GAs to partial mortality because GAs also interacted with other colony-level disturbances and increased mortality. Partial mortality increased over time at an average rate of 0.12 $cm^2\ mo^{-1}$ in Kailua and 0.096 $cm^2\ mo^{-1}$ in Kaloko, further supporting the observations that GAs are actively contributing to colony-level mortality. These findings corroborate previous studies indicating that GAs likely impact long-term coral population dynamics by causing partial mortality, as well as impaired growth and reproduction (Domart-Coulon et al. 2006; Work et al. 2008; Stimson 2010).

Effects of Host Demography

Intrinsic factors, such as host demography, are a fundamental component of the host-pathogen-environment interactions. For example, disease often increases with host abundance when direct or indirect transmission is necessary for pathogen persistence and spread (e.g. Anderson and May 1979; Holt et al. 2003). While GA dynamics may be driven by density-dependent transmission, PorGA prevalence and severity were negatively correlated with colony density, and only weakly positively correlated with *P. lobata* cover. This relationship, however, appears to be driven by strong increased risk of GA development in larger colonies (>40 cm), which were five times more likely to be affected by GAs than small (< 40 cm) colonies (Fig S3.3). The size effect may also partially explain the higher GA levels in Kailua compared to Kaloko, which had average maximum colony diameters of 31.74 and 24.47 cm, respectively.

Strong size-specific patterns in GA risk have also been observed in GA in other scleractinian genera, namely *Montipora capitata* (Burns et al. 2011), *Acropora cytherea* (Irikawa et al. 2011), and *Platygyra* spp. (Loya et al. 1984). While disease severity also increases with size in other coral diseases, such as *Acropora* white syndrome (Roff et al. 2011) and aspergillosis (Kim and Harvell 2004; Bruno et al. 2011), it may be especially pronounced in chronic diseases such as GAs where complete disease-associated mortality is less uncommon. While many large-scale coral disease studies have not assessed colony size, there is conflicting evidence as to the role of host abundance, with some finding a positive relationship with coral cover (Williams et al. 2010; Aeby et al. 2011a) and colony density (Williams et al. 2010), whereas others found a negative or nonexistent relationship (McClanahan et al. 2009; Kaczmarsky and Richardson 2010). We propose that this demographic uncertainty may be partially driven by size, as well as the relative abundance compared to other coral taxa.

While the mechanisms underlying the link between colony size and GA patterns are still unknown, several potential explanations may not be mutually exclusive. First, because GAs rarely cause complete colony mortality, large colonies may simply have had more time to accumulate and develop lesions. Second, if pathogenic microorganisms are involved in GA etiology, larger colonies may be a larger target for pathogens in the environment, similar to other marine organisms (reviewed by Lafferty and Harvell in press). In modular organisms such as corals, the relationship between size and age is seldom linear due to variable size-related growth rates, partial mortality, and coral's ability to fuse tissue fragments (Hughes and Jackson 1980; Hughes 1984; Hughes and Jackson 1985), but in general age and size are loosely related (Loya 1976). Therefore, larger/older colonies may have had a longer time to come into contact with pathogens. In modular organisms, host resistance often decreases with host age and size (Cates

and Rhoades 1977; Puttick 1986; Dube et al. 2002), such as in large, mature sea fan corals that are both more affected by aspergillosis and have lower antifungal response to fungal pathogens (Dube et al. 2002). This change may be attributed to higher allocation of resources to immune defenses in younger, smaller, more valuable tissue (optimal defense theory) or life history trade-offs whereby older individuals preferentially shunt energy to reproduction rather than defense (Zuk and Stoehr 2002; Fedorka et al. 2004). Therefore, older, larger colonies may be less immunocompetent, rendering them more susceptible to GAs. Finally, one of the widely accepted paradigms in vertebrate cancer research is that neoplasms often increase with age due to an accumulation of mutations in genes regulating cell growth (also known as oncogenic mutations) (e.g., Peto et al. 1975, Kennedy et al. 2012). While true neoplasms are less common in corals, age-dependent somatic mutation does occur in invertebrates (Garcia et al. 2010) and cnidarians do have oncogene homologs (Putnam et al. 2007; Spies and Takabayashi 2013). If age-dependent mutations alter genes regulating cell growth and proliferation that lead to GA formation, older, larger colonies may be more prone to GAs than younger colonies. While Spies and Takabayashi (2013) did not find expression patterns of oncogene homologs in *Montipora capitata* GAs consistent with neoplasia in humans, gene expression may change over time following the response to the initial stimulus. GA lesions are highly diverse across scleractinian taxa both in their gross morphology and histopathology. Therefore, future studies should not overlook the role of oncogenes and genetic mutation in *Porites* and should conduct sampling over time following the initial transformative change.

Environmental Drivers of PorGAs

Despite the mounting evidence that coral disease is facilitated by thermal stress (e.g. Bruno et al. 2007; Sato et al. 2009; Maynard et al. 2011), and eutrophication (Bruno et al. 2003;

Voss and Richardson 2006), local hydrology (water motion) was our strongest environmental predictor of GA dynamics. In the present study, GA prevalence and severity increased significantly on reefs with low water motion, suggesting that sheltered embayments are at higher risk of disease. The role of water motion is complicated by the strong predictive power of coral size and the fact that colony size can decrease with increasing water turbulence due to elevated disturbance (Storlazzi et al. 2005). However, the negative relationship between GAs and water motion persists even after applying size corrections, further emphasizing the importance of local hydrology in this disease. Water motion can profoundly influence corals from the physiological to community level (Dollar 1982; Lesser et al. 1994). While elevated disease has been observed in qualitatively sheltered embayments, such as in sea fan aspergillosis (Nagelkerken et al. 1997), few studies have quantitatively addressed the relationship between coral disease and water motion. Our findings support results from Burns et al. (2011) that also detected a negative association between the proportion of *Montipora capitata* colony surface with GA and water motion along the southeastern coast of Hawai‘i Island. In Kenya, PorGA and coral bleaching prevalence are also negatively associated with water motion (McClanahan et al. 2005; McClanahan et al. 2009). Several possible mechanisms link water motion and disease. Water motion may affect microbial dynamics either by facilitating transmission of pathogenic microorganisms under turbulent conditions (Rutzler et al. 1983; Bruckner et al. 1997) or increasing residence time or production of microorganisms in calm conditions (Torréton et al. 2007; Ouillon et al. 2010). Local water motion also affects coral physiology by increasing gas exchange, waste and sediment removal, nutrient exchange and photosynthesis (Dennison and Barnes 1988; Lesser et al. 1994; Finelli et al. 2006). Thus, low water motion may increase physiological stress, rendering corals more susceptible to disease. Regardless of the underlying

mechanisms, the link between local hydrology and disease is intriguing and may also help to partially explain why most of the *Montipora* disease outbreaks on Oahu, Maui, and Kauai are occurring in qualitatively sheltered embayments (Aeby pers. comm., Aeby et al. 2010; Walsh et al. 2013).

Coral disease has been positively associated with terrestrial input from sewage and urbanization (Kaczmarsky et al. 2005; Sekar et al. 2008; Kaczmarsky and Richardson 2010), as well as river discharge (Haapkylä et al. 2011) and is hypothesized to enhance disease by promoting pathogenicity and virulence of microorganisms and/or compromising host immune function (Burge et al. 2013). Contrary to predictions, *P. lobata* GA prevalence and severity was not explained by distance from SGD and nutrient concentration (proxies for terrestrial input) when analyzing both regions together. Overall, nutrient concentration was elevated in Kaloko compared to Kailua (Table 3.1), which was most likely attributed to nutrient inputs from the Kaloko fishpond (near Kaloko 5) and suggests that nutrient input alone may not explain GA patterns. However, when considering each region separately, there was a pronounced decline in *P. lobata* GA prevalence and severity with increasing distance from SGD input, indicating that in addition to the strong role of host size and water motion, some form of terrestrial input unaccounted for in this study may be influencing disease patterns. GAs may be influenced by other pollutants not measured in this study such as toxicants linked with tumor formation in higher-level metazoans (e.g. Malins et al. 1988; Myers et al. 1991). If other forms of terrestrial input are involved in this disease, they may be concentrated and their effects exacerbated under low water flow conditions.

CONCLUSIONS

Despite the chronic nature of GAs, *P. lobata* GAs along WHI were progressive and a significant contributor to coral mortality. These findings, together with impaired growth and reproduction (e.g. Work et al. 2008; Stimson 2010), suggest that GAs likely have deleterious effects on long-term coral population dynamics, which is especially concerning since WHI's PorGA prevalence is 25 times higher than the Main Hawaiian Islands overall (Couch et al. in review). Further *in situ* measurements of the effects of GAs on coral fitness are necessary to address the effects of this disease on population dynamics. Our study augments the growing evidence of the role of environmental stress in disease risk, and specifically highlights the synergistic impact of extrinsic factors like local hydrology with intrinsic factors such as host size. Local hydrology (water motion) and colony size strongly predicted PorGA prevalence and severity, which varied considerably at both the reef (50–300 m) and regional (7 km of coastline) levels. Specifically, reefs dominated by larger colonies (>40 cm in diameter) and low water motion were the most susceptible to PorGAs. These findings also likely explain the elevated PorGA prevalence and severity in qualitatively sheltered embayments along WHI (Couch et al. in review). While nutrient concentration did not strongly predict disease patterns when analyzing both regions in the same models, the pronounced decline in GAs with increasing distance from SGD in each region suggests that other forms of land-based pollution, unaccounted for in this study, may be involved in coral health. The younger reefs along the central and southern coast of WHI represent relatively well-flushed systems, whose coastal watersheds have not experienced the same level of land-use change impacting the northern Kohala Coast reefs. Therefore, as terrestrial input increases, sheltered embayments may be especially susceptible to GAs. Future

studies should address the mechanisms influencing size-specific disease patterns, especially genetic mutations, as well as the synergistic link between colony size and water motion.

ACKNOWLEDGEMENTS

Special thanks to K. Gaab, J. Giddens, N. Rozet, and Kona Diving Company for field support. We also thank K. Olson for assistance with nutrient analyses, as well E. Grossman and L. Marrak helpful feedback on SGD. We are grateful to D. Ruiz Moreno, and B. Miner for assistance with statistical analyses. This study was generously supported by The Kohala Center, The NOAA Coral Reef Conservation Grant Program (grant # NA09NMF4630121 to C.D. Harvell), NSF Graduate Research Fellowship awarded to C. Couch and Cornell University. Thanks to E. Peters, A. Tracy, I. Hewson, and J. Thaler for manuscript review.

REFERENCES

Aeby G, Williams GJ, Franklin EC, Haapkyla J, Harvell CD, Neale S, Page CA, Raymundo LJ, Vargas-Angel B, Willis BL, Work TM, Davy SK (2011a) Growth anomalies on the coral genera *Acropora* and *Porites* are strongly associated with host density and human population size across the Indo-Pacific PLoS ONE 6:e16887

Aeby GS, Ross M, Williams GJ, Lewis TD, T.M. W (2010) Disease dynamics of *Montipora* white syndrome within Kaneohe Bay, Oahu, Hawaii: distribution, seasonality, virulence, and transmissibility. Diseases of Aquatic Organisms 91:1-8

Aeby GS, Williams GJ, Franklin EC, Kenyon J, Cox EF, Coles S, Work TM (2011b) Patterns of coral disease across the Hawaiian Archipelago: relating disease to environment. PLoS ONE 6:e20370

Altizer S, Ostfeld RS, Johnson PT, Kutz S, Harvell CD (2013) Climate change and infectious

diseases: from evidence to a predictive framework. Science 341:514-519

Anderson RM, May RM (1979) Population biology of infectious diseases: Part I. Nature 280:361

Aronson RB, Precht WF (2001) White-band disease and the changing face of Caribbean coral reefs. Hydrobiologia 460:25-38

Baayen RH, Davidson DJ, Bates DM (2008) Mixed-effects modeling with crossed random effects for subjects and items. Journal of Memory and Language 59:390-412

Bak RPM (1983) Neoplasia, regeneration and growth in the reef-building coral *Acropora palmata*. Marine Biology 77:221-227

Bates D, Maechler M (2009) lme4: linear mixed-effects models using S4 classes. R package version 0.999375-32

Battista TA, Costa BM, Anderson SM (2007) Shallow-Water Benthic Habitats of the Main Eight Hawaiian Islands (DVD). In: NOAA Technical Memorandum NOS NCCOS 61 BB (ed), Silver Spring, MD

Bienfang P (1980) Water Quality Characteristics of Honokohau Harbor: A Subtropical Embayment Affected by Groundwater Intrusion. Pacific Science 34:279-291

Bolker BM, Brooks ME, Clark CJ, Geange SW, Poulsen JR, Stevens MHH, White JSS (2009) Generalized linear mixed models: a practical guide for ecology and evolution. Trends Ecology and Evololution 24:127-135

Boyett HV, Bourne DG, Willis BL (2007) Elevated temperature and light enhance progression and spread of black band disease on staghorn corals of the Great Barrier Reef. Marine Biology 151:1711-1720

Bruckner AW, Bruckner RJ, Williams J, Ernest H (1997) Spread of a black-band disease epizootic through the coral reef system in St. Ann's Bay, Jamaica. Bulletin of Marine

Science 61:919-928

Bruno JB, J. F., Ellner SP, Vu I, Kim K, Harvell CD (2011) Impacts of aspergillosis on sea fan coral demography: modeling a moving target. Ecological Monographs 81:123-139

Bruno JF, Petes LE, Harvell CD, Hettinger A (2003) Nutrient enrichment can increase the severity of coral diseases. Ecology Letters 6:1056-1061

Bruno JF, Selig ER, Casey KS, Page CA, Willis BL, Harvell CD, Sweatman H, Melendy AM (2007) Thermal stress and coral cover as drivers of coral disease outbreaks. PLoS Biology 5:1220-1227

Burge CA, Eakin CM, Friedman CS, Froelich B, Hershberger PK, Hoffman EE, Prager KC, Weil E, Willis B, Harvell CD (2013) Climate change influences on marine infectious disease: implications for management and society. Annual Reviews in Marine Science 6: DOI: 10.1146/annurev-marine-010213-135029

Burnham KP, Anderson DR (2002) Model selection and multi-model inference: a practical information-theoretic approach. Springer-Verlag, New York

Burns JH, Takabayashi M (2011) Histopathology of Growth Anomaly Affecting the Coral, *Montipora capitata*: Implications on Biological Functions and Population Viability. PLoS ONE 6:e28854

Burns JHR, Rozet NK, Takabayashi M (2011) Morphology, severity, and distribution of growth anomalies in the coral, *Montipora capitata*, at Wai'opae, Hawai'i. Coral Reefs 30:819-826

Cates R, Rhoades D (1977) Prosopis leaves as a resource for insects. Mesquite: Its biology in two desert scrub ecosystems US/IBP Synthesis Series 4:61-83

CensusScope (2010) Data accessed from <http://www.CensusScope.org> on July 22, 2013. Social Science Data Analysis Network, University of Michigan. <http://www.ssdan.net>

Cheney DP (1975) Hard tissue tumors of scleractinian corals. Advances in Experimental Medicine and Biology 64:77-87

Coles SL, Seapy DG (1998) Ultra-violet absorbing compounds and tumorous growths on acroporid corals from Bandar Khayran, Gulf of Oman, Indian Ocean. Coral Reefs 17:195-198

Commerce (2010) Summary population and housing characteristics. In: US Department of Commerce EaSA (ed). US Census Bureau, Washington, DC.

Couch CS, Barnett C, Vega Thurber R (2012) Examining the Role of Environmental and Viruses in Growth Anomalies of Porites lobata on the Island of Hawaii Final Report. 2009 NOAA Coral Reef Conservation Program. Cornell University Award # NA09NMF4630121.

Couch CS, Garriques JD, Barnett C, Preskitt L, Cotton S, Giddens J, Walsh W (in review) Spatial and temporal patterns of coral health and disease along leeward Hawai‘i Island. Coral Reefs

Dennison WC, Barnes DJ (1988) Effect of water motion on coral photosynthesis and calcification. Journal of Experimental Marine Biology and Ecology 115:67-77

Doddington BJ, Bosch J, Oliver JA, Grassly NC, Garcia G, Schmidt BR, Garner TW, Fisher MC (2013) Context-dependent amphibian host population response to an invading pathogen. Ecology 94:1795–1804

Dollar SJ (1982) Wave stress and coral community structure in Hawaii. Coral Reefs 1:71-81

Domart-Coulon IJ, Traylor-Knowles N, Peters E, Elbert D, Downs CA, Price K, Stubbs J, McLaughlin S, Cox E, Aeby G, Brown PR, Ostrander GK (2006) Comprehensive

characterization of skeletal tissue growth anomalies of the finger coral *Porites compressa*. Coral Reefs 25:531-543

Dube D, Kim K, Alker AP, Harvell CD (2002) Size structure and geographic variation in chemical resistance of sea fan corals *Gorgonia ventalina* to a fungal pathogen. Marine Ecology Progress Series 231:139-150

Fedorka KM, Zuk M, Mousseau TA (2004) Immune suppression and the cost of reproduction in the ground cricket, *Allonemobius socius*. Evolution 58:2478-2485

Finelli CM, Helmuth BS, Pentcheff ND, Wethey DS (2006) Water flow influences oxygen transport and photosynthetic efficiency in corals. Coral Reefs 25:47-57

Franklin EC, Jokiel PL, Donahue MJ (2013) Predictive modeling of coral distribution and abundance in the Hawaiian Islands. Marine Ecology Progress Series 481:121-132

Friedlander A, Aeby GS, Brainard R, Brown E, Chaston K, Clark A, McGowan P, Montgomery T, Walsh W, Williams I, Wiltse W (2008) The state of coral reef ecosystems of the Main Hawaiian Islands. In: Waddell JE, Clarke AM (eds) The State of Coral Reef Ecosystems of the United States and Pacific Freely Associated States: 2008 NOAA Technical Memorandum NOS NCCOS 73 NOAA/NCCOS Center for Coastal Monitoring and Assessment's Biogeography Team, Silver Spring, MD 219-261

Garcia AM, Calder RB, Dollé MET, Lundell M, Kapahi P, Vijg J (2010) Age- and Temperature-Dependent Somatic Mutation Accumulation in *Drosophila melanogaster*. PLoS Genetics 6:e1000950

Gateno D, Leon A, Barki Y, Cortes J, Rinkevich B (2003) Skeletal tumor formations in the massive coral *Pavona clavus*. Marine Ecology Progress Series 258:97-108

Grigg RW, Maragos JE (1974) Recolonization of hermatypic corals on submerged lava flows in

Hawaii. Ecology:387-395

Haapkylä J, Unsworth RK, Flavell M, Bourne DG, Schaffelke B, Willis BL (2011) Seasonal rainfall and runoff promote coral disease on an inshore reef. PLoS ONE 6:e16893

Harvell CD, Mitchell CE, Ward JR, Altizer S, Dobson AP, Ostfeld RS, Samuel MD (2002) Ecology - Climate warming and disease risks for terrestrial and marine biota. Science 296:2158-2162

Harvell CD, Jordán-Dahlgren E, Merkel S, Rosenberg E, Raymundo L, Smith GW, Weil E, Willis BL (2007) Coral disease, environmental drivers and the balance between coral and microbial associates. Oceanography 20:58-81

Harvell D, Altizer S, Cattadori IM, Harrington L, Weil E (2009) Climate change and wildlife diseases: When does the host matter the most? Ecology 90:912-920

Heron SF, Willis BL, Skirving WJ, Eakin CM, Page CA, Miller IR (2010) Summer Hot Snaps and Winter Conditions: Modelling White Syndrome Outbreaks on Great Barrier Reef Corals. PLoS ONE 5:e12210

Holt RD, Dobson AP, Begon M, Bowers RG, Schauber EM (2003) Parasite establishment in host communities. Ecology Letters 6:837-842

Hughes T, Jackson J (1980) Do corals lie about their age? Some demographic consequences of partial mortality, fission, and fusion. Science 209:713-715

Hughes T, Jackson J (1985) Population dynamics and life histories of foliaceous corals. Ecological Monographs:142-166

Hughes TP (1984) Population dynamics based on individual size rather than age: a general model with a reef coral example. American Naturalist:778-795

Hunter C (1999) First records of coral disease and tumors on Hawaiian reefs. Proceedings of the

Hawaii Coral Reef Monitoring Workshop Hawaii Division of Aquatic Resources, Honolulu:73-97

Irikawa A, Casareto BE, Suzuki Y, Agostini S, Hidaka M, van Woesik R (2011) Growth anomalies on *Acropora cytherea* corals. Marine Pollution Bulletin 62:1702-1707

Johnson AG (2008) Groundwater discharge from the leeward half of the Big Island, Hawai'i. Master of Science, University of Hawaii, p158

Jokiel PL, Morrissey JI (1993) Water motion on coral reefs-Evaluation of the clod card technique. Marine Ecology-Progress Series 93:175-181

Kaczmarsky L (2006) Coral disease dynamics in the central Philippines. Dieases of Aquatic Organisms 69:9-21

Kaczmarsky L (2009) Characterizations of the major coral diseases of the Philippines: ulcerative white spot disease and novel growth anomalies of *Porites*. Ph.D., Florida International University, p169

Kaczmarsky L, Richardson LL (2007) Transmission of growth anomalies between Indo-Pacific *Porites* corals. Journal of Invertebrate Pathology 94:218-221

Kaczmarsky L, Richardson LL (2010) Do elevated nutrients and organic carbon on Philippine reefs increase the prevalence of coral disease? Coral Reefs 30:253-257

Kaczmarsky LT, Draud M, Williams EH (2005) Is there a relationship between proximity to sewage effluent and the prevalence of coral disease. Caribbean Journal of Science 41:124-137

Kim K, Harvell CD (2004) The rise and fall of a six-year coral-fungal epizootic. American Naturalist 164:S52-S63

Klaus JS, Frias-Lopez J, Bonheyo GT, Heikoop JM, Fouke BW (2005) Bacterial communities

inhabiting the healthy tissues of two Caribbean reef corals: interspecific and spatial variation. Coral Reefs 24:129-137

Kline DI, Kuntz NM, Breitbart M, Knowlton N, Rohwer F (2006) Role of elevated organic carbon levels and microbial activity in coral mortality. Marine Ecology-Progress Series 314:119-125

Knee K, Street J, Grossman E, Payton A (2008) Submarine Ground Water Discharge and Fate Along the Coast of Kaloko-Honokōhau National Historical Park, Hawai'i; Part 2, Spatial and Temporal Variations in Salinity, Radium-Isotope Activity, and Nutrient Concentrations in Coastal Waters, December 2003-April 2006 USGS Scientific Investigations Report 2008-5128 38

Knee KL, Street JH, Grossman EE, Boehm AB, Paytan A (2010) Nutrient inputs to the coastal ocean from submarine groundwater discharge in a groundwater-dominated system: Relation to land use (Kona coast, Hawaii, USA). Limnology and Oceanography 55:1105-1122

Koelle K, Pascual M, Yunus M (2005) Pathogen adaptation to seasonal forcing and climate change. Proceedings of the Royal Society B: Biological Sciences 272:971-977

Kuta KG, Richardson LL (2002) Ecological aspects of black band disease of corals: relationships between disease incidence and environmental factors. Coral Reefs 21:393-398

Lafferty KD (2009) The ecology of climate change and infectious diseases. Ecology 90:888-900

Lafferty KD, Harvell CD (in press) The Role of Infectious Diseases in Marine Communities. In: Bertness MD, Bruno JF (eds) Marine Community Ecology,

Lesser MP, Weis VM, Patterson MR, Jokiel PL (1994) Effects of morphology and water motion on carbon delivery and productivity in the reef coral, *Pocillopora damicornis* (Linnaeus):

Diffusion barriers, inorganic carbon limitation, and biochemical plasticity. Journal of Experimental Marine Biology and Ecology 178:153-179

Lough J, Barnes D (2000) Environmental controls on growth of the massive coral *Porites*. Journal of Experimental Marine Biology and Ecology 245:225-243

Loya Y (1976) The Red Sea coral *Stylophora pistillata* is an r strategist. Nature:478-480

Loya Y, Bull G, Pichon M (1984) Tumor formations in scleractinian corals. Hegolwiss Meeresunters 37:99-112

Malins DC, McCain BB, Landahl J, Myers MS, Krahn MM, Brown DW, Chan S-L, Roubal WT (1988) Neoplastic and other diseases in fish in relation to toxic chemicals: an overview. Aquatic Toxicology 11:43-67

Maynard JA, Anthony KRN, Harvell CD, Burgman MA, Beeden R, Sweatman H, Heron SF, Lamb JB, Willis BL (2011) Predicting outbreaks of a climate-driven coral disease in the Great Barrier Reef. Coral Reefs 30:485-495

McClanahan T, Maina J, Moothien-Pillay R, Baker A (2005) Effects of geography, taxa, water flow, and temperature variation on coral bleaching intensity in Mauritius. Marine Ecology-Progress Series 298:131-142

McClanahan TR, Weil E, Maina J (2009) Strong relationship between coral bleaching and growth anomalies in massive *Porites*. Global Change Biology 15:1804-1816

Miller J, Muller E, Rogers C, Waara R, Atkinson A, Whelan KRT, Patterson M, Witcher B (2009) Coral disease following massive bleaching in 2005 causes 60% decline in coral cover on reefs in the US Virgin Islands. Coral Reefs 28:925-937

Myers MS, Landahl JT, Krahn MM, McCain BB (1991) Relationships between hepatic neoplasms and related lesions and exposure to toxic chemicals in marine fish from the US

West Coast. Environ Health Perspective 90:7

Myers RL, Raymundo LJ (2009) Coral disease in Micronesian reefs: a link between disease prevalence and host abundance. Diseases of Aquatic Organisms 87:97-104

Nagelkerken I, Buchan K, Smith GW, Bonair K, Bush P, Garzon-Ferreira J, Botero L, Gayle P, Harvell CD, Heberer C, Kim K, Petrovic C, Pors L, Yoshioka P (1997) Widespread disease in Caribbean sea fans: II. Patterns of infection and tissue loss. Marine Ecology-Progress Series 160:255-263

Oki DS (1999) Geohydrology and numerical simulation of the ground-water flow system of Kona, island of Hawaii. In: Report USGSWRI (ed) pp 4073

Ouillon S, Douillet P, Lefebvre J-P, Le Gendre R, Jouon A, Bonneton P, Fernandez J-M, Chevillon C, Magand O, Lefèvre J (2010) Circulation and suspended sediment transport in a coral reef lagoon: The south-west lagoon of New Caledonia. Marine Pollution Bulletin 61:269-296

Parsons ML, Walsh WJ, Settlemier CJ, White DJ, Ballauer JM, Ayotte PM, Osada KM, Carman B (2008) A multivariate assessment of the coral ecosystem health of two embayments on the lee of the island of Hawai ‘i. Marine Pollution Bulletin 56:1138-1149

Pascual M, Bouma MJ, Dobson AP (2002) Cholera and climate: revisiting the quantitative evidence. Microbes and Infection 4:237-245

Pascual M, Cazelles B, Bouma M, Chaves L, Koelle K (2008) Shifting patterns: malaria dynamics and rainfall variability in an African highland. Proceedings of the Royal Society B: Biological Sciences 275:123-132

Patz JA, Olson SH, Uejio CK, Gibbs HK (2008) Disease emergence from global climate and land use change. Medical Clinics of North America 92:1473-1491

Peters EC, Halas JC, McCarty HB (1986) Calicoblastic neoplasms in *Acropora palmata*, with a review of reports on anomalies of growth and form in corals. Journal of the National Cancer Institute 76:895-912

Peterson RN, Burnett WC, Glenn CR, Johnson AG (2009) Quantification of point-source groundwater discharges to the ocean from the shoreline of the Big Island, Hawaii. Limnology and Oceanography 54:890-904

Pinheiro JC, Bates DM (2000) Mixed-Effects Models in S and S-Plus. Springer, New York, NY

Putnam NH, Srivastava M, Hellsten U, Dirks B, Chapman J, Salamov A, Terry A, Shapiro H, Lindquist E, Kapitonov VV (2007) Sea anemone genome reveals ancestral eumetazoan gene repertoire and genomic organization. Science 317:86-94

Puttick GM (1986) Utilization of evergreen and decidous oaks by the Californian oak moth P*hryganidia californica*. Oecologia 68:589-594

Roff G, Kvennefors ECE, Fine M, Ortiz J, Davy JE, Hoegh-Guldberg O (2011) The ecology of 'acroporid white syndrome', a coral disease from the southern Great Barrier Reef. PLoS ONE 6:e26829

Ruiz-Moreno D, Willis BL, Page AC, Weil E, Croquer A, Vargas-Angel B, Jordan-Garza AG, Jordan-Dahlgren E, Raymundo L, Harvell CD (2012) Global coral disease prevalence associated with sea temperature anomalies and local factors. Diseases of Aquatic Organisms 100:249-261

Rutzler K, DL. S, A. A (1983) The black band disease of Atlantic reef corals. Marine Ecology 4:329–358

Sato Y, Bourne DG, Willis BL (2009) Dynamics of seasonal outbreaks of black band disease in an assemblage of *Montipora* species at Pelorus Island (Great Barrier Reef, Australia).

Proceedings of the Royal Society B: Biological Sciences 276:2795-2803

SCD-TSA Kaloko Makai L (2010) Environmental Assessment/ Environmental Impact Statement Preparation Notice:Kaloko Makai Kaloko and Kohanaiki, North Kona, Island of Hawaii. Wilson Okamoto Corporation, Honolulu

Sekar R, Kaczmarsky LT, Richardson LL (2008) Microbial community composition of black band disease on the coral host *Siderastrea siderea* from three regions of the wider Caribbean. Marine Ecology Progress Series 362:85-98

Spies NP, Takabayashi M (2013) Expression of galaxin and oncogene homologs in growth anomaly in the coral *Montipora capitata*. Diseases of Aquatic Organisms 104:249-256

Stimson J (2010) Ecological characterization of coral growth anomalies on *Porites compressa* in Hawai`i. Coral Reefs 30:133-142

Storlazzi C, Brown E, Field M, Rodgers K, Jokiel P (2005) A model for wave control on coral breakage and species distribution in the Hawaiian Islands. Coral Reefs 24:43-55

Street JH, Knee KL, Grossman EE, Paytan A (2008) Submarine groundwater discharge and nutrient addition to the coastal zone and coral reefs of leeward Hawai'i. Marine Chemistry 109:355-376

Sutherland KP, Porter JW, Torres C (2004) Disease and immunity in Caribbean and Indo-Pacific zooxanthellate corals. Marine Ecology-Progress Series 266:273-302

Sutherland KP, Porter JW, Turner JW, Thomas BJ, Looney EE, Luna TP, Meyers MK, Futch JC, Lipp EK (2010) Human sewage identified as likely source of white pox disease of the threatened Caribbean elkhorn coral, *Acropora palmata*. Environmental Microbiology 12:1122-1131

Thurber RV, Willner-Hall D, Rodriguez-Mueller B, Desnues C, Edwards RA, Angly F, Dinsdale

E, Kelly L, Rohwer F (2009) Metagenomic analysis of stressed coral holobionts. Environmental Microbiology 11:2148-2163

Torréton J-P, Rochelle-Newall E, Jouon A, Faure V, Jacquet S, Douillet P (2007) Correspondence between the distribution of hydrodynamic time parameters and the distribution of biological and chemical variables in a semi-enclosed coral reef lagoon. Estuarine, Coastal and Shelf Science 74:766-776

Vargas-Angel B (2009) Coral health and disease assessment in the US Pacific Remote Island Areas. Bulletin of Marine Science 84:211-227

Vargas-Ángel B, Wheeler B (2009) Coral health and disease assessment in the US Pacific Territories and Affiliated States. Proceedings of 11th International Coral Reef Symposium, Ft Lauderdale:175-179

Voss JD, Richardson LL (2006) Nutrient enrichment enhances black band disease progression in corals. Coral Reefs 25:569-576

Walsh WJ, Cotton S, Barnett C, Couch CS, Preskitt L, Tissot B, Osada-D'Avella K (2013) Long-term monitoring of coral reefs of the Main Hawaiian Islands. Final report 2009 NOAA Coral Reef Conservation Report; NA06NOS4260113 97

Whitfield RP (1901) Notice of a remarkable case of combination between two different genera of living corals. Bulletin of the American Museum of Natural History 14:221-222

Williams GJ, Aeby GS, Cowie ROM, Davy SK (2010) Predictive Modeling of Coral Disease Distribution within a Reef System. PLoS ONE 5:e9264

Willis BL, Page CA, Dinsdale EA (2004) Coral Disease on the Great Barrier Reef. In: Rosenberg E, Loya Y (eds) Coral Health and Disease. Springer-Verlag, Berlin, pp 69-104

Work TM, Aeby GS, Coles SL (2008) Distribution and morphology of growth anomalies in

Acropora from the Indo-Pacific. Diseases of Aquatic Organisms 78:255-264

Yamashiro H, Yamamoto M, van Woesik R (2000) Tumor formation on the coral *Montipora informis*. Diseases of Aquatic Organisms 41:211-217

Yamashiro H, Oku H, Onaga K, Iwasaki H, Takara H (2001) Coral tumors store reduced levels of lipids. Journal of Experimental Marine Biology and Ecology 265:171-179

Yasuda N, Nakano Y, Yamashiro H, Hidaka M (2011) Skeletal structure and progression of growth anomalies in *Porites australiensis* in Okinawa, Japan. Diseases of Aquatic Organisms 97:237

Zuk M, Stoehr AM (2002) Immune defense and host life history. American Naturalist 160:S9-S22

Zuur AF, Ieno EN, Walker N, Saveliev AA, Smith GM (2009) Mixed effects models and extensions in ecology with R. Springer

CHAPTER 4

TEMPORAL DYNAMICS AND PLASTICITY IN THE CELLULAR IMMUNE RESPONSE OF THE SEA FAN CORAL, *GORGONIA VENTALINA*

Published as Couch, C. S., Weil, E., & Harvell, C. D. Temporal dynamics and plasticity in the cellular immune response of the sea fan coral, *Gorgonia ventalina*. Marine Biology, 1-12.

ABSTRACT

The temporal dynamics of the invertebrate immune response often determine an organism's success in responding to physiological stress, physical damage and pathogens. To date, most immune challenge studies have been conducted under highly controlled laboratory conditions, with few attempts to study immune function in the wild. In this study, we characterized the temporal dynamics of the Caribbean sea fan, *Gorgonia ventalina*, cellular immune response (granular amoebocyte aggregation and prophenoloxidase (PPO) activation) to allogenic grafts in the laboratory and field using a clonally replicated design. Amoebocyte reaction time differed markedly between the lab (% amoebocyte surface area in tissue sections peaked at 2 d) and field (peak at 6 d). PPO activity decreased between 0 and 6 d after grafting in both ungrafted and grafted tissue, suggesting PPO is decoupled from other cellular components. The reaction norms of the fold induction in % amoebocyte area between disease-grafted and healthy-grafted tissue of each colony across time indicate high intercolony plasticity in cellular immune response. The plasticity between colonies was also evident in the magnitude of cellular immune response, ranging from a 0.88- to 1.60-fold increase in amoebocyte area between initial and 6 d for the diseased-grafted tissue. With the demonstration of highly dynamic cnidarian cellular immune responses, our study expands understanding of the evolutionary ecology of metazoan immune defense mechanisms.

INTRODUCTION

The invertebrate immune system is distinct from that of vertebrates in lacking adaptive

immunity and relying solely on a diverse repertoire of innate immune defenses to recognize foreign materials, mount a response to and eradicate pathogens, remove damaged cells and heal damaged tissue (Aderem and Ulevitch 2000; Ausubel 2005; Mydlarz et al. 2006). Exploration of invertebrate innate immunity provides the foundation for studies on the evolution of immunological responses and disease dynamics (Rolff and Siva-Jothy 2003; Schmid-Hempel 2003; Miller et al. 2007). As an evolutionarily ancient component of immunity, studies are revealing that vertebrates and invertebrates alike rely heavily on a similar rapid innate immune response as their first line of defense (Aderem and Ulevitch 2000; Salzet 2001; Ausubel 2005).

Studying the innate immune system also improves our understanding of disease dynamics, which are mediated by the interaction between a microbe's pathogenicity (ability to cause disease) and host's defenses (Grenfell and Dobson 1995; Hawley and Altizer 2011). For the microbe, pathogenicity determines the ability to infect, multiply, and spread within and among hosts (Collinge and Ray 2006). Host resistance is dependent on the ability to mount an immune response and the population's level of phenotypic and genotypic variation (Schmid-Hempel 2003; Schmid-Hempel 2005). Investigating the dynamics of the innate immune response such as the type, speed, duration, magnitude and plasticity of response is especially important for understanding an organism's capacity to effectively respond to environmental change, pathogens, and damage.

The invertebrate innate immune system is comprised of a synchronized series of humoral and cellular components (reviewed by Loker et al. 2004; Mydlarz et al. 2006). Humoral components exist as free floating compounds that are constitutively present throughout the organism and are therefore generally the first to respond to stimuli (reviewed by Loker et al. 2004; Mydlarz et al. 2006). Cellular immunity is an induced response utilized across a range of

invertebrate taxa (George et al. 1978; Beck et al. 1993; Meszaros and Bigger 1999; Coteur et al. 2002; Malham et al. 2003; Borges et al. 2005; Cerenius et al. 2010) and relies on a coordinated series of events, stimulated by antigens or host signaling molecules (Beck et al. 1993). After activation, immune cells migrate to the affected site, adhere to and phagocytize and destroy the foreign cells by releasing cytotoxic compounds (reviewed by Mydlarz et al. 2006; Cerenius et al. 2010; Song et al. 2010). The timing of these immune responses dictates the efficacy with which the host clears pathogens and repairs physical damage. For example, in the oyster *Crassostrea* spp. hemocyte phagocytosis is especially important during the first three days of infection by *Perkinsus marinus*, the causative agent of Dermo disease, and is quickly followed by the production of reactive oxygen species (ROS) and parasite clearance after hemocyte apoptosis (Goedken et al. 2005). Currently, our understanding of invertebrate immune dynamics is primarily based on laboratory studies in highly controlled conditions (Adema et al. 1991; Korner and Schmid-Hempel 2004; Goedken et al. 2005; Jordan and Deaton 2005; Burge et al. 2007; Palmer et al. 2011c; Perrigault and Allam 2012), thus ignoring the role of natural variation in the biotic and abiotic environment and its implications for host immunity. Furthermore, in light of the rising number of threats, such as emergence of novel pathogens (Woolhouse et al. 2005) and climate change (Harvell et al. 2002) in the marine environment, our understanding of immune function in marine populations lags behind that of their well-studied terrestrial counterparts.

Insight into the evolution of immune function is gained by studying the most basal of metazoans, the cnidarians (Miller et al. 2007; Bosch et al. 2009; Augustin and Bosch 2010). One especially interesting cnidarian for studying *in situ* immune dynamics is the Caribbean sea fan, *Gorgonia ventalina*. Sea fans experienced widespread mortality following outbreaks of the fungal disease aspergillosis (Nagelkerken et al. 1997b; Kim and Harvell 2002; Kim and Harvell

2004; Kim et al. 2006; Mullen et al. 2006), yet some colonies displayed pronounced resistance with many surviving the epizootic (Bruno et al. 2011). This outbreak peaked during the late 1990's causing an estimated 20-90% mortality across the Florida Keys, Mexico and the Bahamas, but has since declined in prevalence (Bruno et al. 2011). Based on the documented intense selection during the epizootic and high recruitment potential of surviving resistant colonies, modeling studies support the hypothesis that the decline of the epizootic could be explained by the evolution of *G. ventalina* resistance (Bruno et al. 2011).

Following widespread mortality of *G. ventalina*, research has focused on characterizing the immune defenses in this species and their role in cnidarian physiology and disease resistance. While most studies have concentrated on the humoral responses and considerable intercolony variability (Kim et al. 2000a; Kim et al. 2000b; Dube et al. 2002; Ward et al. 2007; Couch et al. 2008), only one study has investigated *G. ventalina*'s cellular defenses (Mydlarz et al. 2008). Cnidarian hyaline (agranular) and granular amoebocytes roam the mesoglea, an extracellular matrix between the ectoderm and endoderm (Mullen et al. 2004). Granular amoebocytes phagocytize foreign particles (Patterson and Landolt 1979; Hutton and Smith 1996) and contain acidophilic granules with cytotoxic proteins used to break down phagocytized material (Olano and Bigger 2000). These amoebocytes are commonly associated with an inflammatory response involving wound healing (Meszaros and Bigger 1999; Kramarsky-Winter 2004; Vargas-Angel et al. 2007; Palmer et al. 2011c), phagocytosis of cellular debris and microorganisms (Olano and Bigger 2000), and allogeneic incompatibility (Bigger and Hildemann 1982). Mydlarz et al. (2008) also discovered a strong granular amoebocyte response in aspergillotic tissue, which was induced during exposure to the putative pathogen, *Aspergillus sydowii*, and thermal stress. This study also indicated that *G. ventalina* granular amoebocytes contain melanosomes, and are therefore implicated in the melanin-synthesis pathway. This pathway, which is activated by prophenoloxidase (PPO), is an important innate immune component of cnidarians (Palmer et al.

2010; Mydlarz and Palmer 2011; Palmer et al. 2011a; Palmer et al. 2011b; Palmer et al. 2011c) and other invertebrates (e.g. Cerenius and Soderhall 2004; Nappi and Christensen 2005), and is associated with the production of cytotoxic secondary defense compounds and physiochemical barriers. The role of this pathway in *G. ventalina* defense if further evidenced by the use of melanin to encapsulate fungal hyphae and other endoparasites in the gorgonin (Petes et al. 2003; Mullen et al. 2004; Burge et al. 2012) and elevated PPO activity in diseased tissue compared to healthy tissue (Mydlarz et al. 2008). Modeling studies of sea fan immunity also suggest the importance of timing in cellular immune response as critical to infection dynamics (Ellner et al. 2007), but there have been no empirical studies on the temporal dynamics or variation in cellular immune response, nor studies of the immune response in wild *G. ventalina* populations.

While most studies of *G. ventalina* immune function have been conducted under laboratory conditions, Alker et al. (2004) developed a method for eliciting host responses in the field using allografting (non-self). Alker and colleagues excised diseased tissue from irregular purple lesions (aspergillotic like, see Nagelkerken et al. 1997b for full description) and healthy tissue from a distal region of the same diseased fan, and then grafted (allogenic) these fragments to apparently healthy sea fans (no gross lesions). They found that allografting elicited a pigmentation response in apparently healthy sea fans.

Improving our understanding of immunodynamics in cnidarians in laboratory and wild populations can both enhance our understanding of the evolution of metazoan immune defenses and elucidate disease dynamics particularly in light of rising disease-associated coral mortality. Based on the added physical stress associated with laboratory manipulations and high intercolony variation in constitutive *G. ventalina* immunity we hypothesize that: 1. *G. ventalina* cellular response will not differ in the lab compared to the field; and 2. cellular immune response

will not demonstrate considerable plasticity in timing and magnitude. To test these null hypotheses we conducted a clonally replicated laboratory and field experiment using fragments from apparently healthy colonies grafted with diseased and apparently healthy allografts to determine the magnitude and plasticity of the cellular immune response. In a second field experiment, we used similar grafting methods to measure amoebocyte and PPO response in intact undisturbed colonies in the field.

METHODS

Timeline of immune response in lab

Fragments from the edge of eight apparently healthy (no gross lesions) *G. ventalina* colonies were collected from Looe Key, Florida Keys, USA (24°34.138N, 81° 22.939W) in February 2008. Fragments were wrapped individually in wet bubble wrap, put in separate resealable plastic bags, wrapped in newspaper, surrounded by heat packs and shipped overnight to Cornell University. Fragments were divided into 7 x 4 cm pieces, strung on polypropylene lines with cable ties in artificial seawater-filled aquaria, and acclimated for one week. Using allografting methods described by Alker et al. (2004), fragments were grafted with either a treatment or control. Treatments included a 2 x 2 cm allograft from irregular purple lesions (aspergillotic-like) from one diseased *G. ventalina* colony, henceforth referred to as "diseased graft" (Fig. 4.1A). The control consisted of apparently healthy allografts (henceforth, "healthy graft") from the same diseased colony (2 x 2 cm) (Fig. 4.1A). All grafts were attached to the experimental fragments using 4-inch cable ties threaded through the sea fan mesh

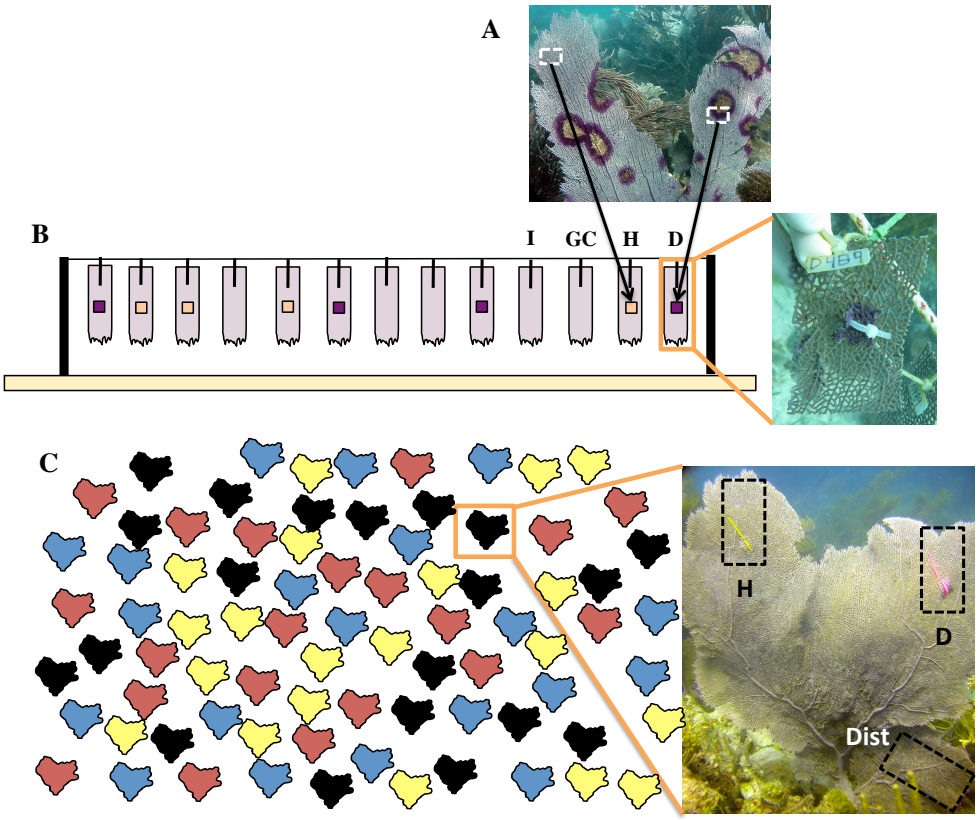

Figure 4.1. Diagram of experimental design (A) Example diseased colony with irregular purple (aspergillotic-like) lesions used as a donor colony for diseased and healthy grafts (white boxes) for laboratory and field experiments. *Note:* multiple donor colonies were used in each experiment and multiple tissue grafts were extracted from each donor colony. (B) Example of clonally-replicated experimental design (lab and field experiment) with 7 x 4 cm *G. ventalina* fragments from one parent colony strung along a nylon line with initial treatments and controls attached with cable ties (I= Initial, GC=graft control, H=healthy-grafted, D=diseased-grafted). *Note: G. ventalina* fragments from all colonies are not shown (C) intact colony experimental design: 80 colonies were grafted with a diseased graft (D) and healthy graft (H) with cable ties at 0 d. A 7 x 4 cm area of tissue around the grafts (D & H), as well as ungrafted distal tissue (Dist) were collected from 20 different colonies at 4 time points (yellow= colonies sampled at 2 d, black = 6 d, red = 10 d, blue = 14 d). *Note:* 15 apparently healthy colonies sampled at t = 0 not shown).

network for the duration of the experiment (Fig. 4.1B). A clonally replicated designed was employed, whereby six fragments from each of the eight sea fans were grafted on day 0 with either a diseased or healthy graft. One diseased-grafted and one healthy-grafted fragment from each colony was photographed, and collected at 1, 2, and 4 d (Fig. 4.1B). A 3 x 3 cm area surrounding and including the grafted area on each fragment was excised, placed in a Whirl-pak® and immediately fixed in 1:4 zinc-buffered formalin (Z-Fix Concentrate, Anatech, Ltd.) diluted with artificial seawater for histological analyses. One fragment from each colony was collected at day 0 (initial) prior to the grafts being applied and fixed in the Z-Fix solution.

Clonally replicated timeline of immune response in field

In May 2008, fragments from the edge of 15 large (> 40 cm^2) apparently healthy colonies (no gross lesions in the field) were collected from a robust *G. ventalina* population at Media Luna Reef, La Parguera, Puerto Rico (17°56.093′ N, 67°02.931′ W). Due to strong weather conditions Media Luna Reef would have been inaccessible during all the proposed sampling time points. Therefore, thirteen 7 x 4 cm fragments from each colony were transplanted to Mario Reef (17°57.167′ N, 67°0388′ W), a protected patch reef located inside the La Parguera reef system and approximately 1.5 km from Media Luna. The reef borders a sandy platform (10-12 feet deep) with a channel, which facilitates good water circulation in the otherwise calm sandy platform. This experiment was not designed to test the immune function of two populations (Media Luna and Mario Reef) in response to changes in environment. Reebar stakes were pounded into the sandy bottom and strung with line 1 meter above the substrate. *G. ventalina* transplants were secured to the line with labeled 4-inch cable ties and acclimated for 2 d prior to grafting (Fig. 4.1B). One fragment from each colony was transplanted back to Media Luna Reef and secured to a line one meter above the substrate to determine the effect of transplantation on

constitutive cellular immune activity (transplant control). At Mario Reef, one fragment from each fan was collected at day 0, placed in a Whirl-Pak®, immediately transported to shore, and fixed in 10% seawater-buffered formalin. Diseased and apparently healthy tissue from the diseased colonies (Fig. 1A) were collected from four diseased fans at Media Luna Reef and divided into 2 x 2 cm allografts on day 0. A similar clonally replicated design was used, whereby the remaining fragments were grafted with either disease allografts (2 x 2 cm), apparently healthy allografts from the diseased colony (2 x 2 cm), or did not receive a graft (graft control) (Fig. 4.1B). Graft controls were used to control for constitutive changes in amoebocytes over time. One fragment from each colony and treatment/control was photographed, collected at 1, 2, 4, and 6 d and transported to shore in a Whirl-Pak®. The transplant control fragments were collected at 6 days post grafting. On shore, each fragment was photographed again without the graft to create a reference point for histological analysis. Each fragment was divided longitudinally through the center of the grafted region. Half was fixed in 10% seawater-buffered formalin for histological analysis while the other half was flash frozen in liquid nitrogen, stored at -80°C and shipped to Cornell University on dry ice for biochemical assays. To examine for the presence of fungal hyphae in the grafts, a subset of apparently healthy (n= 7 on day 4, n=3 on day 6) and diseased grafts (n = 10 on day 4, n = 5 on day 6) were also fixed for histological analysis. All histological samples were also shipped to Cornell University for further processing.

Immune response of intact fans in the field

The cellular immune responses to allografts were tested on un-manipulated apparently healthy fans in June 2009, on a patch reef between Media Luna and Laurel reef in La Parguera, Puerto Rico (17°56.093′ N, 67°02.931′ W). To assess initial amoebocyte area and PPO activity, 7 x 4 cm fragments from the edge of 15 apparently healthy large (> 50 cm^2) fans were collected,

transported to shore, divided in half, and preserved for histological (n = 15) and biochemical immune assays (n = 15) using the methods described above. Diseased and healthy tissue fragments were collected from five diseased fans and divided into 2 x 2 cm sections to serve as allografts. One diseased and one healthy allograft were applied to each of 80 apparently healthy large fans 5 cm from the colony edge (Fig. 4.1C). Diseased and healthy grafts were situated 20 cm from each other on each colony. At 2, 6, 10, and 14 d, a 7 x 4 cm section of tissue surrounding and including each graft was collected from 20 of the fans. An ungrafted region (henceforth, "distal") 20 cm from the grafts was also collected from each fan at each time point to assess systemic induction (n= 20 colonies/time point/treatment + 15 initial apparently healthy colonies). The fragments were transported, photographed, divided longitudinally, fixed or frozen, and shipped as described above. To examine for the presence of fungal hyphae in the grafts, a subset of 6 d apparently healthy (n= 7) and diseased grafts (n = 8) were also fixed for histological analysis.

Histological Preparation

All fixed samples were trimmed to a 3 x 3 cm fragment surrounding the grafted region, placed in a histological cassette, rinsed thoroughly in deionized water, and then decalcified in 10% neutral pH EDTA for 4 d. Samples were embedded in paraffin wax, sectioned at 5 μm thickness and mounted on slides at the Cornell University's Veterinary Histology Laboratory. De-paraffinized sections were stained with hematoxylin and eosin and cover-slipped prior to microscopy.

Quantification of Amoebocyte Surface Area

Amoebocyte surface area was calculated using methods adapted from Mydlarz et al.

(2008). A grid of 5-mm quadrats was drawn on each slide with a permanent marker and covered the entire tissue area (approximately 12–18 quadrats/slide). For initial and no-graft slides, four quadrats were randomly selected using a random number generator. For the grafted tissue slides, four quadrats directly adjacent to the grafted area were chosen. Within each selected quadrat, 3 points were chosen using randomly selected coordinates. At each point, photographs were taken using an Olympus BH-2 compound light microscope and Olympus DP-20 camera system at 40X magnification. Images were transported to Image *J* (National Institutes of Health) then calibrated using a Hausser Scientific Company Bright Line Counting Hemacytometer. Each image was converted into black and white pixels using the binary function and the automatically calibrated threshold. The threshold level was automatically determined by analyzing the histogram of the entire image. The threshold function divides the image into objects and background by taking a test threshold and computing the average of the pixels at or below the threshold and pixels above. For this study, the threshold was automatically set at 1 for all analyses. The darkly stained amoebocytes are the only cell type detected by the threshold analysis. Total surface area of each image was approximately 0.02 mm^2, and amoebocyte coverage was expressed in percent of the image total surface area (coenenchyme).

Extract Preparation and PPO Assay

Approximately 2 g of each frozen sample was ground to a fine powder with a mortar and pestle in liquid nitrogen. The powder was extracted in 0.2 M phosphate buffer, pH 7.8 with 5mM β-mercaptoethanol (Sigma-Aldrich, St. Louis, Missouri) for 45 min on ice. Extracts were centrifuged at 405x g and the supernatant was recovered and centrifuged again at 14,000x g to remove lipids and cellular debris. The protein concentration in each extract was determined using the Bio-Rad DC Protein Assay Kit (Hercules, California) with a bovine serum albumin standard.

Extracts were stored at -80 °C between assays.

Prophenoloxidase (PPO) activity was assayed by aliquoting 20 µl of coral extract into duplicate wells in a 96-well microtiter plate with 100 µl of molecular grade water (Sigma-Aldrich, St. Louis, Missouri). To each well, 20 µl of 0.05 mg ml^{-1} trypsin in molecular grade water was added and the plates were incubated for 15 min at 4 °C. The reaction was initiated by the addition of 50 µl of 10 mM l^{-1} L-1,3-dihydroxyphenylalanine (L-DOPA; Sigma-Aldrich). The absorbance at 490 nm was measured at 0 and 20 min (during the linear portion of the reaction) and the change in absorbance was normalized to mg protein in each sample. The assay was run in duplicate for each sample.

Statistical Analyses

All data were analyzed using R, version 2.13.2 and checked for normality and homoscedasticity. PPO activity was power transformed with a Box-Cox transformation. Amoebocyte data from all experiments were analyzed with linear mixed-effect models (MEM) and maximum likelihood estimation using the lme4 package (Bates and Maechler 2009). In each dataset, treatment and time were specified as fixed effects and slide quadrat nested within colony as well as colony as random effects. To determine effects of our fixed factors, we fitted each model using maximum likelihood estimation, compared each fixed effect model to the null random effects model, and then conducted sequential model selection by comparing single fixed effect models to the full interaction model (Burnham and Anderson 2002; Zuur et al. 2009) using Likelihood ratio tests with chi-square test statistics and Akaike information criterion (AIC) (Burnham and Anderson 2002). The best-fit model was fit with restricted maximum likelihood (REML). Due to the difficulties with performing *post hoc* tests on MEMs, we used the Markov chain Monte Carlo (MCMC) simulation to detect differences between treatments at specific time

points (see Baayen et al. 2008). MCMC generates random samples from a posterior distribution of parameter values for fixed and random effects (Bolker et al. 2009). We conducted 50,000 interations to estimate the highest posterior density (HPD) interval for each parameter, using 95% of the probability distribution (credible intervals). HPD intervals that did not overlap zero indicated conservative significant effects of the specified parameters $\alpha = 0.05$ (Pinheiro and Bates 2000). MEMs with Helmert contrasts and Tukey's HSD *post hoc* tests were used to test whether grafted tissue and ungrafted tissue varied significantly from initial tissue or the transplant control. To determine the magnitude of amoebocyte response, we calculated the fold difference by dividing % amoebocyte area in disease-grafted tissue by % amoebocyte area in healthy-grafted tissue or initial for each colony across time. We applied an arbitrary 10% threshold (10% = 1.10 fold difference) to define amoebocyte response (disease-grafted tissue % amoebocyte area > healthy-grafted or initial tissue). The intact colony PPO data were analyzed with a two-way ANOVA to test PPO activity as a function of treatment and sampling time. The statistical differences in PPO activity as a function of treatment (diseased and healthy grafts) and time were analyzed using Tukey's HSD *post hoc* tests.

RESULTS

Timeline of immune response in lab

Amoebocyte area varied significantly as a function of treatment (AIC=1343.2, χ^2 = 26.103, df= 2, $p<0.0001$) and time (AIC=1345.7, χ^2 = 25.623, df= 3, $p<0.0001$), but was best explained by the interaction treatment and time (AIC=1117, χ^2 = 58.205, df= 5, $p<0.0001$). Diseased-grafted fans demonstrated a transient amoebocyte response with a significant increase from the initial to 1 d (HPD intervals 0.988, 3.570), and a peak in response at 2 d (25.31 ± 1.21

%, n= 8) that was significantly higher than the healthy graft control (18.98 ± 1.02 %, n=8, HPD intervals -7.601, -0.678) and a subsequent relaxation (Fig. 4.2). The healthy graft control showed a gradual decline over time, but was not significantly lower than initial amoebocyte area

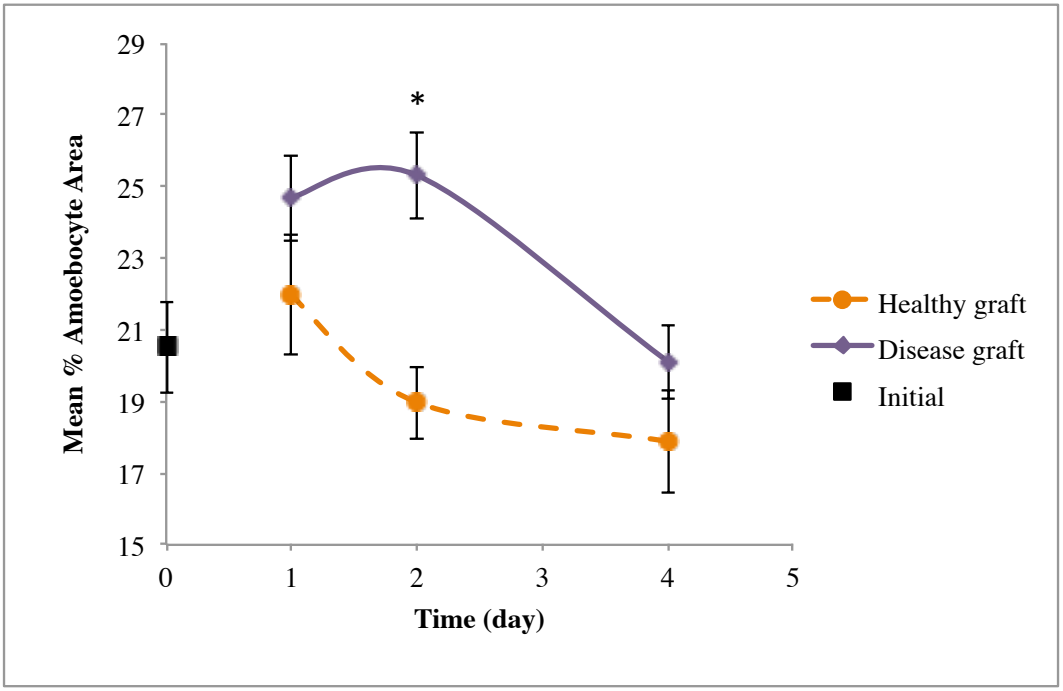

Figure 4.2. Laboratory clonally replicated experiment. Mean ± S.E. % surface area of granular amoebocytes within the coenenchyme measured before grafting and after grafting with a diseased graft (from aspergillotic-like lesion) and apparently healthy tissue (n= 8 per treatment per time sampled). Asterisk indicates significant difference between diseased- and healthy grafted tissue (Tukey's HSD, α= 0.05).

(20.51 ± 1.29 %, n=8) until 4 d (HPD intervals -4.902, -0.385). Quad nested within colony and colonies themselves accounted for 5.32% and 25.55% of the variance in the best-fit interaction model respectively.

Clonally replicated timeline of immune response in field

Similar to the lab experiment, amoebocyte area in the field experiment varied significantly as a function of treatment (AIC=3780.3, χ^2 = 12.063, df= 2, p=0.0024) and time (AIC=3744.1, χ^2 = 50.261, df= 3, p<0.0001), but was best explained by the interaction treatment and time (AIC=3719.8, χ^2 = 90.556, df= 11, p<0.0001). However, diseased-grafted fragments showed a lag in the amoebocyte response relative to the lab experiment (Fig. 4.3). Disease-grafted tissue did not increase in amoebocyte area until 4 d, with a peak at 6 d (30.96 ± 1.67 %, n=14) that was significantly higher than the healthy graft (26.02 ± 1.78 %, HPD intervals 1.993, 3.138), initial (24.13 ± 1.32 %, HPD intervals -2.014, -1.109) and transplant control (24.14 ± 1.48 %, HPD intervals -2.022, -1.063) (Fig. 4.3). Healthy grafted fragments were not significantly different than the graft control (HPD intervals -1.049, 0.281). Amoebocyte response in the graft controls did not vary significantly over time (HPD intervals -0.006, 0.024). Amoebocyte area in the graft control was not significantly different from the mean initial amoebocyte area (HPD intervals -0.421, 0.867). Furthermore, there was no apparent effect of transplantation on amoebocyte response at 6 d compared to initial levels (HPD intervals -1.143, 1.147) and the graft control at 6 d (HPD intervals -1.791, 0.661).

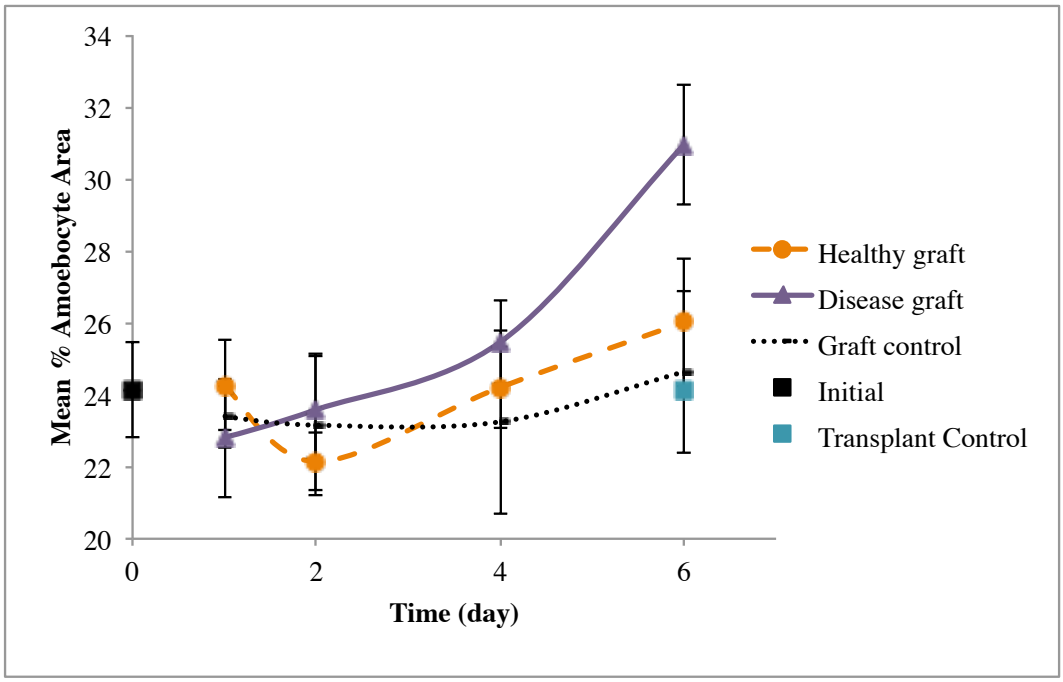

Figure 4.3. Field repeated-measures experiment. Mean ± S.E. % area of granular amoebocytes within the coenenchyme measured before grafting and after grafting with a disease grafted (from aspergillotic-like lesion) and apparently healthy tissue. Ungrafted tissue (graft control) was sampled over time to control for effects of grafting and a transplant control was collected at 6 d from Media Luna Reef. N = 10–14 colonies/treatment/time. Asterisk indicates significant difference between diseased- and healthy- grafted tissue (Tukey's HSD, $\alpha = 0.05$).

Quad nested within colony and colonies themselves accounted for 0% and 26.42% of the variance in the best-fit model, respectively. The reaction norms of the fold induction in amoebocyte area between disease-grafted and healthy-grafted fragments of each colony across time indicated high intercolony plasticity (10% threshold), with one colony demonstrating no response, two colonies peaking at 2 d, two at 4 d, and six at 6 d (Fig. 4.4). This intercolony plasticity was also evident in the magnitude of response, ranging from a 0.88- to 1.60-fold increase in amoebocyte area between initial and 6 d for the diseased-grafted tissue (data not shown). 66% of the diseased and 25% of the apparently healthy grafts contained hyphae within the gorgonin axis (data not shown).

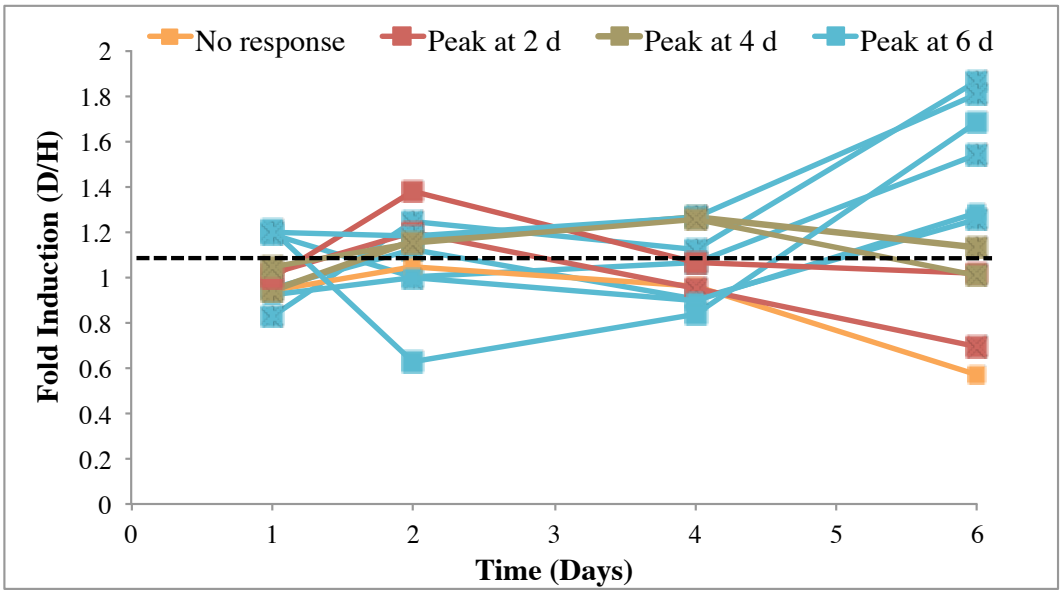

Figure 4.4. Reaction norms of magnitude of amoebocyte response for each colony across time during the clonally replicated field experiment. Lines represent the fold induction in amoebocyte area between diseased-grafted and healthy-grafted tissue. The dotted line at y = 1.10 indicates threshold level of induction of 10% increase in amoebocyte area. This figure highlights the intercolony plasticity in cellular immune response, with 1 colony demonstrating no response (orange), 2 colonies peaking at 2 d (red), 2 at 4 d (tan) and 6 peaking at 6 d.

PPO activity increased significantly between 0 and 1 d in grafted and the graft control (HPD intervals 0.180, 0.465), but did not vary as a function of treatment (AIC=40.875, χ^2 = 0.6332, df= 2, p=0.7286) or time (AIC=36.485, χ^2 = 8.3831, df= 3, p=0.397) between 1 to 4 d (data not shown). PPO activity in the transplant control was significantly higher at 6 d than initial levels (HPD intervals 0.189, 0.451), but did not vary significantly from the disease-grafted, healthy-grafted or graft controls at 6 d (HPD intervals -0.029, 0.237).

Immune response of intact fans in the field

Amoebocyte area varied significantly as a function of treatment (AIC=6254.4, χ^2 = 143.71, df= 2, p<0.0001), but not time (AIC=6396.3, χ^2 = 1.5117, df= 3, p=0.4696), and was best explained by the interaction treatment and time (AIC= 6239 χ^2 = 173.22, df= 11, p<0.0001, Fig. 4.5). While mean % amoebocyte area in grafted tissue (diseased- and healthy-grafted tissue) did not vary significantly over time (AIC= 4268.3 χ^2 = 4.1385, df= 3, p=0.2469), grafted tissue overall showed a similar time course compared to the clonally replicated field experiment, with a lag in response, a peak at 6 d and subsequent decline. Grafted tissue was significantly higher than distal tissue at 6 d (HPD intervals 1.029, 4.009) and 10 d (HPD intervals 1.536, 4.507). Amoebocyte area in distal tissue did not vary significantly over time (AIC= 1861.1 χ^2 = 2.3915, df= 3, p=0.4952), but did decrease slightly between 2 and 10 d, increased at 14 d, and was significantly lower than constitutive mean amoebocyte area in unmanipulated colonies. Quad nested within colony and colonies themselves accounted for 0% and 30.20% of the variance in the best-fit model, respectively. No fungal hyphae were detected within the subset of disease and healthy grafts at 6 d (data not shown).

PPO activity varied significantly as a function of time (ANOVA, df=3, F=5.0406, p=0.0021), but not as a function of treatment (ANOVA, df=2, F=1.6832, p=0.1881) (Fig. 4.6).

PPO activity decreased significantly in all treatments from 0 to 6 d, remained low by 10 d and increased slightly, but not significantly by 14 d (Tukey's HSD, $p<0.01$).

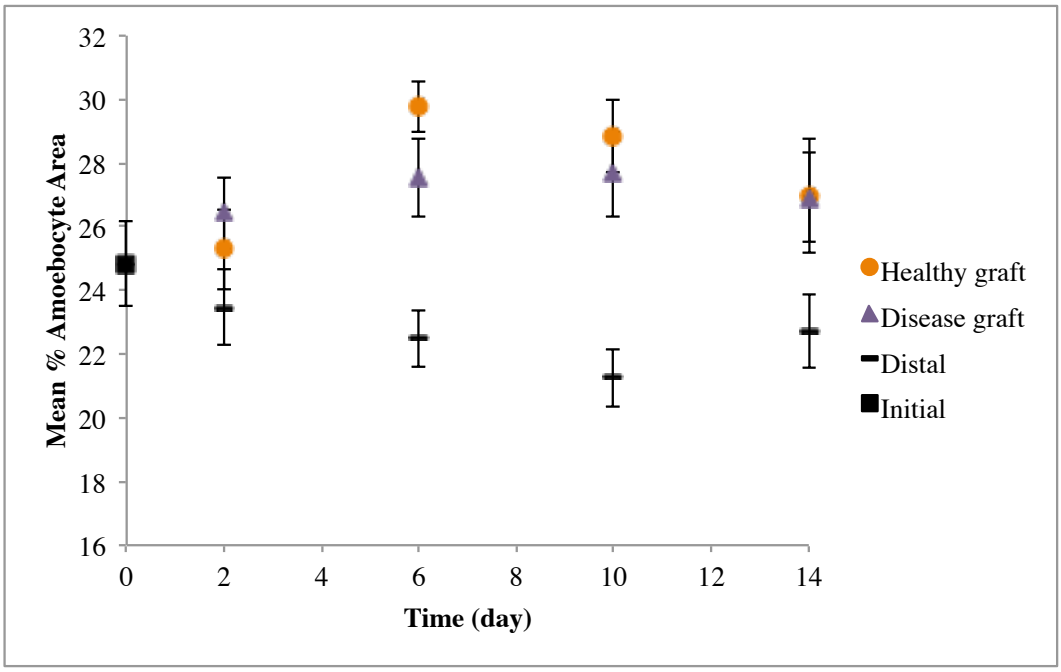

Figure 4.5. Intact colony field experiment. Mean ± S.E. % surface area of granular amoebocytes within the coenenchyme measured after grafting with a diseased graft (from aspergillotic-like lesion) and apparently healthy tissue. Distal ungrafted tissue was sampled from each grafted colony. Initial amoebocyte surface area was quantified in 15 ungrafted colonies at 0 d. Sample size was 15–20 different colonies/time. Asterisks indicate significant difference between grafted (diseased and healthy combined) and distal tissue (Tukey's HSD, $\alpha = 0.05$). Mean % surface area of granular amoebocytes is not plotted with lines because the same colonies were not sampled over time.

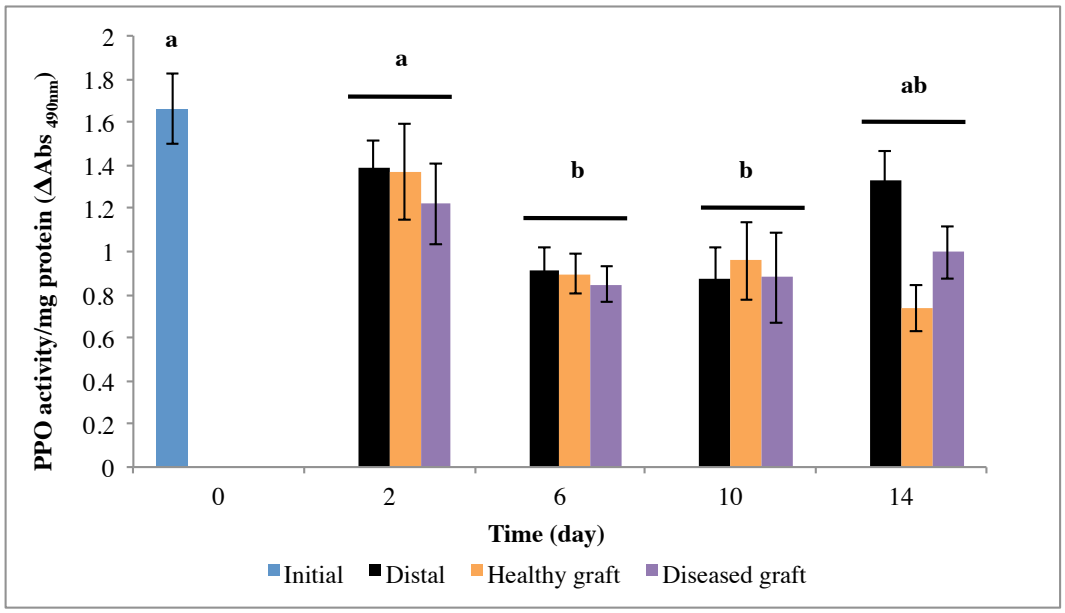

Figure 4.6. Intact colony field experiment. Mean ± S.E. prophenoloxidase (PPO) activity after grafting with a disease graft and apparently healthy tissue. Distal ungrafted tissue was sampled from each grafted colony. Initial PPO activity was measured in 15 ungrafted colonies at 0 d. N = 15–20 different colonies/time. Letters and horizontal bars indicate significant difference between time points for combined treatments and initial PPO activity (Tukey's HSD, $\alpha = 0.05$).

DISCUSSION

In this study we characterized temporal dynamics of the *G. ventalina* cellular immune response (% amoebocyte area and PPO activity) to allografts, and revealed considerable plasticity and systemic changes in immunity. This plasticity was reflected in the magnitude of intercolony variability and the differences in the time course of response between laboratory and field settings.

Under laboratory conditions, amoebocyte area increased significantly in response to diseased grafts relative to healthy grafts (Fig. 4.2). This response peaked at 2 d, and then decreased, which is consistent with previous coral laboratory studies that demonstrated the wound healing process following physical injury. In the scleractinian coral *P. cylindrica,* Palmer et al. (2011c) detected granular amoebocytes aggregation at the wound edge within 6 h, which increased steadily during the course of the experiment, but was not measured past 2 d. On the other hand, in the soft coral *Plexaurella fusifera*, amoebocyte abundance did not vary significantly over time following physical damage, but did peak at 4 days followed by a decrease in cells between 4 to 7 d (Meszaros and Bigger 1999). In other marine invertebrates, most studies have characterized the cellular immune response to pathogens during the first 24 hours after inoculation, making it difficult to compare our results to other systems.

The timing and magnitude of the *G. ventalina* cellular immune response are likely influenced by a combination of factors. The process of signal transduction, activation and migration of amoebocytes may be affected by the composition of the coenenchyme, which contains collagen fibers, and sclerites. Similar to other invertebrates (Canesi et al. 2002; Araya et al. 2010), cnidarians possess mechanisms to initiate and mount a cellular immune response such as signal transduction and immune receptors (Bosch et al. 2009), anti-microbial peptides (e.g.,

Bosch et al. 2009; Vidal-Dupiol et al. 2011)), and cytotoxic compounds (Hutton and Smith 1996; Olano and Bigger 2000; Mydlarz et al. 2008). Given the colonial nature of coral tissue, and the integration of the modules, nutrient translocation and immune responses across modules may be slower across the large surface area relative to non-modular organisms. The ability to respond to stimuli is also highly dependent on the type, pathogenicity and method of delivery of the stimulus (e.g. Mangiaterra and Silva 2001; Borges et al. 2005; Travers et al. 2009). Direct inoculations of microbial agents may elicit a temporally different immune response than physical damage or grafting due to the use of pathogen-associated molecular patterns (PAMPs), by which the host recognizes and responds to microorganisms. Although we expected all of the disease grafts to be infected with fungus, only 66% of them did. However, there was no relationship between presence of fungal hyphae and amoebocyte response, suggesting that other factors or components of the purpling response may be contributing to the difference in amoebocyte response between diseased and healthy grafts.

Contrary to our laboratory experiment, colonies from the clonally replicated field experiment mounted an amoebocyte response to diseased-grafted tissue at 6 d after grafting (Fig. 4.3), thus allowing us to reject the null hypothesis that *G. ventalina* cellular response is the same in the lab and field. To our knowledge, this is the only study of temporal dynamics of marine invertebrate immunity in a field setting. While we measured cellular immune response on slightly different time scales in these two experiments and may have missed early induction in the field experiment, this explanation seems unlikely given the unimodal response curves in other invertebrates to stimuli (e.g. Meszaros and Bigger 1999; Aladaileh et al. 2007). The altered time course between lab and field may be explained by the physiological stress such as temperature fluctuation, relocation, and physical damage, which are unavoidable during

laboratory trials, and are known to elicit a cnidarian cellular immune response (Meszaros and Bigger 1999; Mydlarz et al. 2008; Palmer et al. 2011c). The faster response in the laboratory may be the result of cellular immune priming, which is functionally similar to vertebrate immunity and has been demonstrated in other invertebrates (Kurtz and Franz 2003). For example, following physical damage hemocyte density of moth larvae was twice that of unstressed individuals after injection with a bacterial inoculum (Mowlds et al. 2008). The variation between lab and field studies may also be the result of differences in immune function at the population level as laboratory colonies originated from Florida and field experiments were conducted in Puerto Rico. However, this is a vastly greater difference in timing than expected in immune components. If the temporal dynamics were affected by interregional plasticity, this would support previous studies that have found high geographic variation in *G. ventalina* constitutive immunity (Dube et al. 2002; Couch et al. 2008). Due to the sensitivity of marine microorganisms to environmental fluctuation (Bourne et al. 2007; Thurber et al. 2009), laboratory conditions may have also altered the microbial communities within the water and sea fans themselves, thus affecting the physiological balance of the coral holobiont. While laboratory experiments are crucial for establishing baselines and assessing mechanisms of host-pathogen interactions, our results highlight the critical importance of investigating the host immune response in wild populations.

Contrary to our null hypothesis, the plasticity in timing and magnitude of immune response *in G. ventalina* varied considerably between colonies. Coral colony accounted for 25 to 30 % of the total model variance in all the experiments, and for example, only 58 % of the colonies peaked at 6 d in the clonally replicated field experiment (Fig. 4.4). This variation in amoebocyte response is consistent with previous studies that have characterized highly variable

levels of immune defenses such as peroxidase (Mydlarz and Harvell 2007), antimicrobial activity (Ward 2007), antioxidant (Palmer et al. 2011b), and PPO (Palmer et al. 2011b) in corals. Plasticity in immune function may be explained by a number of factors. First, it is likely due to intercolony genetic variation, which was not investigated in this study. Secondly, given that grafted tissue was collected from multiple colonies, intercolony variation in the donor diseased colony may explain a portion of the plasticity in response. This hypothesis is, however, unlikely because there was no relationship between % amoebocyte area and the identity of the donor colony over time (data not shown).

Given the potential for prior physical damage to affect the rate of immune response and to confirm the timing of response on a wider population level, we tested the cellular immune response of intact colonies in a second field experiment. Interestingly, we measured an increase in amoebocyte area to grafts and a decline in amoebocytes in distal tissue along the same time course (Fig. 4.5). This could be explained if grafting elicited amoebocyte migration from distal regions to affected areas. Similar systemic changes have also been observed in *P. fusifera* following physical damage (Meszaros and Bigger 1999), but not in response to *A. sydowii* in *G. ventalina* (Mydlarz et al. 2008), suggesting that whole colony protection is not ubiquitous across biotic and abiotic assaults. Overall, temporal dynamics to grafted tissue are remarkably similar in both the clonally replicated and intact colony field experiments, with an increase in amoebocyte area until 6 d. Inconsistent with the clonally replicated field experiment, amoebocyte response in the intact colonies to diseased-grafts did not differ from the healthy grafted tissue (Fig. 4.5). One explanation is that active fungal hyphae were present in a subset of disease grafts in the clonally replicated experiment, but not in diseased grafts in the intact colony experiment. Another explanation is that while our study was not intended to characterize *G. ventalina*

histocompatibility, amoebocyte response to healthy grafts may be the result of non-self recognition, which has been documented in other cnidarians (reviewed by Salter-Cid and Bigger 1991; Amar and Rinkevich 2010). Finally, although the identity of the donor diseased colony was not related to the level of cellular immune response, we were unable to collect tissue from the same donor colonies in both years, and therefore cannot rule out the effect of a variation in donor colony or pathogen virulence between the two field experiments.

In addition to characterizing the amoebocyte response, we provide one of the few time series of PPO activity in cnidarians. During the clonally replicated experiment, we observed a significant induction in PPO activity in all treatments and controls from 0 to 1 d, with no effect of treatment on PPO activity over time. Mean initial PPO activity during this experiment was also 2.8 fold lower than the initial levels in the intact colony experiment. This, together with the fact that initial fragments were collected 2 d after acclimation (clonally replicated field experiment), suggests that fragmentation and handling rather than grafting affected PPO activity. In the intact colony experiment, PPO activity decreased in grafted and ungrafted tissue from 0 to 6 d, and increased slightly by 14 d (Fig. 4.6). The decrease in activity in distal tissue over time provides further evidence that allografting causes systemic changes on the entire colony. Interestingly, these results mirror a similar decline in melanin immediately following injury in *P. cylindrica*, and then increased again between 1 and 2 d (Palmer et al. 2011c). These results suggest that PPO and melanin are constitutively present, but are rapidly released into the site of grafting or physical damage and are slowly replenished after wound healing. Our results highlight the complexity of invertebrate immunity and the importance of establishing a time course to interpret immune function.

Invertebrates have evolved a variety of defense mechanisms for detecting and responding

to biotic threats, providing the foundation of host-pathogen interactions. *G. ventalina*'s capacity to mount a transient amoebocyte response and the elevated amoebocyte aggregation and PPO activity in aspergillotic tissue (Mydlarz et al. 2008) suggests the importance of these responses in disease susceptibility and stress tolerance. In scleractinian corals, overall immune function was negatively related to disease susceptibility and thermal stress tolerance (Palmer et al. 2010). In other marine invertebrates such as *Crassostrea* spp., elevated hemocyte density has been associated with increased host survival and resistance to the pathogen *Haplosporidium nelsoni*, also known as MSX (Ford et al. 1993) and seasonal thermal stress (Lambert et al. 2007). Given the importance of plasticity in development and evolution of host defenses (Stearns 1976; Stearns 1989; Gervasi and Foufopoulos 2008), the variation in timing and magnitude of immune response is expected to affect population-wide disease patterns and tolerance to environmental stress. These studies highlight the importance of not only understanding the functional roles of cnidarian cellular immunity, but also how this immune component may affect small-scale disease dynamics and colony survival.

CONCLUSIONS AND FUTURE DIRECTIONS

This is the first study to characterize the temporal dynamics of the cnidarian amoebocyte and PPO response in the field. Since cnidarians are a basal phylum, this study also enhances our understanding of the function of evolutionarily basal immune defense mechanisms. Our results suggest that population level variation in immune response or the physical stress necessary to perform laboratory experiments may alter immune function compared to the wild populations. Although *G. ventalina* amoebocyte response did not peak until 6 d in the field, there are likely physiological costs to maintaining high levels of cellular immune response, which may explain the declining response between 6 and 14 d. Furthermore, our results suggest a systemic depletion

in PPO in response to grafting. The notable intercolony variation in magnitude and timing of amoebocyte response may have important implications for evolution of disease resistance and tolerance to environmental stress.

Our findings provide an important timeline on which to develop future studies of the underlying mechanisms of the cellular immune response and address questions such as: 1. What are the underlying molecular mechanisms mediating stimulus recognition, signal transduction and amoebocyte activation? 2. Is the intercolony variability in cellular immune response due to genetic variation? and 3. Does the magnitude of cellular immune response affect disease susceptibility and colony survival?

ACKNOWLEDGEMENTS

We thank E. Bartels of the Mote Tropical Research Laboratory on Summerland Key for collecting the corals used in the laboratory experiment under Florida Keys National Marine Sanctuary permit number FKNMS-2008-001. We thank D. Anderson, S. Harris, A. Anton and V. Schutte for field support. Funding support was provided by National Geographic and the National Science Foundation grant number OCE0849776. Partial funding was provided by the GEF-World Bank CRTR program to E. Weil and the Department of Marine Sciences, University of Puerto Rico Mayaguez provided partial funding and logistical support. Thanks to C. Burge, M. Mouchka, A. Tracy, N. Douglas, E. Peters, J. Thaler and I. Hewson for manuscript reviews.

REFERENCES

Adema CM, van Deutekom-Mulder EC, van der Knaap WP, Meuleman EA, Sminia T (1991) Generation of oxygen radicals in hemocytes of the snail *Lymnaea stagnalis* in relation to

the rate of phagocytosis. Developmental & Comparative Immunology 15:17-26

Aderem A, Ulevitch RJ (2000) Toll-like receptors in the induction of the innate immune response. Nature 406:782-787

Aladaileh S, Nair SV, Raftos DA (2007) Induction of phenoloxidase and other immunological activities in Sydney rock oysters challenged with microbial pathogen-associate molecular patterns. Fish & Shellfish Immunology 23:1196-1208

Alker AP, Kim K, Dube DH, Harvell CD (2004) Localized induction of a generalized response against multiple biotic agents in Caribbean sea fans. Coral Reefs 23:397-405

Amar KO, Rinkevich B (2010) Mounting of erratic histoincompatible responses in hermatypic corals: a multi-year interval comparison. Journal of Experimental Biology 213:535-540

Araya MT, Markham F, Mateo DR, McKenna P, Johnson GR, Berthe FCJ, Siah A (2010) Identification and expression of immune-related genes in hemocytes of soft-shell clams, *Mya arenaria*, challenged with *Vibrio splendidus*. Fish & Shellfish Immunology 29:557-564

Augustin R, Bosch TCG (2010) Cnidarian Immunity: A Tale of Two Barriers Invertebrate Immunity, pp 1-16

Ausubel FM (2005) Are innate immune signaling pathways in plants and animals conserved? Nature Immunology 6:973-979

Baayen RH, Davidson DJ, Bates DM (2008) Mixed-effects modeling with crossed random effects for subjects and items. Journal of Memory and Language 59:390-412

Bates D, Maechler M (2009) lme4: linear mixed-effects models using S4 classes. R package version 0.999375-32

Beck G, O'Brien RF, Habicht GS, Stillman DL, Cooper EL, Raftos DA (1993) Invertebrate

cytokines III: Invertebrate interleukin-1-like molecules stimulate phagocytosis by tunicate and echinoderm cells. Cellular Immunology 146:284-299

Bigger CH, Hildemann WH (1982) Cellular defense systems of the coelenterata. In: Cohen N, MM S (eds) The reticuloendothelial system. Plenum Press, New York, pp 59-87

Bolker BM, Brooks ME, Clark CJ, Geange SW, Poulsen JR, Stevens MHH, White JSS (2009) Generalized linear mixed models: a practical guide for ecology and evolution. Trends in Ecology & Evolution 24:127-135

Borges JCS, Jensch BE, Garrido PAG, Baptista MB, Mangiaterra CD, Machado JR, Silva C (2005) Phagocytic amoebocyte sub populations in the perivisceral coelom of the sea urchin, *Lytechinus variegatus* (Lamarck, 1816). Journal of Experimental Zoology Part a-Comparative Experimental Biology 303A:241-248

Bosch TC, Augustin R, Anton-Erxleben F, Fraune S, Hemmrich G, Zill H, Rosenstiel P, Jacobs G, Schreiber S, Leippe M (2009) Uncovering the evolutionary history of innate immunity: The simple metazoan *Hydra* uses epithelial cells for host defence. Developmental & Comparative Immunology 33:559-569

Bourne D, Iida Y, Uthicke S, Smith-Keune C (2007) Changes in coral-associated microbial communities during a bleaching event. ISME J 2:350-363

Bruno JB, J. F., Ellner SP, Vu I, Kim K, Harvell CD (2011) Impacts of aspergillosis on sea fan coral demography: modeling a moving target. Ecological Monographs 81:123-139

Burge CA, Douglas N, Conti-Jerpe I, Weil E, Roberts S, Friedman CS, Harvell CD (2012) Friend or foe: the association of Labyrinthulomycetes with the Caribbean sea fan *Gorgonia ventalina*. Diseases of Aquatic Organisms 101:1-12

Burge EJ, Madigan DJ, Burnett LE, Burnett KG (2007) Lysozyme gene expression by

hemocytes of Pacific white shrimp, Litopenaeus vannamei, after injection with Vibrio. Fish & Shellfish Immunology 22:327-339

Burnham KP, Anderson DR (2002) Model selection and multi-model inference: a practical information-theoretic approach. Springer-Verlag, New York

Canesi L, Betti M, Ciacci C, Scarpato A, Citterio B, Pruzzo C, Gallo G (2002) Signaling pathways involved in the physiological response of mussel hemocytes to bacterial challenge: the role of stress-activated p38 MAP kinases. Developmental & Comparative Immunology 26:325-334

Cerenius L, Soderhall K (2004) The prophenoloxidase-activating system in invertebrates. Immunological Reviews 198:116-126

Cerenius L, Jiravanichpaisal P, Liu H, Soderhall I (2010) Crustacean immunity. Invertebrate Immunity 708:239-259

Collinge SK, Ray C (2006) Disease ecology: community structure and pathogen dynamics. Oxford University Press, USA

Coteur G, DeBecker G, Warnau M, Jangoux M, Dubois P (2002) Differentiation of immune cells challenged by bacteria in the common European starfish, *Asterias rubens* (Echinodermata). European Journal of Cell Biology 81:413-418

Couch CS, Mydlarz LD, Harvell CD, Douglas NL (2008) Variation in measures of immunocompetence of sea fan coral, *Gorgonia ventalina*, in the Florida Keys. Marine Biology 155:281-292

Dube D, Kim K, Alker AP, Harvell CD (2002) Size structure and geographic variation in chemical resistance of sea fan corals *Gorgonia ventalina* to a fungal pathogen. Marine Ecology Progress Series 231:139-150

Ellner SP, Jones LE, Mydlarz LD, Harvell CD (2007) Within-Host Disease Ecology in the Sea Fan Gorgonia ventalina: Modeling the Spatial Immunodynamics of a Coral-Pathogen Interaction. The American Naturalist 170:E143-E161

Ford SE, Kanaley SA, Littlewood DTJ (1993) Cellular Responses of Oysters Infected with *Haplosporidium nelsoni*: Changes in Circulating and Tissue-Infiltrating Hemocytes. Journal of Invertebrate Pathology 61:49-57

George SG, Pirie BJS, Cheyne AR, Coombs TL, Grant PT (1978) Detoxication of metals by marine bivalves: An ultrastructural study of the compartmentation of copper and zinc in the oyster *Ostrea edulis*. Marine Biology 45:145-156

Gervasi SS, Foufopoulos J (2008) Costs of plasticity: responses to desiccation decrease post-metamorphic immune function in a pond-breeding amphibian. Functional Ecology 22:100-108

Goedken M, Morsey B, Sunila I, De Guise S (2005) Immunomodulation of *Crassostrea gigas* and *Crassostrea virginica* cellular defense mechanisms by *Perkinsus marinus*. Journal of Shellfish Research 24:487-496

Grenfell BT, Dobson AP (1995) Ecology of infectious diseases in natural populations. Cambridge University Press

Harvell CD, Mitchell CE, Ward JR, Altizer S, Dobson AP, Ostfeld RS, Samuel MD (2002) Ecology - Climate warming and disease risks for terrestrial and marine biota. Science 296:2158-2162

Hawley DM, Altizer SM (2011) Disease ecology meets ecological immunology: understanding the links between organismal immunity and infection dynamics in natural populations. Functional Ecology 25:48-60

Hutton DMC, Smith VJ (1996) Antibacterial properties of isolated amoebocytes from the sea anemone *Actinia equina*. Biological Bulletin 191:441-451

Jordan PJ, Deaton LE (2005) Characterization of phenoloxidase from *Crassostrea virginica* hemocytes and the effect of *Perkinsus marinus* on phenoloxidase activity in the hemolymph of *Crassostrea virginica* and *Geukensia demissa*. Journal of Shellfish Research 24:477-482

Kim K, Harvell CD (2002) Aspergillosis of sea fan corals: disease dynamics in the Florida Keys. In: Porter JW, Porter KG (eds) The Everglades, Florida Bay, and Coral Reefs of the Florida Keys: An Ecosystem Sourcebook. CRC Press, Boca Raton, pp 813-824

Kim K, Harvell CD (2004) The rise and fall of a six-year coral-fungal epizootic. The American Naturalist 164:S52-S63

Kim K, Kim PD, Alker AP, Harvell CD (2000b) Chemical resistance of gorgonian corals against fungal infections. Marine Biology 137:393-401

Kim K, Harvell CD, Kim PD, Smith GW, Merkel SM (2000a) Fungal disease resistance of Caribbean sea fan corals (*Gorgonia* spp.). Marine Biology 136:259-267

Kim K, Alker AP, Shuster K, Quirolo C, Harvell CD (2006) Longitudinal study of aspergillosis in sea fan corals. Diseases of Aquatic Organisms 69:95-99

Korner P, Schmid-Hempel P (2004) In vivo dynamics of an immune response in the bumble bee *Bombus terrestris*. Journal of Invertebrate Pathology 87:59-66

Kramarsky-Winter E (2004) What can regeneration processes tell us about coral disease? In: Rosenberg E, Loya Y (eds) Coral Health and Disease. Springer-Verlag, Berlin, pp 217–230

Kurtz J, Franz K (2003) Innate defence: evidence for memory in invertebrate immunity. Nature

425:37-38

Lambert C, Soudant P, Dégremont L, Delaporte M, Moal J, Boudry P, Jean F, Huvet A, Samain J-F (2007) Hemocyte characteristics in families of oysters, *Crassostrea gigas*, selected for differential survival during summer and reared in three sites. Aquaculture 270:276-288

Loker ES, Adema CM, Zhang SM, Kepler TB (2004) Invertebrate immune systems–not homogeneous, not simple, not well understood. Immunological Reviews 198:10-24

Malham SK, Lacoste A, Gélébart F, Cueff A, Poulet SA (2003) Evidence for a direct link between stress and immunity in the mollusc *Haliotis tuberculata*. Journal of Experimental Zoology Part a-Comparative Experimental Biology 295A:136-144

Mangiaterra MBBCD, Silva JRMC (2001) Induced inflammatory process in the sea urchin *Lytechinus variegatus*. Invertebrate Biology 120:178-184

Meszaros A, Bigger C (1999) Qualitative and quantitative study of wound healing processes in the coelenterate, *Plexurella fusifera*; spatial, temporal, and environmental (light attenuation) influences. Journal of Invertebrate Pathology 73:321-331

Miller DJ, Hemmrich G, Ball EE, Hayward DC, Khalturin K, Funayama N, Agata K, Bosch TCG (2007) The innate immune repertoire in Cnidaria - ancestral complexity and stochastic gene loss. Genome Biology 8:R59

Mowlds P, Barron A, Kavanagh K (2008) Physical stress primes the immune response of Galleria mellonella larvae to infection by *Candida albicans*. Microbes and Infection 10:628-634

Mullen K, Peters EC, Harvell CD (2004) Coral resistance to disease. In: Rosenberg E, Loya Y (eds) Coral Health and Disease. Springer-Verlag, New York, pp 377-399

Mullen KM, Harvell CD, Alker AP, Dube D, Jordán-Dahlgren E, Ward JR, Petes LE (2006) Host range and resistance to aspergillosis in three sea fan species from the Yucatan. Marine Biology 149:1355-1364

Mydlarz LD, Harvell CD (2007) Peroxidase activity and inducibility in the sea fan coral exposed to a fungal pathogen. Comparative Biochemistry and Physiology Part A Molecular & Integrative Physiology 146:54-62

Mydlarz LD, Palmer CV (2011) The presence of multiple phenoloxidases in Caribbean reef-building corals. Comparative Biochemistry and Physiology Part A Molecular & Integrative Physiology 159:372-378

Mydlarz LD, Jones LE, Harvell CD (2006) Innate immunity environmental drivers and disease ecology of marine and freshwater invertebrates. Annual Review of Ecology and Systematics 37:251-288

Mydlarz LD, Holthouse SF, Peters EC, Harvell CD (2008) Cellular responses in sea fan corals: Granular amoebocytes react to pathogen and climate stressors. Plos One 3:e1811

Nagelkerken I, Buchan K, Smith GW, Bonair K, Bush P, Garzon-Ferreira J, Botero L, Gayle P, Harvell CD, Heberer C, Kim K, Petrovic C, Pors L, Yoshioka P (1997) Widespread disease in Caribbean sea fans: II. Patterns of infection and tissue loss. Marine Ecology-Progress Series 160:255-263

Nappi AJ, Christensen BM (2005) Melanogenesis and associated cytotoxic reactions: Applications to insect innate immunity. Insect Biochemistry and Molecular Biology 35:443-459

Olano CT, Bigger CH (2000) Phagocytic activities of the gorgonian coral *Swiftia exserta*. Journal of Invertebrate Pathology 76:176-184

Palmer CV, Bythell JC, Willis BL (2010) Levels of immunity parameters underpin bleaching and disease susceptibility of reef corals. The FASEB Journal 24:1935-1946

Palmer CV, Bythell JC, Willis BL (2011a) A comparative study of phenoloxidase activity in diseased and bleached colonies of the coral *Acropora millepora*. Developmental & Comparative Immunology 35:1096-1099

Palmer CV, Traylor-Knowles NG, Willis BL, Bythell JC (2011b) Corals Use Similar Immune Cells and Wound-Healing Processes as Those of Higher Organisms. Plos One 6:e23992

Palmer CV, McGinty ES, Cummings DJ, Smith SM, Bartels E, Mydlarz LD (2011c) Patterns of coral ecological immunology: variation in the responses of Caribbean corals to elevated temperature and a pathogen elicitor. Journal of Experimental Biology 214:4240-4249

Patterson MJ, Landolt ML (1979) Cellular reaction to injury in the anthozoan *Anthopleua elegantissima* Journal of Invertebrate Pathology 33:189-196

Perrigault M, Allam B (2012) Differential immune response in the hard clam (*Mercenaria mercenaria*) against bacteria and the protistan pathogen qpx (quahog parasite unknown). Fish & Shellfish Immunology 32:1124-1134

Petes LE, Harvell CD, Peters EC, Webb MAH, Mullen KM (2003) Pathogens compromise reproduction and induce melanization in Caribbean sea fans. Marine Ecology-Progress Series 264:167-171

Pinheiro JC, Bates DM (2000) Mixed-Effects Models in S and S-Plus. Springer, New York, NY

Rolff J, Siva-Jothy MT (2003) Invertebrate ecological immunology. Science 301:472-475

Salter-Cid L, Bigger CH (1991) Alloimmunity in the gorgonian coral *Swiftia exserta*. Biological Bulletin 181:127-134

Salzet M (2001) Vertebrate innate immunity resembles a mosaic of invertebrate immune

responses. Trends in Immunology 22:285-288

Schmid-Hempel P (2003) Variation in immune defense as a question of evolutionary ecology. Proceedings of the Royal Society Biological Sciences Series B 270:357-366

Schmid-Hempel P (2005) Evolutionary Ecology of Insect Immune Defenses. Annual Review of Entomology 50:529-551

Song LS, Wang LL, Qiu LM, Zhang HA (2010) Bivalve Immuity Invertebrate Immunity. Springer-Verlag Berlin, Berlin, pp 44-65

Stearns SC (1976) Life-history tactics: a review of the ideas. Quarterly Review of Biology 51:3-47

Stearns SC (1989) Trade-offs in life-history evolution. Functional Ecology 3:259-268

Thurber RV, Willner-Hall D, Rodriguez-Mueller B, Desnues C, Edwards RA, Angly F, Dinsdale E, Kelly L, Rohwer F (2009) Metagenomic analysis of stressed coral holobionts. Environmental Microbiology 11:2148-2163

Travers M-A, Le Bouffant R, Friedman CS, Buzin F, Cougard B, Huchette S, Koken M, Paillard C (2009) Pathogenic *Vibrio harveyi*, in contrast to non-pathogenic strains, intervenes with the p38 MAPK pathway to avoid an abalone haemocyte immune response. Journal of Cellular Biochemistry 106:152-160

Vargas-Angel B, Peters EC, Kramarsky-Winter E, Gilliam DS, Dodge RE (2007) Cellular reactions to sedimentation and temperature stress in the Caribbean coral *Montastraea cavernosa*. Journal of Invertebrate Pathology 95:140-145

Vidal-Dupiol J, Ladriere O, Destoumieux-Garzon D, Sautiere PE, Meistertzheim AL, Tambutte E, Tambutte S, Duval D, Foure L, Adjeroud M, Mitta G (2011) Innate Immune Responses of a Scleractinian Coral to Vibriosis. Journal of Biological Chemistry

286:22688-22698

Ward JR (2007) Within-colony variation in inducibility of coral disease resistance. Journal of Experimental Marine Biology and Ecology 352:371-377

Ward JR, Kim K, Harvell CD (2007) Temperature affects coral disease resistance and pathogen growth. Marine Ecology-Progress Series 329:115-121

Woolhouse ME, Haydon DT, Antia R (2005) Emerging pathogens: the epidemiology and evolution of species jumps. Trends in Ecology & Evolution 20:238-244

Zuur AF, Ieno EN, Walker N, Saveliev AA, Smith GM (2009) Mixed effects models and extensions in ecology with R. Springer

APPENDIX I

SUPPLEMENTARY FIGURES AND TABLES

CHAPTER 1

The following are supplementary tables and figures.

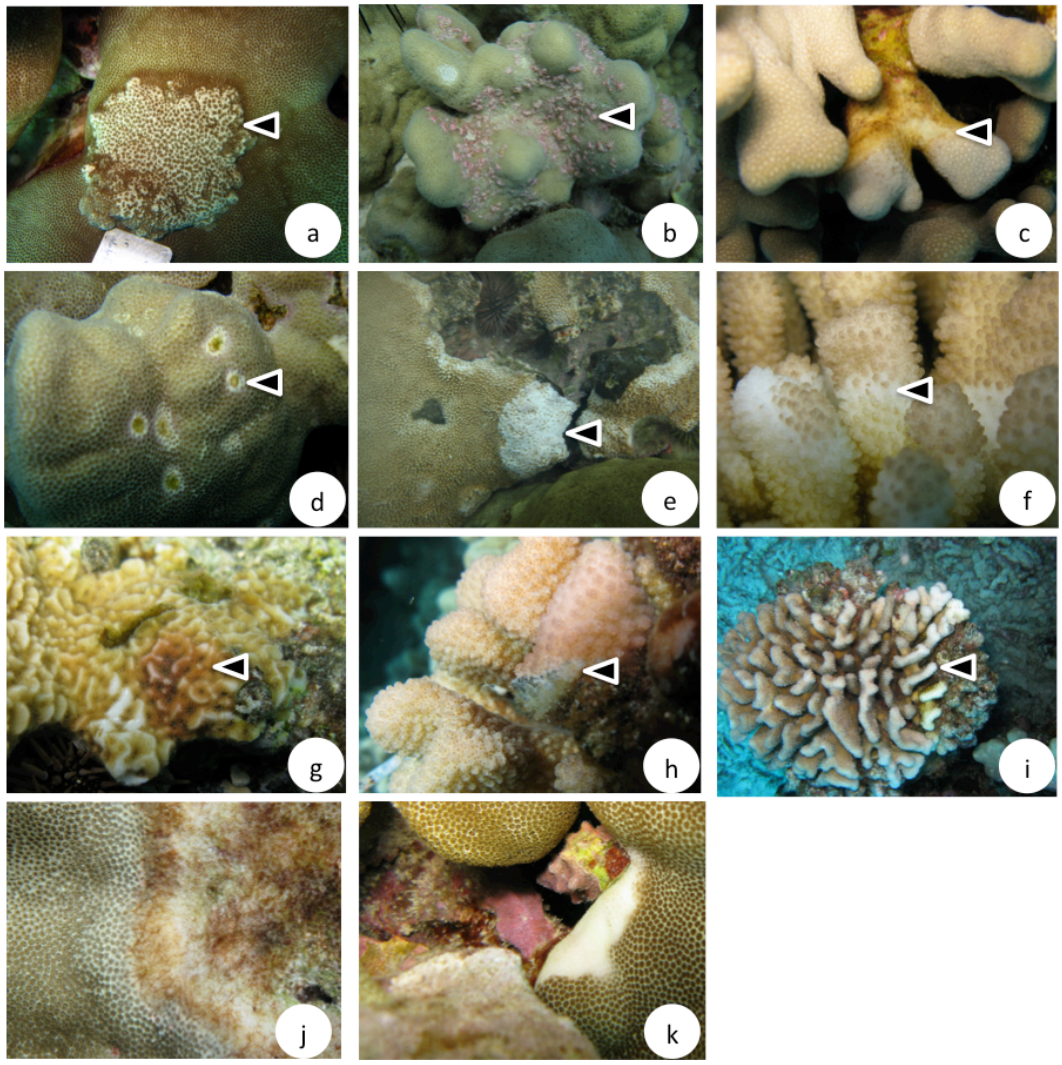

Figure S1.1. Coral diseases observed in West Hawai'i between January 2010-August 2011: a) *Porites* growth anomaly (PorGA), b) *Porites* trematodiasis (PorTRM), c) *Porites* tissue loss syndrome (PorTLS), d) *Porites* multifocal tissue loss syndrome (PorMFTL), e) *Montipora* growth anomaly (MonGA), g) *Pocillopora* tissue loss (PocTLS), h) *Pavona varians* hypermycosis (PavHYP), i) Ciliate infection (CIL). j) Algal overgrowth (ALOG), k) *Drupella cornus* predation. Arrows indicate lesions. Note: No cases of *Montipora* white syndrome were observed during this study. Lesion descriptions: Aeby et al. (2011b): PorGA, PorTRM, PorTLS, PorMFTL and MonGA; Work et al. (2008a): PavHYP; PocTLS: distinct areas of subacute tissue loss at the base of branches revealing intact white skeleton progressing basally to a green patina. PS: discoloration characterized by diffuse indistinct areas of pallor encompassing 25-50% of the colony. CIL: black speckled band (clusters of ciliates) adjacent to healthy tissue and exposed skeleton progressing basally to a green patina.

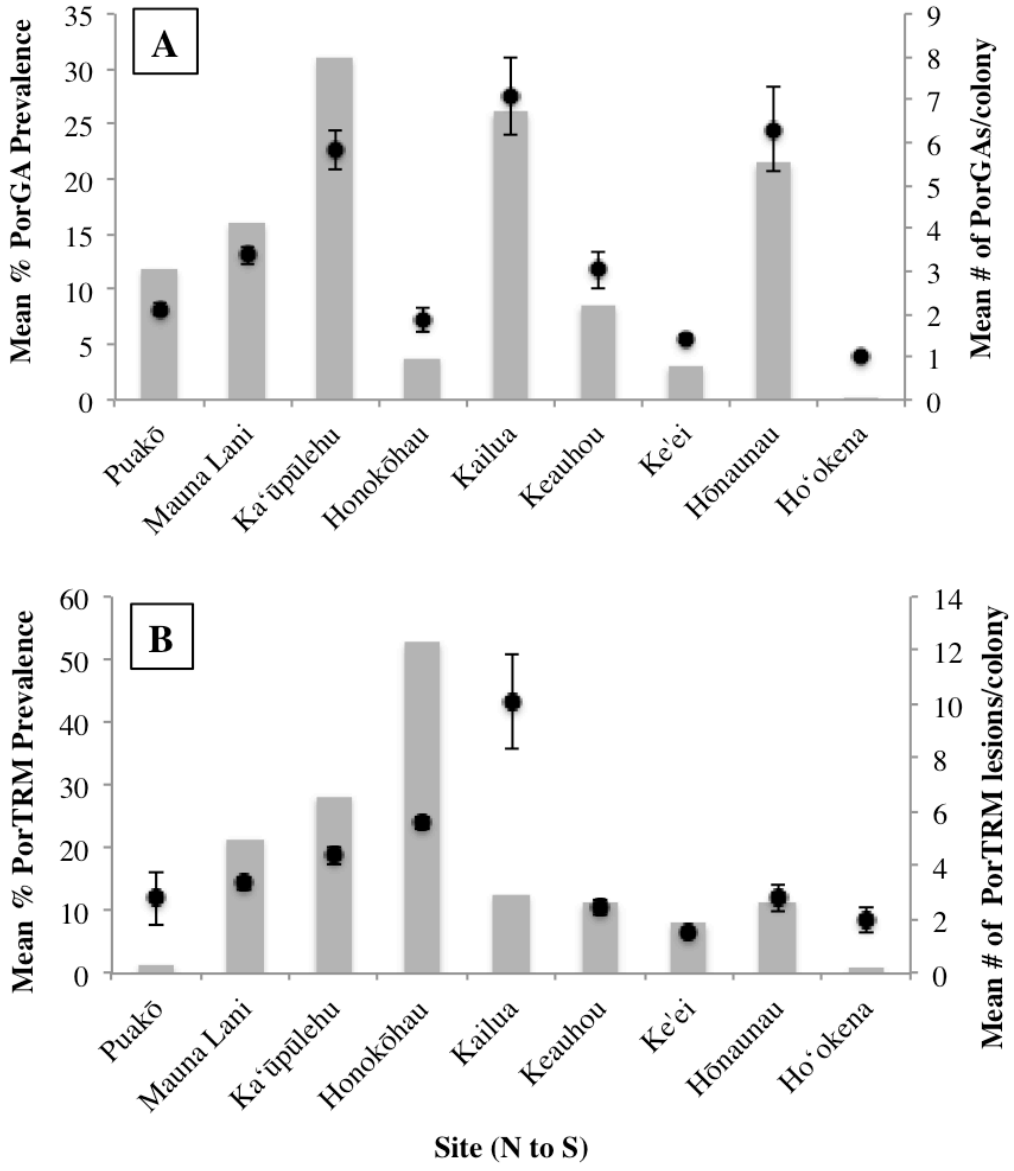

Figure S1.2. (A) Mean % PorGA prevalence (gray bars) and mean ± SE severity (number of PorGA lesions/colony) (black dots) across shallow study sites. (B) Mean % PorTRM prevalence (gray bars) and mean ± SE severity (number of PorTRM lesions/colony) (black dots) across shallow study sites. n= 4 transects/site

Table S1.1. List of acronyms.

Acronym	**Definition**
AICc	corrected Akaike's information criterion
ALOG	Algal Overgrowth
BLE	Bleaching
BR	Breakage
CIL	Ciliate Infection
COTS	Crown of Thorns Starfish
COTSPRD	Crown of Thorns Starfish Predation
DC	Discoloration
GastPRD	Gastropod Predation
GLM	Generalized Linear Model
LMEM	Linear Mixed-Effect Model
MHI	Main Hawaiian Islands
MonGA	*Montipora* Growth Anomalies
PavHYP	*Pavona varians* Hypermycosis
PorGA	*Porites* Growth Anomalies
PorMFTL	*Porites* Multifocal Tissue Loss
PorTLS	*Porites* Tissue Loss Syndrome
PorTRM	*Porites* Trematodiasis
PR	*Porites* Pigmentation Response
SED	Sedimentation
WHAP	West Hawaii Aquarium Project
WHI	West Hawaii Island

Table S1.2. Mean % prevalence and frequency of occurrence of diseases and biological interactions found in shallow and deep zones along WHI. Standard error of mean indicated in parentheses.

	Prevalence		Frequency of Occurrence
Disease	**Shallow**	**Deep**	**All Sites**
PorGA	18.9 (2.3)	13.3 (1.41)	100.00
PorTRM	12.4 (2.1)	6.00 (0.99)	98.40
PorTLS	0.47 (0.13)	0.79 (0.15)	56.25
PorMFTL	0.52 (0.25)	0.42 0.15)	34.38
MonGA	0.01 (0.01)	0.002 (0.002)	4.69
PocTLS	0.11(0.07)	0	2.12
PavHYP	4.97 (3.3)	0	10.94
CIL	0.23 (0.16)	1.56 (0.93)	10.94
Biological Interaction			
ALOG	10.6 (0.76)	8.37 (1.2)	98.44
GastPRD	2.09 (0.31)	2.75 (0.53)	95.31
COTSPRD	0.10 (0.08)	0.16 (0.05)	15.63
PR	5.04 (0.91)	2.95 (0.70)	81.25
DC	0.86 (0.18)	0.19 (0.05)	57.81
PS	0.29 (0.17)	0.28 (0.20)	7.81
BLE	0.59 (0.15)	0.50 (0.09)	59.38
BR	0.58 (0.24)	0	17.19
SED	0.10 (0.08)	0	3.13

PorGA = *Porites* growth anomaly PorTRM = *Porites* trematodiasis, PorTLS = *Porites* tissue loss syndrome, PorMFTL = *Porites* multifocal tissue loss syndrome, PorSP = *Porites* swollen patches, MonGA = *Montipora* growth anomaly, PocTLS = *Pocillopora* tissue loss, PavHYP = *Pavona varians* hypermycosis, CIL = Ciliate infection, ALOG = Algal overgrowth, GastPRD = Gastropod predation, COTSPRD = Crown-of-thorns starfish predation, PR = *Porites* pigmentation response, DC = discoloration, PS = *Pocillopora* senescence, BLE = Bleaching, BR = Breakage, SED = Sedimentation.

Table S1.3. Mean % *Porites* growth anomaly (PorGA), *Porites* trematodiasis (PorTRM) and *Porites* tissue loss syndrome (PorTLS) prevalence (SE indicated in parentheses) along West Hawai‘i (WHI) compared to previously published prevalence for the Main (MHI) and Northwestern Hawaiian Islands (NWHI) (Aeby et al. 2011b).

	WHI	**MHI**	**NWHI**
PorGA	16.1 (1.4)	0.64 (0.15)	0.32 (0.3)
PorTRM	9.2 (1.2)	1.1 (0.3)	10.7 (2.2)
PorTLS	0.63 (0.1)	0.11 (0.03)	0.82 (0.28)

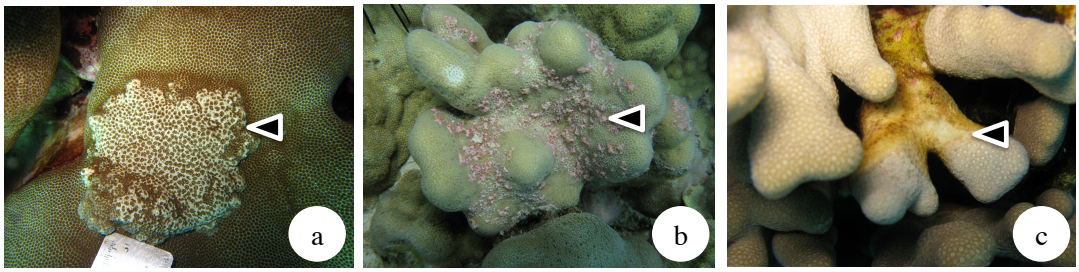

Figure S2.1. Three most common *Porites* diseases observed in West Hawai‘i (a) *Porites* growth anomaly (PorGA), (b) *Porites* trematodiasis (PorTRM), (c) *Porites* tissue loss syndrome (PorTLS), See for Aeby et al. (2011b) lesion descriptions.

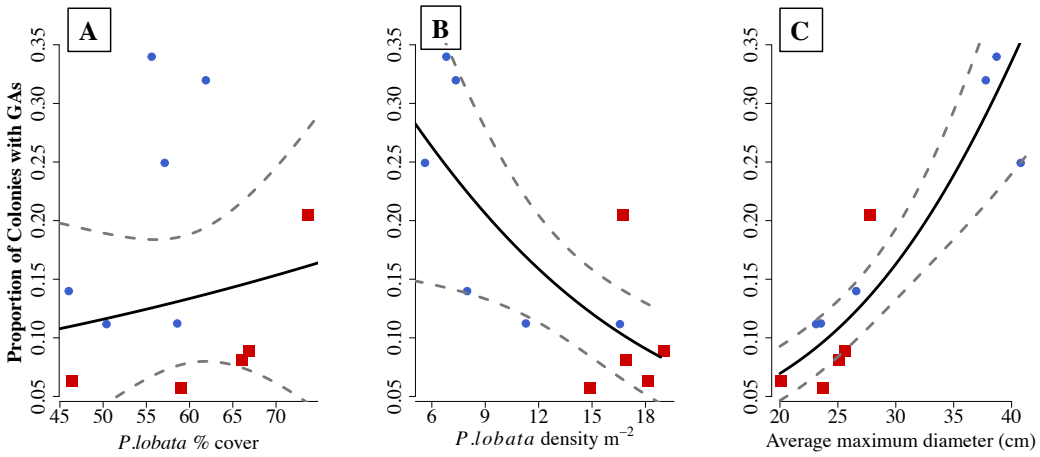

Figure S3.1. Generalized regressions of relationship between the proportion of *P. lobata* colonies with GAs and A) *P. lobata* % cover, B) *P. lobata* colony density, and C) Average *P. lobata* maximum diameter. Blue circles = Kailua, Red squares= Kaloko. Solid line: logistic regression (with quasibinomial errors). Grey dashed lines: upper and lower 95% confidence and prediction intervals.

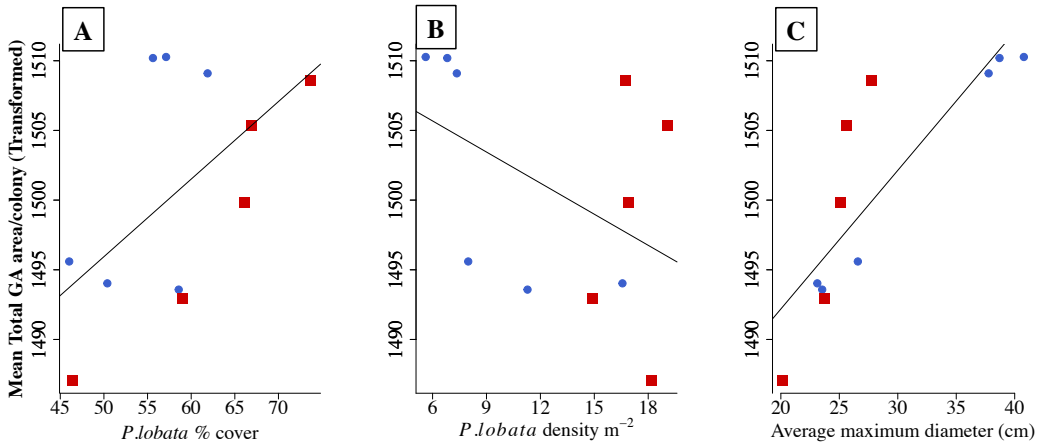

Figure S3.2. Linear regressions of relationship between the GA severity (mean total GA area/colony) and A) *P. lobata* % cover, B) *P. lobata* colony density, and C) Average *P. lobata* maximum diameter. Blue circles = Kailua, Red squares= Kaloko.

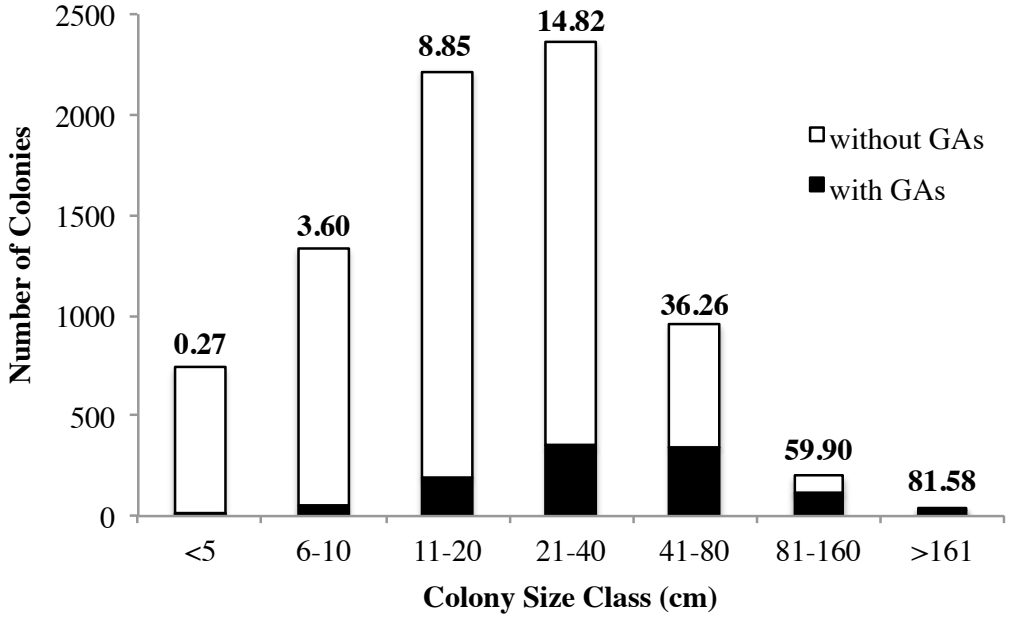

Figure S3.3. Size frequency distribution of *P. lobata* colonies without growth anomalies (white) and with GAs (black). Numbers indicate proportion of *Porites* colonies (%) with GAs across all transects.

Table S3.1. Parameters estimates from the two best-fit GLMMs with GA prevalence as the response.

	β (S.E.)	**z**	***p***
Prevalence	-5.32 (1.07)	-4.96	< 0.00001
Size	0.09 (0.02)	6.14	< 0.00001
Water Motion	-0.24 (0.07)	-3.52	0.000429
Size x Water Motion	-0.01 (0.001)	-5.33	< 0.00001
Prevalence	-79.71 (16.00)	-4.98	< 0.00001
Temperature	3.09 (0.62)	4.99	< 0.00001
Water Motion	-0.14 (0.01)	-13.40	< 0.00001

Table S3.2. Parameters estimates from the two best-fit LMEMs with GA severity as the response. P <0.05 when HPD intervals do not overlap 0, α= 0.05.

	β (S.E.)	**t**	***p***
Severity	1468.41 (6.43)	228.26	<0.05
Size	1.14 (0.21)	5.43	<0.05
Severity	1484.05 (7.63)	7.6332	<0.05
Size	0.91 (0.18)	0.1811	<0.05
Water Motion	-0.66 (0.31)	0.3146	<0.05

APPENDIX II

HISTOPATHOLOGY OF TISSUE LOSS AND DISCOLORATION LESIONS IN CORALS FROM HAWAIʻI ISLAND.

Field assessments and were conducted in collaboration with Hawai'i DAR and histopathological assessments were conducted by Dr. Thierry Work (USGS).

INTRODUCTION

Tissue loss diseases have caused widespread coral mortality across the Indo-Pacific, yet the etiology of many tissue loss diseases is still unknown. Several putative agents have been hypothesized for *Montipora* white syndrome, including helminthes, ciliates (Work et al. 2012), and/or *Vibrio owensii* (Ushijima et al 2012), but the etiology and transmissibility of tissue loss diseases in other coral taxa is not well understood. Tissue loss syndrome (TLS) and discolored lesions are also often misidentified in the field due to the limited repertoire of responses corals demonstrate to a range of biotic and abiotic stressors. Histopathology can provide crucial information on the underlying cause of the lesion, yet few studies augment field observations with histopathological assessments. In this study, we conducted histopathology on a subset of common lesions identified as subacute TLS and discoloration to confirm field identification.

METHODS

Of 33 samples collected for histopathology, 26 comprised normal/lesion tissue pairs from 20 colonies whereas the remainder were lesions only each from a single colony, including ten *Porites compressa*, four *Pocillopora meandrina*, four *Porites evermanni* and two *Porites lobata* (Fig. S5.1). Samples were collected from Kaloko-Honōkohau, South Oneo Bay (19.63°N, -

155.99°W), Keauhou (19.56°N, 155.96°W), Ho‘okena (19.36°N, 155.89°W), Okoe Bay (19.13°N, 155.91°W) and Manuka (19.07°N, 155.90°W) between February and July 2010. 3 x 3 cm samples were collected with a hammer a chisel, placed in separate Whirl-paks® and immediately fixed in 1:5 zinc-buffered formalin (Z-Fix Concentrate, Anatech, Ltd.) diluted with artificial seawater. Fixed samples were sent to the National Wildlife Health Center Honolulu Field Station for further histological preparation. Samples were decalcified in Cal-ExII (Fisher Scientific), embedded in in paraffin wax, sectioned at 5µm thickness, and stained with hematoxylin and eosin, and mounted on slides. De-paraffinized sections were stained with hematoxylin and eosin and cover-slipped prior to microscopy.

RESULTS AND DISCUSSION

The most common gross lesions for all species were diffuse subacute tissue loss. For *Porites*, the two main lesions seen were necrosis or fragmentation associated with algae (Fig. S5.2C). In *P. meandrina*, this manifested as distinct areas of tissue loss at the base of branches revealing intact white skeleton progressing basally to a green patina (Fig. S5.1A). Discoloration in *P. meandrina* was characterized by diffuse indistinct areas of pallor encompassing 25-50% of the colony (Fig. S5.1C). We hypothesize that this lesion is the result of a senescence reaction and is associated with discoloration and tissue loss. In both types of *P. meandrina* lesions, microscopically, we observed severe atrophy with depletion of zooxanthellae (bleaching). This condition has been observed throughout the Hawaiian Archipelago (B. Vargas-Ángel and G. Aeby pers. comm.), but a population-wide survey with histopathology over time is necessary to confirm whether this is truly a senescence reaction.

In *P. compressa*, tissue loss manifested as localized areas of tissue loss revealing intact

skeleton covered by variable amounts of light growths of turf algae sometimes separated from normal tissues by a thin (1-3 mm) brown band (Fig. S5.1B). These lesions were also associated with discoloration that consisted of localized distinct to indistinct areas of brown material overlying tissues. Similar to Palmer et al. (2008), we observed a cellular inflammation response in *P. compressa*, which was associated with subacute tissue loss. Interestingly, the formation of hyaline membranes associated with the inflammation response, appear to originate from calicodermis. Observed in other corals including *Porites* (T. Work pers. obs), our study is the first documented case and provides insight into *Porites* response to TLS.

In the one *P. lobata*, colony, tissue loss was similar to that of *P. compressa* except that margins of the lesion consisted of a wide (ca. 1 cm) distinct brown band, which was associated with necrosis. We also observed subacute tissue loss with a distinct brown band, which lacked progressing turf algae across the skeleton and was associated with fragmentation. This type of lesion is often associated with COTS predation, but can be easily confused with other TLS lesions at first glance.

In *P. evermanni* with discoloration, one colony had multiple small to coalescing punctated distinct pink area (Fig. S5.1D). In the other three colonies, discoloration of tissues surrounded skeleton covered by turf algae and included distinct amorphous areas of pallor of coenosarc (Fig. S5.1D). In one case (*P. evermanni*), necrosis manifested either as diffuse areas of cells showing lack of nuclear or cytoplasmic details adjacent to normal tissue (liquefaction necrosis) (Fig. S5.2D). In the remainder, necrosis manifested as areas of cytoplasmic fragmentation, hypereosinophilia, pyknosis, and karyorrhexis associated with hyaline membranes (Fig. S5.2E) that appeared to originate from calicodermis (Fig. S5.2G). In two cases, granular black cells infiltrated within mesoglea of basal body wall adjacent to algae (Fig. S5.2E,

F). In one case, hypertrophied calicodermis contained small ovoid bodies that resembled coccidian parasites (Fig. S5.2G). The *P. evermanni* samples were collected from a unique population the Keauhou region. This population is comprised of approximately 50-80 colonies, most of which are over 1m and as large as 9 m in diameter. While we have not have not assessed the prevalence or severity of the discoloration and tissue loss lesions within this population, many colonies had multiple lesions. The origins of this syndrome are unclear, but were observed as early as 2004, with approximately 30% of the colonies affected (G. Aeby, pers. comm.).

Similar to TLS in *Acropora* and *Montipora,* PorTLS manifested as necrosis and progressive cellular degradation that may or may not be the result of microorganisms (Work and Aeby 2011; Work et al. 2012). Microorganisms can either initiate lesion formation or opportunistically infect the tissue following wounding. While we observed bacterial aggregates in *Porites* (Fig. S5.2F), which are commonly associated with healthy and diseased Poritids (Domart-Coulon et al. 2006; Sudek et al. 2012), these aggregates were not associated with necrosis. In fact Sudek et al. (2012) documented a 74% decline in bacterial aggregate density in diseased *P. compressa* colonies, suggesting their symbiotic role in coral physiology. We also documented structures that resembled coccidian parasites without sporozoites in several *Porites* (Fig. S5.2H). These protozoans are a common aquatic parasite infecting range of taxa, including the Caribbean Acroporids, found within the mesenterial filaments Upton & Peters (1986). Given their rarity in coral tissue, it is unlikely that they are causing pathology. Necrosis was also associated with algal infiltration, but in most cases the putative causes of necrosis were unclear. Microalgae has also been associated with necrosis in *Porites* bleaching with tissue loss, which is a common type of PorTLS lesion observed in *P. compressa* across the Main Hawaiian Islands (pers. obs., Sudek

et al. 2012). Fragmentation was also a common microscopic observation, which in several cases was associated with algae, but may also be associated with predation. Histopathology and colony monitoring could shed light on whether predation provides the initial lesion for the development of TLS, which has not been investigated. By augmenting our field surveys with histopathological assessments, we also enhanced our understanding of coral pathology and improved lesion identification in this newly characterized region.

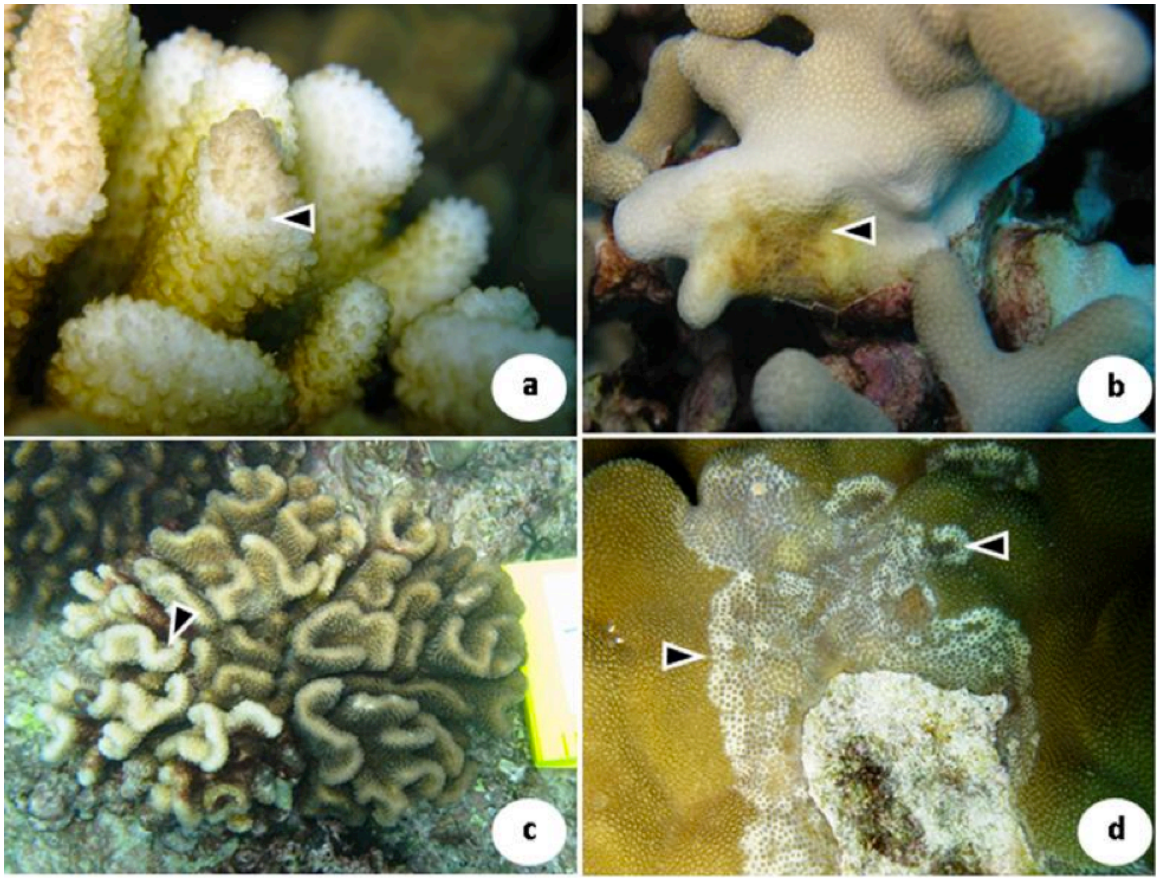

Figure S5.1. Gross lesions in *Pocillopora meandrina* (a,c) and *Porites* sp. (b, d). a) *P. meandrina* subapical subacute tissue loss; note distinct area of bare skeleton progressing to patina of green algae (arrow). b) *P. compressa* subacute tissue loss; note skeleton covered by light patina of algae surrounded by an indistinct broad border band of pale tissues. c) *P. meandrina* discoloration; note diffuse indistinct area of pallor on left side (arrow). d) *P. evermanni* discoloration; note localized area of skeleton covered by organic matter (bottom) surrounded by distinct irregular border of tissues manifesting pale swollen coenosarc.

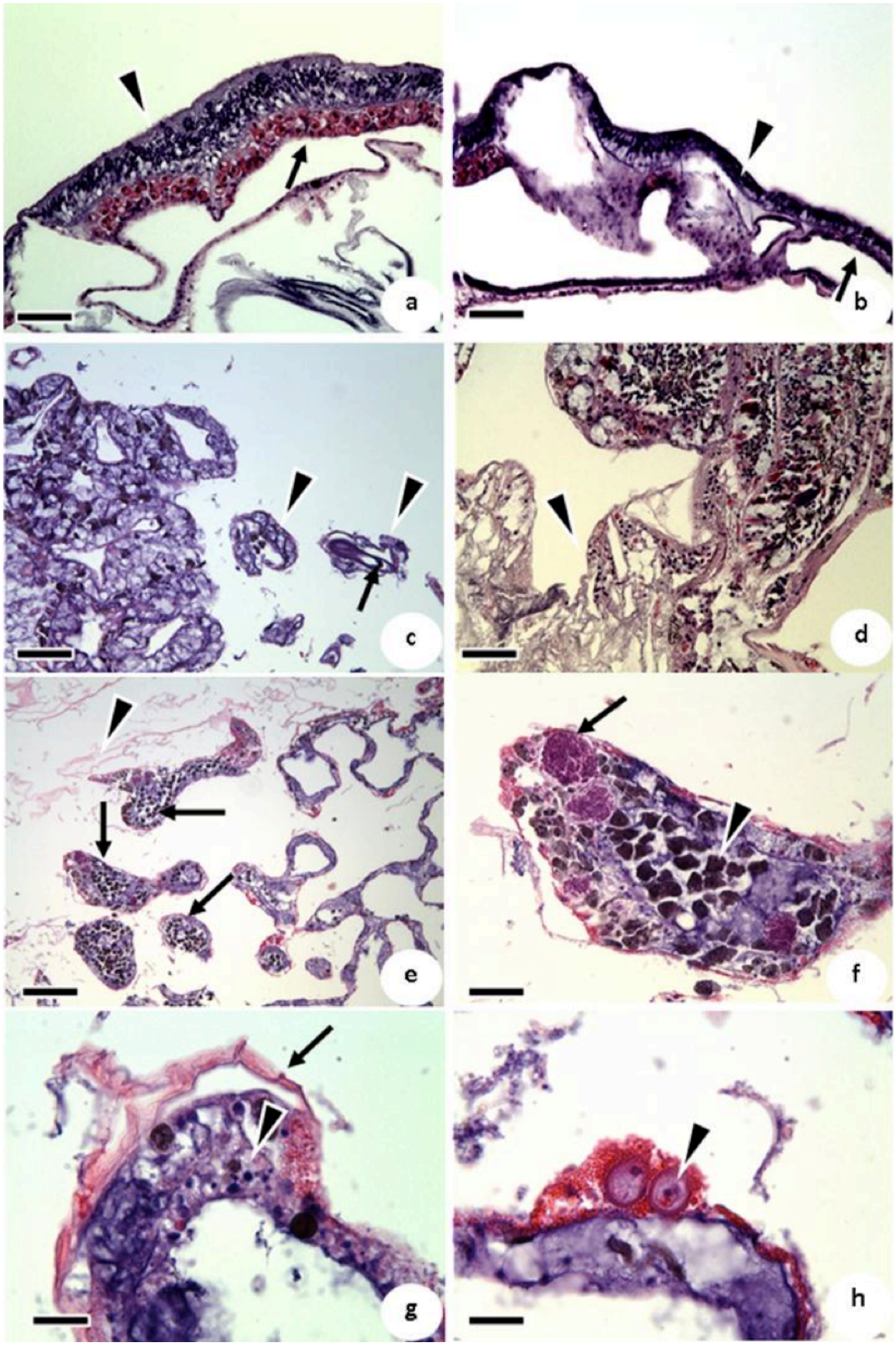
a
b
c
d
e
f
g
h

Figure S5.2. a) Normal *P. meandrina* coenosarc upper body wall; note gastrodermis replete with zooxanthellae (arrow) and tall columnar epidermis (arrowhead). Bar= 20 um. b) *P. meandrina* with gross evidence of discoloration upper body wall coenosarc; note massive atrophy of gastrodermis with no zooxanthellae (arrow) and flattened to cuboidal epidermis (arrowhead). Bar=20 um. c) *Porites compressa* with subacute tissue loss; note fragmentation of tissues of basal body wall (arrowhead) associated with algae (arrow). Bar=50 um. d) *Porites evermanni* discoloration; note diffuse liquefaction necrosis (lower left arrowhead) of basal body wall and mesenterial filaments with intact tissues upper right. Bar=20 um. *Porites compressa* tissue loss (e-h). e) Note hyaline membranes (upper left arrowhead) and marked infiltrates of granular brown cells within basal body wall (arrowheads). Bar=100 um. f) Close up of e. Note symbiotic bacterial aggregate (arrow) and granular brown cells (arrowhead). Bar=20 um. g) Basal body wall; note nuclear fragments (arrowhead) within gastrodermis and hyaline membrane originating from calicodermal surface (arrow). Bar=10 um. h) Basal body wall. Note hypertrophied calicodermis containing two ovoid structures (arrowhead). Bar= 10 um.

REFERENCES

Domart-Coulon IJ, Traylor-Knowles N, Peters E, Elbert D, Downs CA, Price K, Stubbs J, McLaughlin S, Cox E, Aeby G, Brown PR, Ostrander GK (2006) Comprehensive characterization of skeletal tissue growth anomalies of the finger coral *Porites compressa*. Coral Reefs 25: 531-543 doi 10.1007/s00338-006-0133-6

Palmer CV, Mydlarz LD, Willis BL (2008) Evidence of an inflammatory-like response in non-normally pigmented tissues of two scleractinian corals. Proceedings of the Royal Society B: Biological Sciences 275: 2687-2693 doi 10.1098/rspb.2008.0335

Sudek M, Work T, Aeby G, Davy S (2012) Histological observations in the Hawaiian reef coral, *Porites compressa*, affected by *Porites* bleaching with tissue loss. Journal of Invertebrate Pathology:121-125

Upton SJ, Peters EC (1986) A new and unusual species of coccidium (Apicomplexa: Agamococcidiorida) from Caribbean scleractinian corals. Journal of Invertebrate Pathology 47: 184-193

Ushijima B, Smith A, Aeby GS, Callahan SM (2012) *Vibrio owensii* induces the tissue loss disease *Montipora* white syndrome in the Hawaiian reef coral Montipora capitata. PLoS ONE 7: e46717

Work TM, Aeby GS (2011) Pathology of tissue loss (white syndrome) in *Acropora* sp corals from the Central Pacific. Journal of Invertebrate Pathology 107: 127-131 doi 10.1016/j.jip.2011.03.009

Work TM, Russell R, Aeby GS (2012) Tissue loss (white syndrome) in the coral *Montipora capitata* is a dynamic disease with multiple host responses and potential causes. Proceedings of the Royal Society B: Biological Sciences 279: 4334-4341

COURTNEY SALONSTALL COUCH

EDUCATION

2008-2014	Ph.D.	**Cornell University,** Ithaca, NY (Successfully defended 8/21/13). Dept. of Ecology and Evolutionary Biology, Advisor: Dr. C. Drew Harvell. Dissertation Title: "Intrinsic Host and Extrinsic Environmental Drivers of Coral Health and Disease"
2004	B.Sc.	**St. Lawrence University**, Canton, NY Biology *Magna cum laude*

RESEARCH EXPERIENCE

Started Oct 1, 2013: "Promoting Pacific Coral Health through the Action Network for Coral Health and Resilience (ANCH&R)." (Postdoctoral Researcher)
HIMB, The Nature Conservancy, Papahānaumokuākea Marine National Monument (NOAA)

- Will develop quantitative sampling designs and conduct surveys to characterize coral disease and determinates of disease in Main Hawaiian Islands, PMNM and Big Ocean Network. Will conduct coral disease training workshops to increase coral reef manager capacity to address coral disease and coordinate the Action Network for Coral Health and Resilience.

2012-present: "Coral Health in COREMAP: Building Resilience in Climate-Impacted Coral Reefs of Indonesia" (collaborator, organizer)
Cornell University, Mote Marine Laboratory, Hasanuddin University, Indonesia

- Conducting field surveys and training programs to determine whether marine protected areas established by COREMAP act as a refuge from coral disease outbreaks and assess the link between socio-economic status and coral health.

2010-present: "Environmental Monitoring of Coral Disease and Bleaching." (collaborator)
NOAA/Hawai`i Division of Aquatic Resources, Kailua-Kona, HI

- Developing an experimental predictive tool to assess the risk of bleaching and disease outbreaks in Hawai'i, based on satellite-derived environmental metrics.

2010-present: "Ecosystem Services and Impacts of Submarine Groundwater Discharge to Coral Reef Health and Bleaching in Hawai'i." (co-PI)
USGS/UC Berkley/Cornell University, Kailua-Kona, HI

- Determining the risks to coral reef health associated with climate change and land use including municipal groundwater development.

2010: "Survey of the Coral Reefs Pelekane Bay" (collaborator)
The Nature Conservancy, Cornell, Scripps Institution of Oceanography and OceanInk

- Assessed the effects of chronic sedimentation on the Pelekane Bay coral reefs to understand how restoration of terrestrial environments can help restore downstream marine ecosystems.

2009-2013: "Intrinsic Host and Extrinsic Environmental Factors of Coral Health and Disease" (Doctoral research with Prof. C. Drew Harvell, in collab. with Dr. Rebecca Vega Thurber)

- Conducted independent and collaborative research in coral disease ecology and pathology using field surveys, water quality monitoring, histopathology, and micro and molecular biology.

2006-2009: "Coral, pathogens and the environment: what's influencing coral immunity?"
Cornell University, Ithaca, NY (research technician and lead investigator)

- Investigated the dynamics of coral innate immune response to pathogens and environmental stressors.

2005: Ecological Consulting Internship
PBS&J, Miami, Fl

- Investigated benthic community structure of Florida coastal ecosystems and the Flower Garden Banks National Marine Sanctuary.

2004: CARICOMP San Salvador, Bahamas (volunteer)

- Conducted coral reef health and benthic community structure surveys

2004: Coral Reef Community Health Project (undergraduate researcher)
St. Lawrence University, Florida Keys and Bahamas

- Surveyed benthic invertebrate and fish populations, and conducted a *Diadema antillarum* restoration project.

2003: "Feeding behavior of the sea urchin *Lytechnius variegatus"* (undergraduate research)
St. Lawrence University, Canton, NY

- Conducted laboratory experiments on the feeding preferences of *Lytechnius variegatus*.

2002: Limnological NYSF Fellowship (undergraduate research assistant)
St. Lawrence University, Canton, NY

- Surveyed biodiversity and water quality of two lakes, incorporating pelagic sampling, SCUBA sampling, lab analyses, and GIS.

PROFESSIONAL ACTIVITIES

ADVISORY AND ADMINSTRATIVE EXPERIENCE

2010-present: Coral Disease Specialist- HI Division of Aquatic Resources, Kailua-Kona, HI

- Coral disease advisor for Hawai'i DAR, conducted baseline coral disease surveys and trainings for staff.

2009- 2011: Marine Science Specialist for The Kohala Center, Kamuela, HI

- Scientific advisor for marine ecosystem health and citizen science program, water quality data analysis, educational outreach.

2007-2009: Coral Disease Working Group Coordinator at Cornell University, Ithaca, NY

- Acted as the project coordinator for the Coral Disease Working Group, part of the International "Coral Reef Target Research and Capacity Building Program" funded by the Global Environmental Facility and the World Bank.

WORKSHOPS

2012	*Ecology of Infectious Marine Disease NSF Research Coordination Network* (invited participant), Seattle, WA
2009-2011	*Environmental Monitoring of Coral Disease and Bleaching Workshops* NOAA/Hawai`i Division of Aquatic Resources (invited member), Honolulu, HI
2009	*Pan-Pacific Coral Health and Disease Workshop*, CRTR Coral Disease Working Group (organizer and participant), Kailua-Kona, HI
2007-2009	CRTR Coral Disease Working Group Annual Capacity Building workshops (organizer and participant), Philippines, Fl, Cornell
2007	*CRTR Future Leaders Forum* (invited participant), Brisbane, Australia

TEACHING EXPERIENCE

2013	**Teaching Assistant:** Biodiversity and Biology of Marine Invertebrates, Cornell University, Shoals Marine Laboratory
2012	**Mentor:** Cornell's Biology Research Fellows Program
2012	**Guest Lecturer:** Marine Ecology, Cornell University
2009-2011	**Guest Lecturer:** Oceanography, Cornell University
2011	**Lecturer:** Conservation Oceanography, Cornell EES Program, HI
2010	**Guest Lecturer:** Chemical Ecology, Cornell University, Ithaca, NY
2009	**Guest Lecturer:** Conservation Oceanography, Cornell EES Program, HI
2004	**Marine Science Instructor:** Seacamp, Big Pine Key, Fl
2004	**Marine Science Instructor:** Newfound Harbor Marine Institute, Big Pine Key, Fl

OUTREACH EXPERIENCE

2011-present	Community Coral Health Survey Program (leader)/Eyes of the Reef, Kona, HI
2012	Ithaca Sciencenter invited presenter, Ithaca, NY
2010-11	Hawai'i Island Meaningful Outdoor Education for Students, Hawai'i Island
2010-11	Expanding Your Horizon's (co-leader), Cornell, Ithaca, NY
2009-11	Coral disease training workshops (leader), Kona, HI
2004	Coral Reef Ecology (co-leader), San Salvador Central High School, Bahamas

FUNDING

2012	Paul P. Feeny Graduate Student Research Fund ($1,000)
2012	Orenstein Endowment Fund ($750)
2011	Cornell ACSF's Sustainable Biodiversity Fund ($6,000)
2011	Cornell University Graduate Research Travel Grant ($2,000)
2009	NOAA Coral Reef Conservation Grant Program, "The role of environment and viruses in *Porites lobata* growth anomalies" (author and senior personnel with C. Drew Harvell [PI]). ($47,700)
2009	NSF Graduate Research Fellowship ($120,000)
2009	The Kohala Center Student Fellowship ($45,000

AWARDS AND HONORS

2004	Phi Beta Kappa National Honorary Society, St. Lawrence University
2003	Linda Reeve's Merit Scholarship Award, St. Lawrence University
2003	St. Lawrence University Faculty Scholar, Canton, NY

PUBLICATIONS

IN REVIEW

Couch, C. S., J. Garriques, C. Barnett, L. Preskitt, S. Cotton, J. Giddens, W. Walsh (in review). Spatial and Temporal Patterns of Coral Health and Disease along Leeward Hawai`i Island. Coral Reefs.

PEER-REVIEWED

Bell R.C., A. Belmaker, J.M. Brown, **C.S. Couch,** K.S. Francisco, M. Manuel, K.M. Marchetto, J.L. Simonis, R.Q. Thomas, J.P. Sparks. (2013). Effectiveness of *Erythrina* gall wasp bio-control and implications for the recovery of threatened Wiliwili trees (Fabaceae: *Erythrina sandwicensis*). The Journal of the Torrey Botanical Society 140(2):215-224

Couch, C. S., L. D. Mydlarz, C. D. Harvell, and N. L. Douglas. (2008). Variation in measures of immunocompetence of sea fan coral, *Gorgonia ventalina*, in the Florida Keys. Marine Biology. 155(3): 281-292.

Couch, C. S., E. Weil, C. D. Harvell. (2013). Temporal dynamics and plasticity of the sea fan coral, *Gorgonia ventalina* cellular response. Marine Biology. 160 (9), 2449-2460.

Groner, M.L., C.A. Burge, **C.S. Couch**, C.J.S. Kim, G.F. Siegmund, S.Singhal, S.C. Smoot, A. Jarrell, J.K. Gaydos, C.D. Harvell, S. Wyllie-Echeverria. (in press). Host demography

influences the prevalence and severity of eelgrass wasting disease. Diseases of Aquatic Organisms

Hewson, I, Brown, J, Burge, CA, **Couch, CS**, LaBarre, BA, Mouchka, ME, Naito, M, & Harvell CD. (2012). Viral assemblages associated with healthy and aspergillosis affected tissues of the *Gorgonia ventalina* holobiont. Coral Reefs. 31: 487-491.

Mouchka, M and **C.S. Couch**. (2010). The effects of aquaculture effluent on *Porites cylindrica* innate immune function. Building capacity in coral reef science: an anthology of CRTR scholars' research: 13-20.

Mydlarz LD, **CS Couch**, E Weil, CD Harvell. (2009) Immune defenses of healthy, diseased and bleached *Montastraea faveolata* during the 2005 Caribbean bleaching event. Diseases of Aquatic Organisms. 16 (1-2): 67-78.

BOOKS

Raymundo, L. J., **C. S. Couch**, and C. D. Harvell (eds). 2008. Coral Disease Handbook: Guidelines for Assessment, Monitoring & Management. Melbourne: Currie Communications. 121pp.

TECHNICAL REPORTS

Couch, C.S., C. Barnett, R. Vega Thurber, (2012). Examining the role of environmental and viruses in growth anomalies of *Porites lobata* on the Island of Hawai'i Final Report. 2009 NOAA Coral Reef Conservation Program. Cornell University Award # NA09NMF4630121.

Minton, D., E. Conklin, **C. Couch**, M. Garren, M. Hardt, R. Amimoto, K. Pollack, and C. Wiggins. (2011). Survey of the coral reefs of Pelekane Bay. Report prepared for The Kohala Center.

Mouchka, M. E., **C. S. Couch**, L. J. Raymundo, M. Garren, M. J. Pueblos, J. Guest, M. Defley, C. D. Harvell, and F. Azam. 2008. Follow-up study report on the impact of fish aquaculture effluent on *Porites cylindrica* health and disease. Coral Reef Targeted Research Program Report. 21pp.

Walsh, W., R. Sparks, C. Barnett, **C. Couch**, S. Cotton, D. White, K. Stone, E. Conklin. 2013. Long-term monitoring of coral reefs of the Main Hawaiian Islands Final Report. 2009 NOAA CRCP. State of Hawai`i Monitoring Report. NA06NOS4260113.

SELECTED PRESENTATIONS & SYMPOSIA

2012	Cornell Ecology and Evolutionary Biology GSA Symposium, "Ecological and Environmental Drivers of Coral Disease Dynamics on Hawai'i Island. "
2012	37th Eastern Fish Health Workshop, Lake Placid, NY, "The Role of Host Demographics and Environment in *Porites lobata* Growth Anomaly Dynamics
2012	along West Hawai'i." (invited oral)
2011	41st Benthic Ecology Meeting, Norfolk, VA, "The Role of Host Demographics and Environment in *Porites lobata* Growth Anomaly Dynamics along West Hawai'i." (oral)
2010	Cornell Ecology and Evolutionary Biology GSA Symposium, "The Role of Environmental Factors in *Porites lobata* Growth Anomaly Dynamics." (oral)
2010	International Marine Conservation Congress, Victoria, BC, "The Role of Environmental Factors in *P. lobata* Growth Anomaly Dynamics." (poster)
2010	Big Island Water Resources Meeting, Hilo, HI, "The Role of Environmental Factors in *Porites lobata* Growth Anomaly Dynamics." (oral)
2009	Reef Teach Presentation to community, Kona, HI, "Just How Healthy are West Hawai`i's Corals?" (oral)
2009	Ecology and Evolution of Infectious Diseases, Cornell, NY, "Temporal Dynamics of *Gorgonia ventalina* Cellular Response in La Parguera, Puerto Rico." (poster)
2008	Environmental Monitoring of Coral Disease and Bleaching in the Hawaiian Islands Wksp, Honolulu, HI, "CRTR Coral Disease Working Group: a review of five years of research." (oral)
2007	International Coral Reef Symposium, Ft. Lauderdale Fl. "How Quickly does *Gorgonia ventalina* Mount a Cellular Response to Elicitors?" (poster)
	Cornell Ecology and Evolutionary Biology GSA Symposium, "Variation in measures of immunocompetence of sea fan coral, *Gorgonia ventalina*, in the Florida Keys" (oral)
2004	Benthic Ecology Meeting, Mobile, Al, "Ranked feeding preferences of the sea urchins, *Lytechinus variegatus* and *Arbacia punctulata*." (poster)

SERVICE ACTIVITIES

2013-2010	Student Member: Dive Safety Control Board, Cornell University
2012	Chair of E&EB Professional Development Working Group
2011	Sigma Xi Member
2008-2011	International Society for Reef Studies (ISRS)
2005-2011	American Association of Underwater Scientists (AAUS)
2004	NAUI Skin Diver Instructor
2003	Beta Beta Beta Biological Honor Society

REVIEWER

Journals: Ecology, Marine Biology, Diseases of Aquatic Organisms

Grants: NOAA's Coral Reef Conservation Program, Cornell's Atkinson Center for a Sustainable Future

SCUBA DIVING EXPERIENCE

2012 Most recent CPR/First aid/Oxygen renewal
2005-present Scientific Diver through American Academy of Underwater Sciences
2004 NAUI Rescue Diver
2002 PADI Advanced Open Water Diver
2001 PADI Open Water Diver